Ministério da
Ciência e Tecnologia

sid.inpe.br/mtc-m19/2010/09.10.18.49-TDI

THE ROLE OF HYDROGEN AND BERYLLIUM ISOTOPES AS TRACERS OF SOLAR AND CLIMATE VARIABILITY

Alessandra Abe Pacini Schmidt Marques

Doctorate Thesis at Post Graduation Course in Space Geophysics, advised by Drs. Ezequiel Echer, and Heitor Evangelista da Silva, approved in september 28, 2010.

URL do documento original:
<http://urlib.net/8JMKD3MGP7W/388CFJS >

INPE
São José dos Campos
2010

PUBLISHED BY:

Instituto Nacional de Pesquisas Espaciais - INPE
Gabinete do Diretor (GB)
Serviço de Informação e Documentação (SID)
Caixa Postal 515 - CEP 12.245-970
São José dos Campos - SP - Brasil
Tel.:(012) 3208-6923/6921
Fax: (012) 3208-6919
E-mail: pubtc@sid.inpe.br

Ministério da
Ciência e Tecnologia

sid.inpe.br/mtc-m19/2010/09.10.18.49-TDI

THE ROLE OF HYDROGEN AND BERYLLIUM ISOTOPES AS TRACERS OF SOLAR AND CLIMATE VARIABILITY

Alessandra Abe Pacini Schmidt Marques

Doctorate Thesis at Post Graduation Course in Space Geophysics, advised by Drs. Ezequiel Echer, and Heitor Evangelista da Silva, approved in september 28, 2010.

URL do documento original:
<http://urlib.net/8JMKD3MGP7W/388CFJS >

INPE
São José dos Campos
2010

Dados Internacionais de Catalogação na Publicação (CIP)

Marques, Alessandra Abe Pacini Schmidt.
M348r The role of hydrogen and beryllium isotopes as tracers of solar and climate variability / Alessandra Abe Pacini Schmidt Marques. – São José dos Campos : INPE, 2010.
xxiv+ 94 p. ; (sid.inpe.br/mtc-m19/2010/09.10.18.49-TDI)

Tese (Doutorado em Geofísica Espacial) – Instituto Nacional de Pesquisas Espaciais, São José dos Campos, 2010.
Orientadores : Drs. Ezequiel Echer, e Heitor Evangelista da Silva.

1. Relações Sol-Terra. 2. Isótopos naturais 3. Clima terrestre. 4. Ciclo solar. 5. Mudanças globais. I.Título.

CDU 550.3:551.58

Aprovado (a) pela Banca Examinadora em cumprimento ao requisito exigido para obtenção do Título de Doutor(a) **em**

Geofísica Espacial

Dr. **Alisson Dal Lago**

Presidente / INPE / São José dos Campos - SP

Dr. **Ezequiel Echer**

Orientador(a) / INPE / SJCampos - SP

Dr. **Heitor Evangelista da Silva**

Orientador(a) / UERJ / Rio de Janeiro - RJ

Dr. **Eurico Rodrigues de Paula**

Membro da Banca / INPE / SJCampos - SP

Dr. **Kalevi Mursula**

Convidado(a) / OULU / Finlândia -

Dr. **Sambasiva Rao Patchineelam**

Convidado(a) / UFF / Rio de Janeiro - RJ

Aluno (a): Alessandra Abe Pacini Schmidt Marques

São José dos Campos, 28 de setembro de 2010

“I don't pretend we have all the answers. But the questions are certainly worth thinking about..”

Sir Arthur C. Clarke
Writer (1917 – 2008)

With love, to my parents, ***Áderson e Emília****,*

my little nieces, ***Letícia e Paola****,*

and my students.

ACKNOWLEDGEMENTS

“I get by with a little help from my friends
I get high with a little help from my friends
Going to try with a little help from my friends...”
– Beatles

During the last four years, my life had been orbiting this thesis... Sometimes, it was easy to keep on this orbit... But sometimes, it was really hard. I can say that it would have been impossible to finish this work if I was alone during that long way. But I wasn’t. Actually, I was surrounded by people that helped me a lot, for different reasons, in different ways... All of them helped me to take the most important step of my academic life. All of them helped me to conclude this thesis. And because of that, I’ll always be grateful:

to my dear advisors ***Ezequiel*** and ***Heitor***, for the great opportunity to work with them and for their time, advices, support, motivation, patience, confidence in my work and essential friendship;

to Drs. **Alisson Dal Lago**, **Kalevi Mursula**, **Sambasiva Rao Patchineelam** and **Eurico de Paula**, which kindly participated of the examination crew of this thesis, helping me to improve the final version and opening important discussions concerning the results present here.

to my kind colleagues, friends and teachers from INPE, for all these six years of support, help and friendship. I deeply thank my supervisors Drs. ***Jonas Rodrigues, Alexandre Pimenta*** and ***Alisson Dal Lago*** for their comprehension and help along these four years. Thanks also to ***Drs. Daniel Nordemann, Nivaor Rigozzo*** and ***Eurico de Paula*** for their support since the very beginning of this work. A special thanks goes to my beloved “joseense” family (***Jonas, Cida, Ceci, Pedrina e Christiano***) and to all of my inestimable friends which turned São José dos Campos in the best place in the world to me (with “caldinho”, “chimarrão” and home), in special: ***Aline, Valents, Rô, Marizinha, Wanturs, Diana, Sérgio, Clara, Cléo, Paulinho, Marcos, Vivian, Cris, Rafael, Laysa, Juliano and Amelinha***.

to my “cariocas” colleagues from LARAMG/UERJ, for having kindly welcomed this “paulistana” in their “almost-so-amazing-town-as-São Paulo”. A special thanks goes to ***Gustavo, Raquel*** and ***Bruno***, for their help with the measurements, and to my lovely friends ***Márcio, Dany, Els, Aldrey, Marcus*** and ***Alencar*** for their crucial presence.

to my generous colleagues from Finland, for their help and support in the last year of my thesis. In special, I would like to thanks ***Dr. Kalevi Mursula*** for having kindly received me as a member of the Space Physics group of the University of Oulu; to ***Dr. Ilya Usoskin*** for his support, friendship and invaluable opportunity to work with him, improving significantly the results of this thesis and opening new doors in my life; to ***Dr. Ari-Pekka Leppänen***, for his valuable collaboration in the analysis; to my dear friends of Oulu for their fundamental company in this far-far-away land: ***Katri, Olesya, Lyiun, Tomi, Ilpo, Ilka, Ville, Timo, Riku, Jaakko, Paulo, Sofia, Cecília, Miikka, Alex, Carlos, Rodrigo*** and ***Santa Claus***, of course.

to ***Dr. Hiroko Miyahara,*** for all discussions about my results and ideas, and for her example of how to be, simultaneously, a great person, generous friend and incredible young researcher.

to people from PROANTAR and LAMIRE, for their support with the rock sampling. A special thanks goes to ***Dr. Vivian Pelizari*** for make my participation on that Antarctic Operation XVI possible, and to all members of that Operation, in special ***Ema, Lia, Beto, Mikolaj, Drs. Vincent Jomelli*** and ***Erling Johnson***.

to LGPA/UERJ staff for their kind help with the rock samples processing.

to people from IRD and Van de Graff / PUC labs, for their generous help with the rock measurement experiences. A special super-thanks goes to ***Dr. Kenya Dias da Cunha*** for her advices, support and precious friendship.

to people from Lab. of Environmental Monitoring / Eletronuclear, specially ***Dr. Sérgio Ney***, for making Angra’s data available for this work.

to the CAPES/CNPq resolution (number 001 from March 11, 2004) for the opportunity to live the most enriching experience of my life: be a teacher at CEFET-Química (Nilópolis-RJ) and UERJ during the period of this work.

to my mates of teacher's room in CEFET and UERJ, for their friendship and generosity. In special: ***Antônio ACAF, Heitor, Adriano, Antônio Carlos, Príscila, Grazi, Aloa, Tiago, Mari, Vítor, Freitas*** and, specially, ***Eduardo*** (and his lovely family (which I consider a little bit mine: **Cá-amore, tia Norma, tio Célio, D. Noemia, Léo, GK, Ricardo** and **S. Nelson** (*in memory*)).

to my students, for their kindness and support. They were my biggest motivation to finish this thesis. A special thanks goes to my ex-students and friends ***Isabelle, Raquel*** and ***Monique***.

to my previous advisor, ***Dr. Jean-Pierre Raulin*** and old colleagues from CRAAM / Mackenzie, for being an important part of my academic past, present and future.

to my personal best-friends for their crucial existence and support: ***Juliana & Artur, Juliana & Paulinho, Valquíria & Assunção*** and ***Chico***.

to CAPES and CNPq for the fundamental fellowship received.

In closing, I wish to thanks my "extended" and beloved family, ***Vini, papai, mamãe, vovó, Aline, Zé, Lélis, Lola, Sílvio, Luíza*** and other ***Abe-Pacini-Schmidt-Marques-Bordallo-Matsumoto*** for EVERYTHING. I have no words to express my gratitude for their support, sacrifices and love. Everything is meaningless without you, family...

Alessandra Pacini

September 03, 2010

ABSTRACT

The history of Earth's climate and the role of solar activity as a driver of the observed changes can be recovered through the study of natural records. Among them, stable isotopes of hydrogen and cosmogenic radioisotopes of beryllium are usually analyzed, especially from ice cores and air samples. In this thesis, deuterium/hydrogen ratio from ice cores and ^{7}Be activity from air samples are analyzed to study the role of different climatic and solar phenomena in their variation. Deuterium isotope data were obtained from polar (Greenland, Antarctic) and equatorial (Andes) regions for the last four decades (1951-1994). It has been found that deuterium series present a decadal cycle, which might be a direct influence of solar irradiance modulation on the hydrological cycle. Furthermore, the results emphasize the importance of the local climatic system on the deuterium isotopic temporal variability. Berylium-7 data were obtained from near-ground air samples measured since 1987 around the Angra's Nuclear Power Station (with 3-month time resolution) , in Rio de Janeiro, Brazil, and also from air-samples acquired by our own instrumentation installed in the campus of University of Rio de Janeiro State since late 2008 (with weekly time resolution). Data and model results from Oulu University, Finland, were also used in the ^{7}Be variability study. For the Brazilian isotopic data, the dominant driver of its modulation was found to be the regional precipitation pattern, with the local production by cosmic-rays having a minor effect on its variability. Moreover, our results indicate that anomalous events of tropospheric dynamics may also imprint information about air masses 3-D movement in the near-ground air ^{7}Be data. Thus, this thesis explores the information contained in the studied isotopic time series, showing the potential scientific uses of them and highlighting the necessity of more careful interpretations of the isotopic modulation as proxies of climatic and solar variations.

O PAPEL DOS ISÓTOPOS DE HIDROGÊNIO E BERÍLIO COMO TRAÇADORES DA VARIABILIDADE SOLAR E CLIMÁTICA

RESUMO

A história do clima terrestre e sua relação com a atividade solar podem ser reconstruídas a partir de informações encontradas em registros naturais. Dentre esses registros, os isótopos estáveis do hidrogênio e os radioisótopos cosmogênicos do berílio são usualmente analisados, retirados de diferentes matrizes naturais, especialmente de testemunhos de gelo e amostras de ar. Nesta tese, a razão deutério/hidrogênio, extraída de testemunhos de gelo, e a atividade do ^{7}Be, medida em amostras de ar, foram utilizadas para o estudo do papel de diferentes fenômenos climáticos e solares em suas variações. Os dados de deutério foram obtidos a partir de testemunhos de gelos das regiões polares (Groenlândia e Antártica) e equatoriais (Andes) para as últimas quatro décadas (1951 – 1994). Foi encontrada uma periodicidade decadal nessas séries isotópicas, que parece ser o resultado de uma influência direta da modulação da irradiância solar no ciclo hidrológico global. Além disso, os resultados encontrados enfatizaram a importância dos regimes climáticos locais na variabilidade do deutério medido. Os dados de berílio-7 foram extraídos de amostras de ar coletadas próximas ao solo desde 1987 (com resolução temporal trimestral) nas cercanias da Usina Nuclear de Angra, no Rio de Janeiro, Brasil, e também de amostras de ar coletadas e medidas (semanalmente) pela nossa própria instrumentação instalada desde o final de 2008 no campus da Universidade Estadual do Rio de Janeiro. Dados e modelos numéricos da Universidade de Oulu, Finlândia, foram também utilizados na análise das origens da variabilidade do ^{7}Be. Os resultados indicam que o forçante dominante da modulação dos dados de ^{7}Be do Rio de Janeiro é o padrão regional de chuvas, tornando as variações locais da produção cosmogênica (causada por raios-cósmicos) não evidentes nos dados. Além disso, nossos resultados indicaram que eventos anômalos da dinâmica troposférica podem imprimir nos dados de ^{7}Be as informações dos movimentos 3-D das massas de ar. Assim, essa tese explora as informações contidas nas séries temporais dos isótopos estudados, mostrando os potenciais usos científicos de cada um deles e destacando a necessidade de interpretações mais cuidadosas das modulações isotópicas utilizadas como traçadores de variações climáticas e solares.

LIST OF FIGURES

Pg.

LIST OF TABLES

Pág.

TABLE OF CONTENTS

Pág.

1 INTRODUCTION

1.1. Foreword

The motivation of this thesis has arisen during a period full of discussions about the origin of the recent climate changes observed in our planet. It was late 2006, and at that time it was already known that the huge amount of biomass burned by anthropogenic and industrial activities was responsible for the release of greenhouse gases to the atmosphere, contributing to the observed global warming. However, it was also known that this amount of greenhouse gases could not fully drive all the recent evolution of the terrestrial climate. On that year, there was not a consensus about the relative importance of the Natural Forcing (linked to solar energy input variations, cosmic rays flux modulation and volcano eruptions for example) and the Anthropogenic ones (mainly greenhouse gases). Even today, we still haven't found this answer…

One of the most controversial topics about the Natural Forcing was related to the effects of the solar magnetic cycles on Earth's climate and atmosphere. Many works showed evidences of the linkage between the solar activity and the terrestrial climate, but there was no physical model able to explain the suggested connection. The lack of sufficient information about the role of Solar Activity Forcing could be noticed at the Intergovernmental Panel on Climate Changes (IPCC / UNO) report, published on early 2007 (the technical summary regarding to the physical sciences basis of IPCC report can be found at http://www.ipcc.ch/publications_and_data/ar4/wg1/en/ts.html).

The IPCC report was the result of six years of studies about the climate changes developed by more than 2500 researchers, from 130 countries. On 2nd Feb 2007, this report announced an alarming projection for the future of the Earth's climate, and caused a huge impact on the world population. According to that report, the greenhouse gases released by the anthropogenic activities are causing an environmental catastrophe along the next century (increasing

the sea level, the average surface temperature of the planet and the occurrence of hurricanes and storms). Meanwhile, this “inconvenient result” was obtained based on numerical climatic models which considered only well known radiative forcing on climate changes. The most important radiative forcings (RF) considered on that report are presented on Figure 1.1, as well as the average of their contribution (local or global) to the warming (showed in red) or cooling (in blue) of the planet. According to the IPCC definition, RF “is a measure of the influence that a factor has in altering the balance of incoming and outgoing energy in the Earth-Atmosphere system and is an index of the importance of the factor as a potential climate change mechanism”. In the 2007 IPCC Report, RF values were relatives to a pre-industrial background at 1750, and were expressed as a global and annual average value [in W·m²]. As one can see, only the solar irradiance variability (that is one of the manifestations of the solar magnetic cycles) was considered as a natural forcing. Nevertheless, the level of scientific understanding about this forcing, indicated by the LOSU index, was “low”.

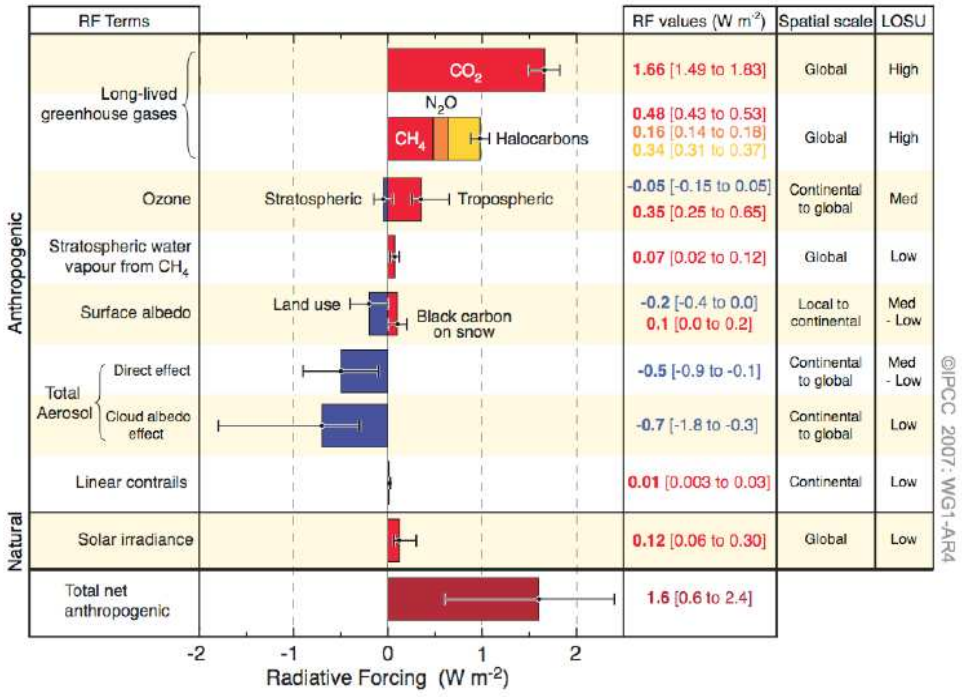

Figure 1.1 – Most relevant radiative forcings presented at 2007 IPCC Report

Source: http://www.ipcc.ch/publications_and_data/ar4/wg1/en/tssts-2-5.html

Although the LOSU index is a subjective information on the reliability of the studies considered about each forcing agent, the “low” LOSU clearly shows the lack of enough investigations on the impact of solar irradiance modulation on climate. Moreover, the role of other possible mechanisms of the solar activity forcing (like the modulation of cosmic-rays) was not even considered on that report. Furthermore, other problems started to appear later, suggesting that some results presented at 2007 IPCC report were obtained based on tons of missing crucial information, wrong uncertainties estimations, non-scientific references, misunderstanding data and apparently manipulated analysis (SCHIERMEIER, 2010). These facts provided a new criticism light over the IPCC results, inducing the creation of a report explaining these obscure point (just-published, 30th Aug 2010: http://reviewipcc.interacademycouncil.net/report.html) and bringing the natural forcings’ studies to the core of the scientific discussion. A new version of the IPCC report will be published at 2013 based on new scientific results (obtained with improved models and reduced uncertainties) and including a group of solar-terrestrial physicists in its scientific workgroup.

The key to better establish the role of solar forcing on climate change is to understand their long term modulation. Since the available records are not long enough for this kind of study, some natural isotopes has been used as proxies of these environmental conditions, improving the understanding on the terrestrial climate dynamics and allowing the analysis of the relative importance between natural and anthropogenic forcings on the global changes. On this context, a better knowledge of the response of these natural tracers to solar and climate variations is crucial to make the studies on Solar Activity and Terrestrial Climate connections more reliable, and to improve the quality of the climate change projections for the near future.

This thesis reports a study of the solar and climate information provided by time series of hydrogen and beryllium isotopes, found in different natural archives

(ice cores, air and rocks). Our study was developed at the Space Geophysical Division, at National Institute for Space Research (DGE/INPE – Brazil), in collaboration with the Radioecology and Global Changes Laboratory, at University of Rio de Janeiro State (LARAMG/UERJ – Brazil), and with the Space Physics Department of University of Oulu (Oulun Yliopisto – Finland). This institutional cooperation was justified by the fact that the solar-climate investigation is strongly interdisciplinary, involving researches on solar physics, space physics and climatology. Moreover, this study was based on instrumental work, data analysis and numerical models, implying in a search for know-how in different institutions. Besides of the international and interdisciplinary collaboration, each step of this thesis' development was presented and discussed at several international scientific meetings along these four years of work (from 09/2006 to 09/2010), putting our results on the context of the modern knowledge regarding to the Solar-Climate connection proxies. The scientific background required to this work is presented at the next sub-section (1.2) and the closing sub-section of the introduction chapter (1.3) presents the outline of this thesis.

1.2. General scientific background

The energy source that drives most of Geospace processes, including the near-Earth's environment, is the Sun. This energy flux comes from the solar core and goes to the interplanetary medium through electromagnetic waves and accelerated particles, presenting temporal variabilities related to the solar magnetic activity.

As the main source of energy of the Earth, some physical processes on the planet, including some climatic phenomena, are strongly dependent on the solar activity cycles. To establish the relations between solar activity and terrestrial phenomena is necessary to understand how these parameters varied in the past. For this kind of study it is possible to apply some proxies of these solar and geophysical processes.

This section succinctly introduces the scientific basis of this study regarding to the solar activity origins, its effects on climate and the knowledge on the natural tracers of this relationship.

1.2.1. An overview of our variable Sun

Far from the Earth almost 150 millions of kilometer, the Sun is our nearest star providing us light, heat and energy. Besides its importance in our sky (solar apparent bright is 200 billion times higher than the Alpha Centaurus bright, which is the second most close start from the Earth), the Sun is considered a really common star. Table 1.1 shows the main solar characteristics.

Table 1.1 – Main characteristics of the Sun

Age	$4{,}5 \times 10^9$ years
Mass	1.989×10^{30} kg
Radius	696000 km
Mean density	1409 kg/m^3
Mean distance from the Earth	1.499×10^8 km
Luminosity	3.9×10^{26} W
Black body temperature	5785 K
Temperature of the core	15 MK
Superficial gravity	274 m/s^2
Escape velocity	618 km/s
Main chemical composition	H ≈ 90%, He ≈ 10%, other (C, N, O) ≈ 0.1%
Mean rotational period (at the Equator)	26.8 days
Mean rotational period (at the latitude 75°)	31.8 days

Source: Briggs & Carlisle (1996); Kivelson and Russell (1995).

In the study of its structure, the Sun is usually divided in two main parts: its Interior and its Atmosphere (BRIGGS; CARLISLE, 1996).

The solar interior, which includes the core and the radiative and convective layers, cannot be directly observed. Some theoretical models suggests that nuclear fusion reactions are occurring at the solar core, under extreme temperature conditions (around 15 MK), releasing energy. Through this process, 5 millions of tons of hydrogen are converted to helium every second, resulting in a gamma-ray (γ) and neutrinos (ν) fluxes. Table 1.2 shows the most probable nuclear reactions occurring at the solar core producing the solar energy.

Table 1.2 – Nuclear reactions occurring at the solar core and involving isotopes of hydrogen (H) and helium (He), gamma-ray photons (γ), electrons (e-), positrons (e+) and neutrinos (ν)

$4\,^{1}H \rightarrow {}^{4}He + 5\,\gamma + 2\,\nu$
$2\,(^{1}H + {}^{1}H) \rightarrow 2\,(^{2}H + e^{+} + e^{-} + \nu)$
$2\,(e^{+} + e^{-}) \rightarrow 2\,\gamma$
$2\,(^{2}H + {}^{1}H) \rightarrow 2\,(^{3}He + \gamma)$
$^{3}He + {}^{3}He \rightarrow {}^{4}He + 2\,^{1}H + \gamma$

Source: Kivelson and Russell (1995).

The huge amount of energy produced by the solar core is surrounded by the radiative layer. This layer works as an isolator shelve, keeping the high temperatures at the solar core necessary to the nuclear reaction occurrence. The γ-ray photons resulting of these nuclear reactions are absorbed and reemitted continuously through the radiative layer, wasting some energy along the path and spending 50 million years to reach the solar surface.

Under the solar surface, the temperature decreases with radius quickly, creating an unstable region above the radiative layer. In this region, called convective layer, the radiative process is much less significant and the energy is mainly transported outward from the Sun by the convection process. Heated parcels of plasma located at the bottom of this layer become rarefied and rise up. At the same time, cooler material from the top of the layer descends, creating giant convective plasma cells.

Due to the upward and downward motion of these cells, magnetic fields are formed, representing an important role to the solar activity (KIVELSON; RUSSELL, 1995). It is possible to see the top of each convective cell in the photosphere (see a movie of these photospheric granular features on the webpage: http://solarscience.msfc.nasa.gov/images/SVST_granulation.mpg).

The innermost layer of the Solar Atmosphere is called photosphere, and it can be seen with the naked eye, since its energy (that comes from the solar interior through the convective cells) is emitted mostly in the visible part of the electromagnetic spectrum. The mean photospheric temperature is 6000 K.

Above the photosphere there are two more layers in the solar atmosphere: the chromosphere and the corona. The corona is expanded to the interplanetary medium, due to the hydrostatic balance, creating a continuous flow of particles, called solar wind, which travels away from the sun and propagates into the entire solar system.

Figure 1.2 shows schematically the solar structure.

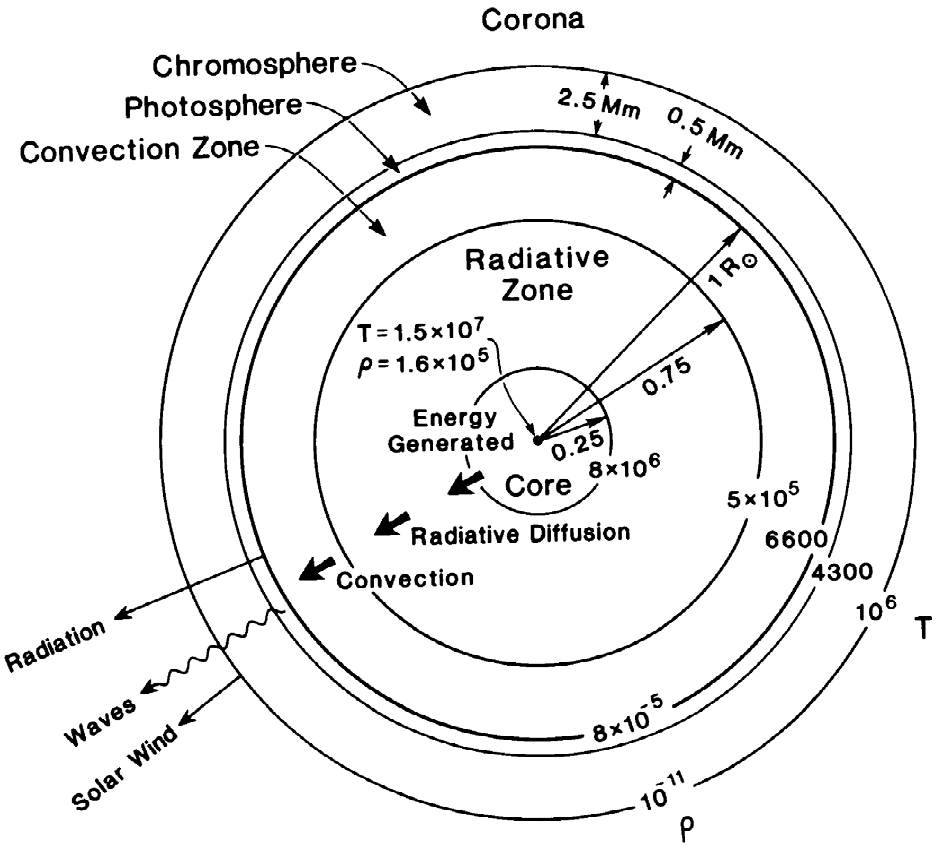

Figure 1.2 – Solar structure showing how the temperature (T) and density (ρ) vary according to the distance.

Source: Kivelson and Russel (1995).

Even though the quiet Sun is considered very much interesting to astronomers (due to its proximity to the Earth, making a detailed observation of the solar spatial features possible), the most part of the important geophysical effects come from the active solar magnetic behavior.

During calm periods, the solar magnetic field is mainly dipolar (poloidal field). Due to a continuous flux of charged particles (solar wind) propagating from the surface of the Sun through the solar system, the magnetic field lines are frozen and dragged forming the so called Interplanetary Magnetic Field (IMF). The region controlled by the solar magnetic field is called Heliosphere.

Because of the solar rotation, the IMF configuration follows the spiral trajectory, which is known as Arquimedes' spiral (or Parker's spiral), as showed in Figure 1.3.

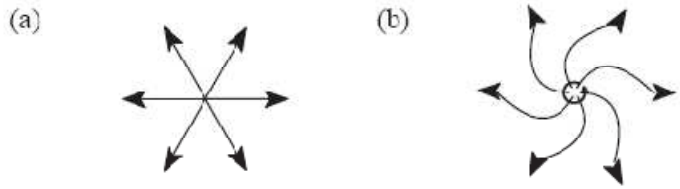

Figure 1.3 – Interplanetary Magnetic Field configuration seen from the solar north pole (a) radial direction of solar wind flow, e; (b) Arquimedes' spiral due to the solar rotation.

Source: Briggs and Carlisle (1996).

Different from a rigid body, the ball of ionized gas called Sun rotates faster at the equator than the pole (see Table 1.2). Due to this differential rotation, the original poloidal magnetic field is sheared near the bottom of the convection zone, producing a toroidal component. This process is represented in Figure 1.4, panels a and b.

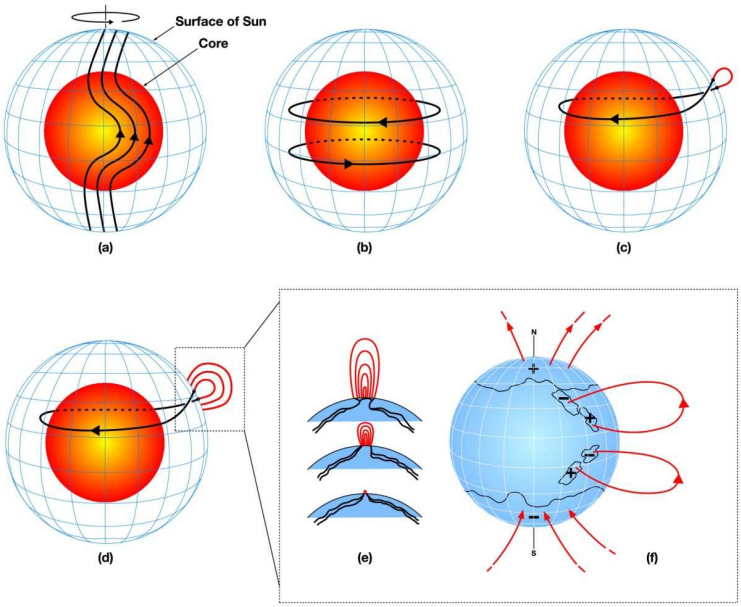

Figure 1.4 – Physical processes in the solar dynamo model described on the text.

Source: http://www.nasa.gov/images/content/144061main_CycleDiagramLG.jpg

When the toroidal field is strong enough, some magnetic loops rise to the surface (first in a large number in latitudes around 40°, and then increasing the occurrence in lower latitudes), twisting as they rise due to rotational influence (Figure 1.4, panels d, e and f). The feet of these magnetic loops block the convective movement occurring on the base of the photosphere, creating cold (~ 2000 K) and black regions on the solar surface, called Sunspots.

During solar flares, the magnetic energy accumulated in the sunspot active regions is converted into other types of energy, like thermal (local plasma heating); mechanical (Coronal Mass Ejections) and kinetic (particle acceleration). While this magnetic energy has been released during solar flares, a meridional magnetic flow carries the superficial magnetic flux towards the poles (Figure 1.5, panel g). Some of this flux is then transported downwards to the bottom of the solar surface and towards the equator, causing the reversion of the main poloidal field (Figure 1.5, panel h). This reversed poloidal flux is then sheared again near the bottom by the differential rotation to produce the new toroidal field opposite in sign to that shown in Figure 1.4, panel b, and all the process is repeated.

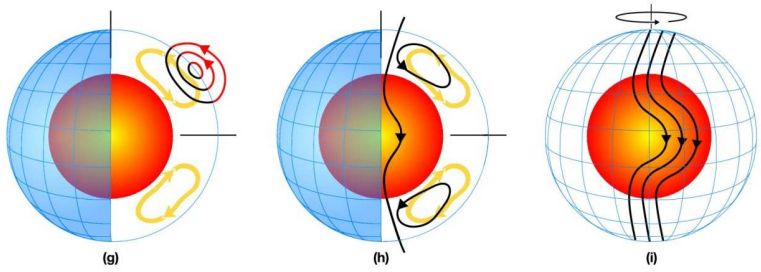

Figure 1.5 – Continuation of the description of the solar dynamo model.

Source: http://www.nasa.gov/images/content/144061main_CycleDiagramLG.jpg

The cyclicity of the solar magnetic phenomena characterizes the solar activity, which is measured by solar indices. The oldest and most famous solar index is the Sunspot number (SSN), that is the counting of sunspot groups and individual sunspots in the visible solar disc. This index presents several

periodicities, and the most evident is the 11-year cycle, called Schwabe cycle or, simply, Solar Cycle. The amplitude of the 11-year Schwabe cycle (which has, in fact, a variable length of 9 to 14 years) varies significatively, modulated for longer periodicities. Behind the Schwabe cycle is the 22-year magnetic polarity cycle, knowing as Hale cycle (HALE et al., 1919). Figure 1.6 shows the evolution of the averaged SSN from 1700 to August 1st, 2010. The black line is an average over one year while the red line is the monthly mean.

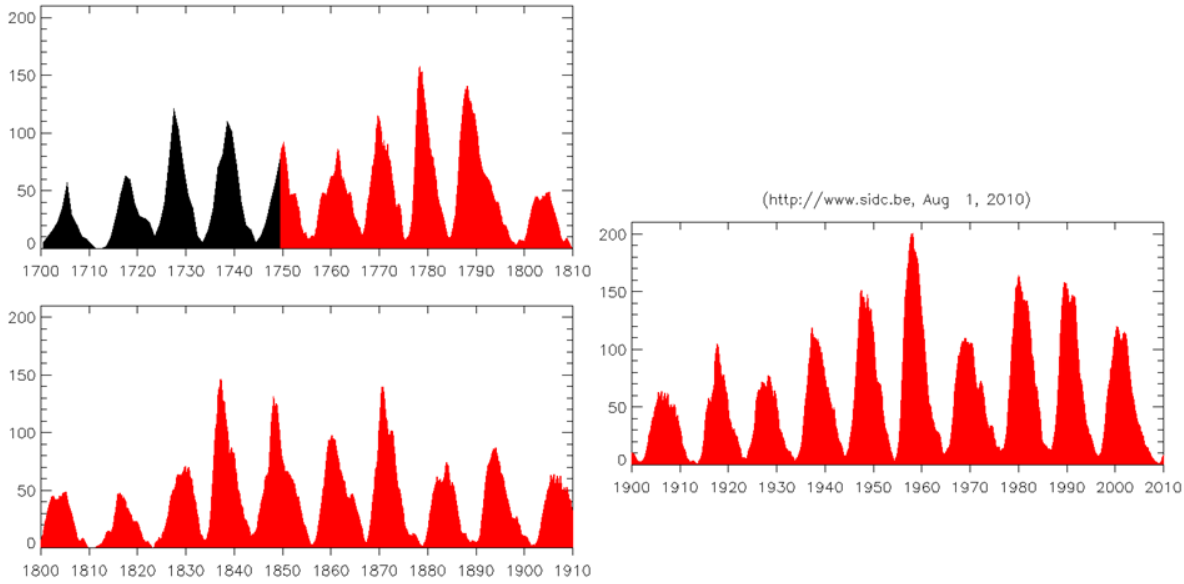

Figure 1.6 – Sunspot numbers (yearly, in black, and monthly, in red).

Source: http://sidc.oma.be/html/wolfaml.html

During periods of solar cycle maximum, the Sun becomes highly active, with a higher occurrence of explosive events related to the active regions (Sunspot regions). Although the number of dark regions in the solar disk increase during the solar activity cycle, the total electromagnetic energy emitted by the Sun integrated over the whole spectrum (the Total Solar Irradiance, IRR) do not decrease, as the common sense could suppose. The IRR varies in phase with the SSN variations due to the presence of bright areas which surround the dark sunspots (called faculae). The combination of the electromagnetic depletion

caused by the dark regions and the electromagnetic enhancement flux caused by the faculae is shown in Figure 1.7.

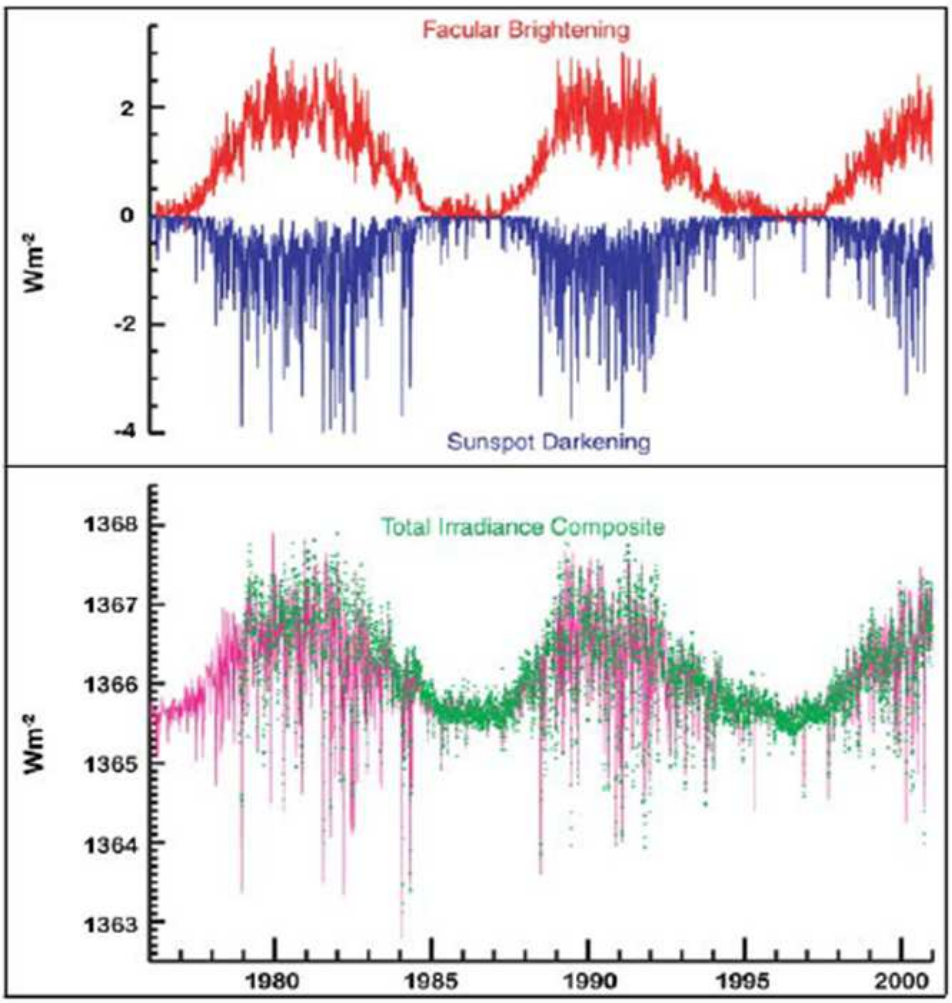

Figure 1.7 – Total Solar Irradiance variations along the solar activity cycle, due to the contribution of dark and bright regions associated to the sunspots.

Source: Lean and Fröhlich (1998)

Furthermore, the cyclic activity of the solar magnetic field also drives the IMF behavior, through the variations in the solar wind flux, making the IMF more intense and irregular during solar maximum. The characteristics found in the interplanetary medium modulate the cosmic ray flux (CR). The cosmic ray flux is composed by energetic particles, mainly protons, originated in different astronomical sources (like stars, supernovas, black holes and active galactic

nuclei) which enter in the Heliosphere interacting with the terrestrial neighborhood (VALDEZ-GALICIA, 2005).

Terrestrial surface measurements of CR flux show a clear 11-year solar cycle anti-correlation, delayed with respect to the sunspot time series (USOSKIN et al. 1998). The time profile of CR flux (measured by three different neutron monitors) is shown in Figure 1.8 (panel b), compared to the sunspot numbers for the same period (panel a).

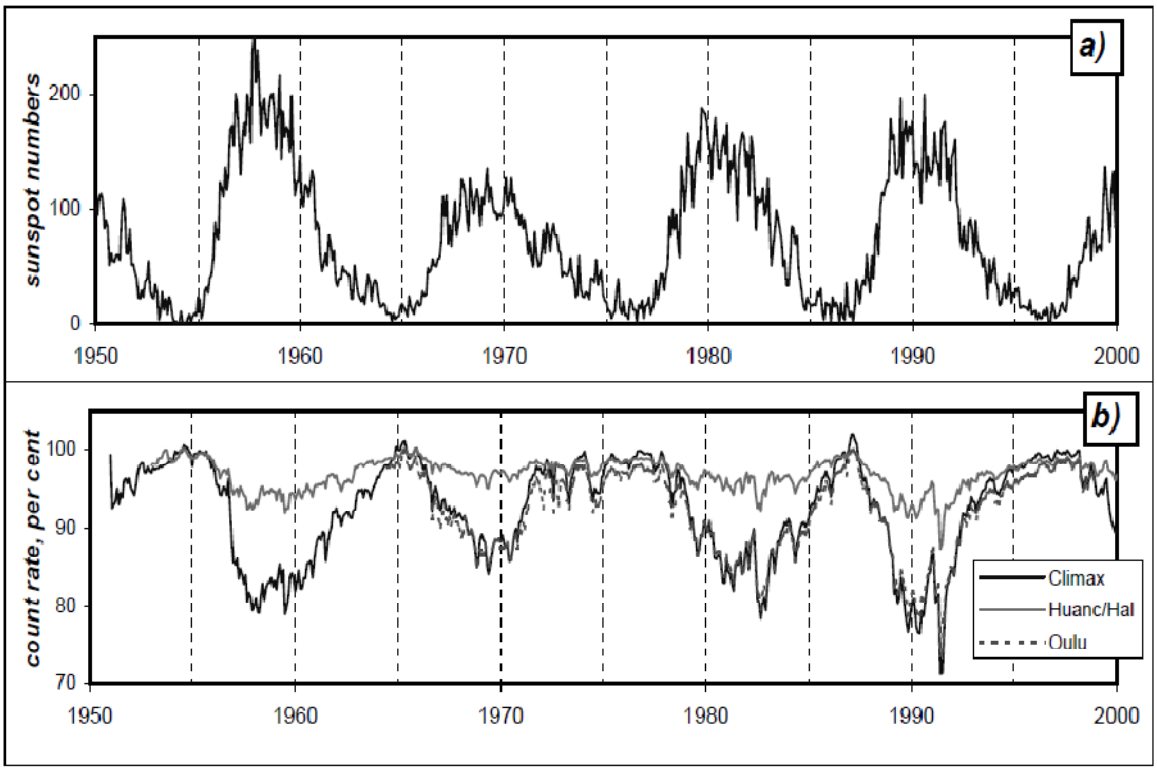

Figure 1.8 – Comparison between the time evolution of Sunspots number (panel a) and cosmic ray flux (panel b), measured by different neutron monitors (100% count rate corresponds to May 1965).

Source: lecture private notes, Usoskin.

Besides the 11-year anti-correlation, some other solar features can be also noted. A Hale cycle is imprinted on CR time series as a modulation of the shape of the cycles (with sharp or flat maxima), and some short-term fluctuations,

related to the solar rotation, flares and CMEs, for example, can also be noted in a high time resolution CR data.

The solar sporadic events (like the solar flares and the CMEs), as well the characteristics of the interplanetary medium (solar wind, IMF and cosmic rays) are modulated by the solar activity cycles, and are able to produce effects in the Earth's environment (BAKER, 2000; USOSKIN, 2004; BAZILEVSKAYA et al. 2000). In the next section, a brief revision of the recent results regarding to this solar modulation imprints over terrestrial climate data will be present.

1.2.2. Effects of solar activity variability on climate

Evidences of the solar activity variability imprints on the terrestrial climate modulations have been found in different natural archives, but such correlations alone are not sufficient to provide a final understanding on the solar forcing on climate change. One of the most famous possible links is related to the Little Ice Age, a cold period registered at the North Hemisphere during the solar activity minimum periods in the late XV century, early XVI (EDDY et al, 1976). The lack of a physical mechanism to explain such link keeps the study of the solar activity – Climate connection a controversial subject even nowadays.

It is important to note that this thesis is not gathering information about Earth's orbital influences on climate (related to the well known Milankovitch Cycles, which changes the total amount and distribution of Sunlight over the terrestrial surface over cycles of thousands of years, 100, 41 and 23, and are associated with the Ice Ages and holocenes). This review is only about the effects of the solar magnetic activity variability on climate.

A huge amount of works have been published in the last years reporting statistical evidences of the solar activity imprints on different climatic parameters (like air and sea surface temperature, different atmospheric layers

characteristics and cloud covering) in all timescales (a good review of those works can be found in Haigh, 2007).

The current scientific knowledge concerning the solar activity imprints on the terrestrial climate points to three major solar phenomena as the possible responsible for this connection: the total solar irradiance, the ultraviolet spectral flux and the CR modulation (caused by the IMF / solar wind variable conditions along the solar cycle). Table 1.3 summarizes the possible routes through which the solar variability may influence the terrestrial climate.

Table1.3 – Solar activity forcings and its climate possible consequences.

Total solar irradiance (IRR)	Direct impact on sea surface temperatures and hydrological cycle.
Solar ultraviolet irradiance (UV)	Heating the upper and middle atmosphere, dynamical coupling down to troposphere. Middle and lower atmosphere chemistry and composition, impacts temperature structure and radiative forcing.
Cosmic Rays modulation (CR)	Ionization of different atmospheric levels, impact on composition, temperature and electric field. Impact on condensation nuclei. Magnetosphere – ionosphere – thermosphere coupling.

Source: modified from Haigh (2007).

The total solar irradiance (IRR, or TSI), that is the integral over the wavelength of the solar radiation flux, has been directly measured since 1979 showing a 11-year cyclic variations (in phase with the sunspot cycle) with amplitude around 0.1% (REID, 2000). This percentage would not be able to produce significant changes in Earth's climate (STOTT et al., 2003), although some evidences of the 11-year solar cycle imprints over climatic data have been found (WHITE et al. 1997). Some recent studies have been developed aiming to reconstruct the past IRR variability and find longer and stronger trends (for example, SOLANKI;

KRIVOVA, 2004). Variations in the order of 0.6% of the IRR could explain abrupt changes in the Earth's temperature, like that ones occurred during the Little Ice Age (LEAN & RIND, 1999).

Some possible mechanisms could be responsible for amplify the small IRR's variability along the solar cycle and produce some climatic responses in the troposphere, like the simultaneous effect in cloud cover caused by CR, changes in the global atmospheric electric circuit, or the coupling between the "top down" mechanism (stratospheric warming caused by UV flux, propagating to the terrestrial surface) and the "bottom up" one (involving the air-sea heat changes, bringing the sea direct heating up to the tropopause) (MEEHL, 2009).

The CR charged particles interaction with the terrestrial atmosphere ionizes its constituents and cause changes on its chemical characteristics. The resulting ionization is able to change the thunderstorm distribution and intensity patterns, producing an 11-year cycle in the electric storms temporal evolution (REID, 2000). Moreover, changes in the ionic concentration around the tropopause height and below can provide an effect on the production rate of the condensation nuclei, creating a relation between solar cycle and cloud cover, which could be more evident in high latitudes (DICKINSON, 1975). An interesting and complete review concerning the possible physical mechanisms linking CR and clouds was recently published by Usoskin and Kovaltsov (2008a). Independent of the linkage physical mechanism between CR flux and terrestrial climate, several empirical evidences have been found and published recently (for example, the better correlation between the surface temperature and the 22-year solar cycle, associated to the CR flux due to the solar polarity inversion period, compared to the correlation found with the 11-year cycle. (MIYAHARA et al. 2008).

Studies relating the ultraviolet spectral flux (UV) variations with the climatic changes are still controversial, since there is no consensus regarding the

physical coupling between stratosphere and troposphere. The UV solar spectrum varies by a few percent along the solar cycle (100 times larger than the IRR variation) and is mostly absorbed in the terrestrial stratosphere by the ozone (O_3) molecules, producing stratospheric heating and driving the balance of ozone in the stratosphere. These effects have been associated (not in a conclusive way) to the changes in the tropospheric winds, which are a controlling parameter of the climate conditions in the Earth's surface (KODERA et al. 1990; HAIGH, 1996, 1999; SHINDELL et al. 1999).

To understand the solar activity and climate changes relationship it is necessary to know the past variation of both phenomena. Therefore, the use of natural proxies of the involved physical processes and their connection becames necessary.

1.2.3. Natural isotopes as tracer of solar activity and climate dynamics

It is well known that the concentration of determined natural isotopes found in the Earth's surface depends on some environmental conditions. This allows paleo-environmental studies using these sensitive tracers as proxies of the past variations occurred in the physical phenomena involved in their modulation. Some isotopes, found in different natural archives, keep the register of the past environmental conditions from decades up to thousands of years, representing an important tool for this kind of paleo-environmental studies. Several works have been published using natural isotopes, both stable and radioactive, as environmental proxies.

Changes of water's isotopic composition occurred during the global hydrological cycle stages are registered in natural archives, providing paleoclimatic information (GAT, 1996). This record can be found, for example, in ice-cores, in biological matrices (like skeletons of plankton and corals), in sediments and in speleotherms (HAIGH, 2007). The record of the variability of the water stable isotopes' concentration measured in ice cores is one of the most detailed and

used information on the past climate conditions, and have been used (individually or combined) as a paleo-thermometer for the oceans and also as a humidity and precipitation rate proxy (EPISTEIN; SHARP, 1963; DANSGAARD, 1964; JOUZEL et al, 1997; VIMEUX et al, 1999, PETIT et al, 1999). Studies using these climatic proxies include several sources of uncertainties, since the cause-consequences phenomena involved in the isotopic fractionation are complex and regional, hindering paleoclimatic and hydrological interpretation (LUZ et al., 2009).

Concerning the radioactive isotopes which are used as proxies of some environmental parameter, one can say that the cosmogenic isotopes plays a central role in this kind of study. Cosmogenic isotopes are created mainly in the atmosphere by the interaction between cosmic rays and the air molecules, and because of that, their production rate is modulated by the CR flux (which is anti-correlated with the solar activity cycles, see section 1.1.1). After their production in the atmosphere, the cosmogenic isotopes arrive in the Earth's surface and are stored in some natural archives, recording the information of the physical processes occurred since their production. Despite the production process of the two most used long-lived cosmogenic radioisotopes (^{14}C and ^{10}Be) are similar, they follow different dynamics in the atmosphere before be stored in the terrestrial surface, imprinting these different atmospheric / climatic information in the natural archive.

After its production in the atmosphere, the cosmogenic carbon-14 (^{14}C) oxidizes and follows the carbon global cycle, being partially dissolved in the oceans and assimilated in the organic cycle of plants and animals. On the other hand, the beryllium-10 (^{10}Be) follows the aerosols dynamics in the atmosphere, which is also climatic dependent. Although these two cosmogenic isotopes registered different climatic information in their variabilities, they also carry the same solar activity information that modulates their production. Using these cosmogenic isotope concentrations measured in tree rings or in ice cores, recent works have

been presented a reconstruction of the past solar activity behavior (USOSKIN et al, 2002; USOSKIN et al, 2004; MIYAHARA et al, 2004; SOLANKI et al, 2004; MUSCHELER et al, 2007). All of these works are based on the following logic: 1) The solar activity cycles (represented by the SSN index) modulates the heliospheric condition (represented by the solar function ϕ, that is a parameter related to the solar open magnetic flux); 2) The heliospheric condition modulates the cosmic ray flux; 3) The cosmic ray flux modulates the cosmogenic isotopic production. Each stage of this logical sequence must be based on a solid physical explanation, which has been studied nowadays (e.g VIEIRA; SOLANKI, 2010). Thus, these cosmogenic isotopes may be used as tracers of climatic changes, of atmospheric dynamics and also of solar activity conditions. All of these paleo-information are mixed into the cosmogenic data measured in the terrestrial surface. To the better use of them as tracers of the processes involved in their modulation, it is necessary to understand the relative importance and the role of all environmental drivers of this variability.

The use of these natural isotopes as a proxy of environmental conditions would help us to understand the terrestrial climate dynamics, as well the behavior of the solar activity in the past, improving the knowledge concerning their link and also the evaluation of relative importance between natural and anthropogenic forcings on the global changes.

1.3. Goal and Outline of the thesis

The research described here is an effort to understand the role of different climatic and solar phenomena in the modulation of certain isotopes found in different natural archives in the terrestrial surface. We have focused on the investigation of the natural drivers of the modulation of hydrogen and beryllium isotopic concentration. Therefore, we have used a database composed by temporal series of the isotopic concentration, solar data and climatic indices. Part of this database was made available online by the responsible scientific groups or through institutional collaboration with our group. The other part was

acquired by our own instrumentation as an experimental stage of this work. The periodical features of these data series were identified and compared through the employment of spectral programs. Moreover, conceptual models were developed and used together with specific numerical models to improve the knowledge of the coupling between the environmental conditions and the isotopic modulation.

After this first chapter, in which the fundamental concepts were introduced, this thesis is divided in three more chapters. In the second chapter, the results obtained with the hydrogen isotopic data are shown, as well as the description of the correspondent analysis. The third chapter gathers the results obtained with the beryllium isotope, including the description of the data acquisition, analysis, methods and models applied in the investigation. In closing, the conclusion and the perspectives are highlighted in the fourth, and last, chapter.

2 HYDROGEN ISOTOPE: δD

Deuterium, ^{2}H or D, is a stable isotope of Hydrogen, with one proton and one neutron in its nucleus. Its atomic mass is 2.014102 u, while the hydrogen's one is 1.007947 u (*u* is the atomic mass unit and is equivalent to $1.66 \cdot 10^{-27}$ kg). The most acceptable theory to explain the natural D formation points to the primordial explosion of the universe, the Big-Bang, as its main source. Evidences of a nonprimordial production of this isotope were found in several astronomical objects, as supernovas (COLGATE, 1974), super-massive stars (HOYLE; FOWLES, 1973) and the Sun (CHUPP et al. 1973). However, the contribution of this nonprimordial abundance in the interstellar medium is not considered significant. This consideration is based mainly on Epstein et al. (1976) study, where several astronomical scenarios were analyzed as potential sources of nonprimordial deuterium. Their results show that, although these objects have an environment capable to synthesize D, they also create a condition able to destroy it, making insignificant the resulting concentration of nonprimordial deuterium available in nature.

On the other hand, measurements of the interstellar D/H ratio indicate a non-homogeneous spatial isotopic distribution, suggesting the existence of some significant non-primordial D sources. Mullan & Linsky (1998) associate this inhomogeneity to the ejection of an important parcel of nonprimordial deuterium synthesized in active stellar atmospheres to the interstellar medium, providing an isotopic enrichment of D in some regions (as measured in the solar wind by Anglin, 1973). The deuterium synthesis in active stars is explained by Mullan & Linsky (1998) as a result of a p-n nuclear reaction, where a high energetic proton (with energy above 6.3 MeV), accelerated during flares, collides with an atmospheric neutron, producing a D nucleus and emitting a γ-ray photon of 2.3 MeV (MULLAN; LINSKY, 1998).

On Earth, the natural abundance of D is represented by the SMOW (Standard Mean Ocean Water) value, which is the typical value of D/H ratio measured in the oceans: $155.95 \cdot 10^{-6}$ (or, expressed in per mill units: 156 ppm) (DEWIT et al. 1980). The available deuterium is linked to oxygen atoms creating a special kind of water molecules, called “heavy-water” (D_2O or HDO, which is the most abundant molecule of heavy-water found in nature). The heavy-water follows the global hydrological cycle, making the D distribution in our planet dependent on the isotopic fractionation occurred in each step of the water-cycle (for example, during the evaporation and condensation processes, or during the mixing of air-masses with different origins) (FRIEDMAN, et al. 1964, JOUZEL, et al. 2005). The fractionation occurs due to the lower values of vapor pressure and freezing point parameters of the molecule HDO compared to the H_2O. These characteristics implies in a higher concentration of D in water during its solid phase compared to the liquid one, and a higher D concentration in liquid phase than the vapor one (FRIEDMAN et al. 1964).

All the information concerned to physical and geophysical processes involved in the isotopic fractionation are registered in natural archives along the time, allowing paleo-environmental studies using deuterium as a sensible tracer of these changes occurred in the past, in different time scales (from inter-annuals to thousands of years) (GAT, 1996)

The parameter used in this kind of studies is the δD, that is expressed in units of δ (ppm, or ‰) and represents the relation between the D/H ratio measured in natural samples (ice-cores, for example) and the D/H standard ratio (SMOW). Equation 2.1 shows this relation:

$$\delta D[‰] = \left[\frac{(D/H)_{SAMPLE}}{(D/H)_{SMOW}} - 1\right] \cdot 10^3 \qquad (2.1)$$

The temporal behavior of the δD parameter is usually associated to changes on the environmental conditions during the rain/snow precipitation on the ice-core sampling sites. Positive δD values mean an enrichment of deuterium relative to the standard values and negative ones indicate a D concentration depletion (GAT, 1996). In continental areas of high and medium latitudes, for example, the δD time profile measured in ice-cores was well correlated to the surface air temperature in the precipitation site (MERLIVAT; JOUZEL, 1979).

To obtain information on the physical conditions at the evaporation site (the source site of the air-masses which results on the sampled ice-core), another parameter was created, called deuterium-excess. This d-excess parameter is resulting of the combination between δD and the simultaneous measurements of oxygen isotope $\delta^{18}O$ in the same ice-core (d-excess (‰)=$\delta D - 8 \cdot \delta^{18}O$), and is related to the humidity and temperature of the air and of the sea surface at the oceanic area involved in the evaporation process (FROEHLICH et al. 2002, MERLIVAT; JOUZEL 1979).

An analysis of the δD time variability of ice-cores from Antarctic and Greenland initiated by Rigozo & Evangelista in 2006 suggested a significant contribution of a solar-cycle type periodicity. According to the current isotopic fractionation models, there is no consistent explanation for that. We considered in this work two possible hypotheses to explain the solar activity signal on δD modulation:

a) The nonprimordial deuterium synthesized in the Sun during solar flares provide the isotopic enrichment of the solar wind, and through its interaction with the terrestrial environment would contribute to the periodical increase of the measured δD, following the solar activity cycle;

b) The 11-year solar cycle would be influencing directly, or indirectly, the isotopic fractionation process, through its impact over the climatic

parameters involved in the global hydrological cycle (see the possible mechanisms in sub-section 1.2.2).

In order to evaluate these hypotheses, improving the knowledge concerning the solar and climate information carried by δD proxy, ***we have made an investigation of the main natural drivers of the δD global features observed in isotopic time series obtained from different geographical latitudes***. In the next section (2.1), the data and methodology employed in this investigation is presented, and the last section of this chapter (2.2) shows the results obtained and the plausible discussions on the δD response on climate and solar variability.

2.1. Data & Methods

We have employed five globally distributed δD time series, derived from ice-cores of 3 different continents: Antarctica (King George Island – KGI at 64°07'S and 58°37'W, Talos Dome – TD at 72°48'S and 159°06'E, and Dronning Maund Land – DML at 75°00S and 00°04'E); South America (Nevado Illimani / Bolivia – ANDES at 16°39'S and 67°47'W); and Greenland - GISP2 at 72°36'N and 38°30'W. Figure 1 depicts the geographical sites covered in this study.

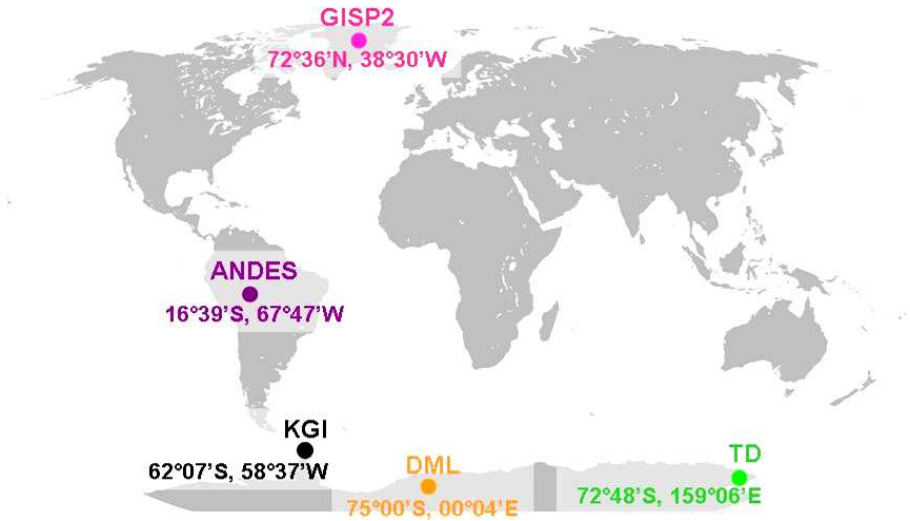

Figure 2.1 – Geographical distribution of the ice cores which provided the annual δD time series employed in this analysis.

The isotopic time series were made available from NOAA Paleoclimatology Program (STENNI et al., 2002) – in the case of TD; EPICA (OERTER et al., 2004) for DML; and GISP2/GRIP (BARLOW, 1999) for Greenland. The Andean time series (Nevado Illimani/Bolivia) was kindly shared by Dr. Françoise Vimeux group (IRD / France). The isotopic data from Antarctic Peninsula (KGI) were extracted from an 49.9 m ice-core sampled in a Lange Glacier, in the Summer of 1995 / 1996, by Brazilian researchers (from NUPAC / UFRGS and LARAMG / UERJ groups) of the Brazilian Antarctic Program (PROANTAR). A complete description of the sampling method and isotopic measurement can be found in Simões et al. (2004) paper.

All of the δD time series have annual resolution and cover the same time range: from 1951 to 1994 (an exception is GISP2 that covered the interval 1941-1984). This time range was defined by the shortest δD time series analyzed here (KGI). Figure 2 shows the δD database.

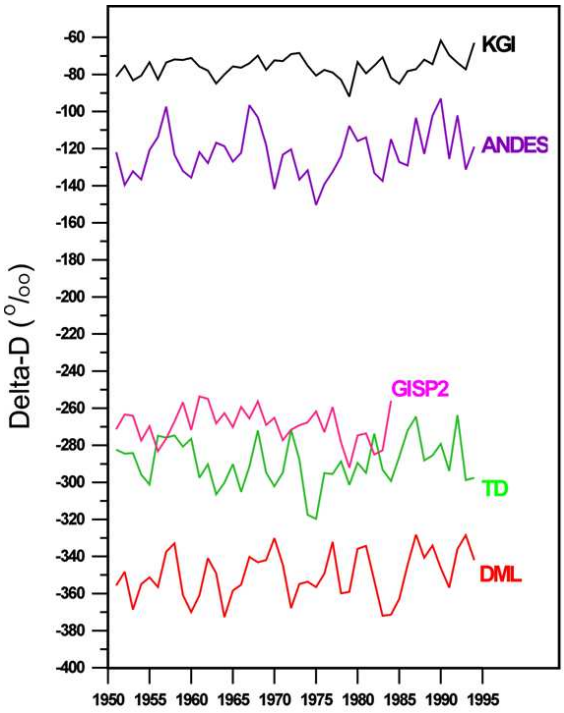

Figure 2.2 – δD database used in this work from five different regions: Greenland (GISP 2), Nevado Illimani (ANDES) and Antarctica (TD, DML and KGI).

Usually, a time series can be decomposed in a trend component, periodic signals and a random residue. In this analysis we focus in the periodic component of the isotopic time series, considering that a detected periodicity in δD time series is a response of some natural related phenomena that occurs at a corresponding periodicity band, within physically acceptable lag intervals. The first step was to retrieve the periodicities of the deuterium database through two spectral methods: the ARIST method (RIGOZO et al., 2005) and Morlet Wavelet analysis – MWA (TORRENCE; COMPO, 1998).

The ARIST method uses a simple sine function with three unknown parameters: β = amplitude, υ = angular frequency and ϕ = phase (WOLBERG, 1967; RIGOZO; NORDEMANN, 1998; RIGOZO et al. 2005). The starting point of the method is the definition of the so-called conditional function $F = Y - \beta sin(\upsilon t + \phi)$ where $\underline{Y}$ is the original signal (time series), $\underline{t}$ is time and $\underline{\beta}$, $\underline{\upsilon}$ and $\underline{\phi}$ are the three parameters to be determined. One of the main advantages of this method is that it gives the standard deviation of every determined parameter. This allows a selection of the most representative important amplitude/deviation ratio. That is, when amplitude is higher than two standard deviations of amplitude.

The MWA is recognized as an adequate technique to detect rapid changes of patterns and cyclicities even in non-stationary signals. The MWA consists of a plane wave modulated by a Gaussian function and can be used for analyzing localized variations of power within a time series at many different frequencies. For the wavelet spectrum, we estimate the significance level for each scale using only values in the domain of the 95% significance level (TORRENCE; COMPO, 1998).

We have considered all the δD time series described here as a sum of simple oscillating functions (Equation 2.2):

$$(\delta D)_i = \sum_k f(\Delta T_k)_i \qquad (2.2)$$

where, *i* denotes a specific δD station (KGI, TD, DML, ANDES or GISP2) and $f(\Delta T_k)$ corresponds to the sinusoidal function, *f*. Each sinusoidal function was characterized by the k-th periodicity (ΔT_k) found by ARIST method (the value of k varies according to the δD station).

Once those spectral methods verified the existence of a possible solar activity component in the δD database (as one can see in the next section), we started the investigation of the hypotheses a and b postulated in the previous subsection.

In order to test the hypothesis a (related to the transport, by the solar wind, of the D atoms synthesized during solar flares to the terrestrial environment), it was done a rough estimative of the flux of the nonprimordial D arriving in Earth along the solar cycle, and then a comparison with the δD modulation observed in the five selected ice-cores.

This estimative was based on Mullan and Linsky (1998) work that presented the following linear relation between the number of nonprimordial deuterium atoms (D_{np}) produced during solar flares and the total energy released by this flare (E_{flare}):

$$D_{np}\,[\text{nuclei/m}^2] = 0{,}3 * E_{flare}\,[\text{erg/m}^2] \qquad (2.3)$$

The E_{flare} value was defined as a product between the number of solar flares able to accelerate protons to energies up to 6.3 MeV (and so, able to create D_{np} nuclei), the typical energy and duration of this kind of flare (type X, according to the GOES classification, with energy ~ 10^{-4} W/m² in the range 1 – 8 Å, and duration ~ 10 min). Due to the fact that the X-ray flux is measured near-Earth

(by the GOES satellite), it was necessary to apply a distance correction, considering an isotropic distribution from the Sun to the Earth (applying the $4\pi(1AU)^2$ factor, where AU is the Astronomical Unit, or the mean Sun-Earth distance). The number of flares used in this calculation was obtained from the solar activity reports available in NOAA webpage (www.sec.noaa.gov).

Assuming that 100% of the D_{np} atoms created by the solar flare was ejected to the interplanetary medium, it was possible to estimate the parcel of them able to reach the Earth ($\%D_{np}$):

$$\%D_{np} = D_{np} * \pi R_{\oplus}^2 \tag{2.4}$$

where $\pi R_{\oplus}^2$ is the Earth's cross section and $R_{\oplus}$ = 6400 km.

To illustrate this estimation, let's calculate an example. Assuming that all of the solar flares type X occurred in 1989 (60 flares) have a peak flux of 10^{-4} W/m², the total energy released in this year by these flares is

$$E_{flare} = 10^{-4}\left[\frac{J}{s \cdot m^2}\right] \cdot (10 \cdot 60)[s] \cdot 60 = 3{,}6\left[\frac{J}{m^2}\right] = 3{,}6 \cdot 10^7\left[\frac{erg}{m^2}\right] \tag{2.5}$$

And, according to our conceptual rough model, the portion of the nonprimordial D synthesized by these 60 solar flares in 1989 would be:

$$\%D_{np} = \frac{3{,}6 \cdot 10^7 \cdot (4\pi(1AU)^2)}{(4\pi(1AU)^2)} \cdot (\pi R_{\oplus}^2) \cdot 0{,}3 \cong 1{,}4 \cdot 10^{21}[nuclei] \tag{2.6}$$

Thus, a time series of a number of nonprimordial D nuclei produced by solar flares arriving at the Earth along the solar cycle was found. This $\%D_{np}$ time series and the discussion of its relation with the δD time series are presented in the next section.

In order to test the hypothesis b (related to the impact of the solar activity cycle on the climatic parameters involved in the isotopic fractionation), we compared the modulation patterns of the δD time series with the spectral feature present on solar and climate parameters considered important to create global impacts on the hydrological cycle. Thus, we have used a database composed by the Global Air Surface Temperature (GAST, available at data.giss.nasa.gov/gistemp/), Planetary Energy Imbalance (PEI: HANSEN et al., 2005), Global Sea Surface Temperature (SST), Southern Oscillation Index (SOI: www.bom.gov.au/climate/current/soihtm) and Total Solar Irradiance (IRR: LEAN et al., 1995), as representative of changes in the incoming solar radiation during different periods of solar activity cycles. Other mechanisms of solar activity and climate changes linkage were not tested in this work due to the lack of know-how and enhancement of associated difficulty (for example, related to the need of theoretical 3-D models concerning the oceans and atmosphere dynamics and coupling).

The PEI parameter represents the difference between the incoming solar irradiance and the outgoing long-wave terrestrial radiation. PEI data were included in the study since there are consistent evidences that link it to the global ocean temperature conditions. Accurate measurements of the ocean heat content over the last 10 years indicate that Earth is absorbing 0.85 ± 0.15 watts per square meter more than it is emitting to the outer space (HANSEN et. al., 2005). For the period from 1948 and 1998, Levitus et al. (2000) demonstrated that most of the global energy imbalance is actually driven by the heating of the ocean. These estimates are consistent with the above findings by Hansen. Since PEI parameter definition considers the ocean energy output, which is mainly converted to the evaporation mechanism, it is plausible to accept that fractioning of stable isotopes of oxygen and hydrogen would respond to PEI trends and variabilities. GAST and SST time series were used

since they are basic parameters in the isotopic fractionation and are associated to evaporation and precipitation processes.

A theoretical approach concerning the teleconnections between ENSO and the Antarctic border climatology was proposed by Liu et al. (2002). Their model suggests a mechanism that links the ENSO variability to the regional Ferrel atmospheric cell, resulting in meridional eddy heat flux divergence and convergence. During strong El Niño events, positive anomalous SST in the tropical Pacific enhances the tropical convection and meridional thermal gradient from the equator polewards in through the Pacific sea. Meanwhile, a high-pressure system at the Bellingshausen Sea (Antarctic Peninsula) creates a regional circulation that brings warm air to the polar region (YUAN, 2004). Considering the potential teleconnectiveness of ENSO phenomena through the transport of heat and water vapor between the tropics and the Antarctic region, we have considered an ENSO derived index, in this case the SOI. Figure 2.3 shows the solar / climatic database used in this analysis' stage.

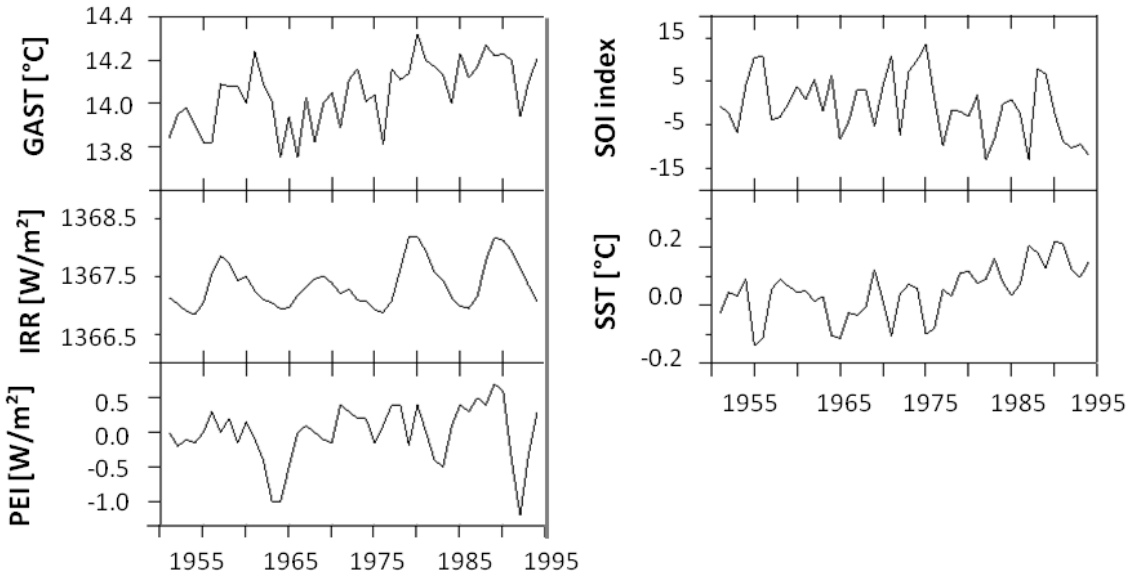

Figure 2.3 – Solar irradiance and climate database used in this analysis.

The same spectral decomposition method was applied to the solar-climatic parameters (PEI, IRR, GAST, SST or SOI) obtaining their sinusoidal functions (see equation 2.2). The correlation level between the isotopic, solar and climatic time series, as well as between their periodicities, was obtained through the use of the traditional bivariate Pearson's coefficient. It allowed us to write the δD time series as a function of the environmental periodicities. Therefore, a linear regression was applied between each sinusoidal function, of i-th periodicity detected, simultaneously, in the isotopic time series and in any of the solar-climatic parameters. Thus, each periodical component found at the δD time series was written as:

$$f(\Delta T_k)_i = \sum_j \left((\alpha_k)_j + (\beta_k)_j \cdot g(\Delta T_k)_j \right) \tag{2.7}$$

Where, $g(\underline{\Delta T_k})_j$ is a sinusoidal component with the n-th period interval ($\underline{\Delta T_k}$) from the decomposition of the *j* environmental parameter (PEI, IRR, GAST, SST or SOI). $(\alpha k)_j$ and $(\beta k)_j$ are the linear and angular coefficients of the $f(\underline{\Delta T_k})_i$ *versus* $g(\underline{\Delta T_k})_j$ correlation, respectively.

However, the correlation coefficients alone do not allow the study of the details of the relationships between the series. For instance, it does not properly consider the possible phase difference between the series, neither does it take into account possible strengthening or weakening of the coherence. Due to this fact, we have applied the Morlet wavelet coherence between each time series to compare the spectral features found at the database.

The wavelet coherence is defined as the normalized wavelet cross-spectrum (TORRENCE; COMPO, 1998; GRINSTED et al. 2004) and determines both the absolute magnitude, defined between 0 (no coherence) and 1 (100% coherence), and the phase shift between the series, as a function of the frequency/time scale and time. The wavelet coherence can be regarded as

localization of the correlation in the time and frequency domains, and reveals the locations in both time and frequency where the coherence is higher.

The results obtained with the methods described above, as well as the associated discussions, are present in the next subsection.

2.2. On the δD response on climate and solar variations

Each location on Earth exhibits specific climatic and geographic characteristics that result in fractionation processes, which are reflected in the water isotopic composition of precipitated snow. This fact is evidenced in Figure 2.2 that shows a great difference of δD values from sites of polar climatology as GISP2, TD and DML and others of tropical Andean, Illimani, and sub-Antarctic (low altitude), KGI, characteristics.

According to Merlivat and Jouzel (1979) and Fröhlich et al. (2002), $\delta^{18}O$ and δD values from sites at moderate and high latitude continental regions are associated to local surface air temperature during the period of precipitation, while the deuterium excess (or d-excess) is related to the physical conditions of the oceanic source area of the precipitation (such as humidity, air temperature and sea surface temperature). Specifically, the northern part of the Antarctic Peninsula is under the direct influence of several synoptic-to-meso scales air mass systems derived from South America, the South Pacific and the Austral Circumpolar oceans. Further, King George Island (KGI) in the South Shetlands, is under the mean position of the Antarctic atmospheric front and near the winter limit of sea ice extension. Due to the constant influence of these systems, the region exhibits rapid variations in air temperature (VAUGHAN, 2003; FERRON et al., 2004). Taking into account the global stable isotope model proposed by the Global Network for Isotopes in Precipitation (GNIP) programme (ARAGUÁS-ARAGUÁS et al., 2000), there is a high similarity between the mean δD at KGI and the South American one - enclosing all the Andean

cordillera from the Northern Patagonia to the subtropics. From δD iso-ratios structure of GNIP, it is clear the great difference of δD values in the eastern and western parts of the Antarctic Peninsula, which results from the two different climatic regimes (VAUGHAN, 2003; VAN DEN BROEKE et al., 2004).

To search the main periodicities in the isotopic database, we have applied the spectral methods described in section 2.2 which results are shown in the following figures. Figure 2.4 shows the amplitude spectra of δD, solar and climatic time series as determined by the ARIST method, while Figure 2.5 depicts the wavelet results, showing the periods of time when the periodic signals were better evidenced or not.

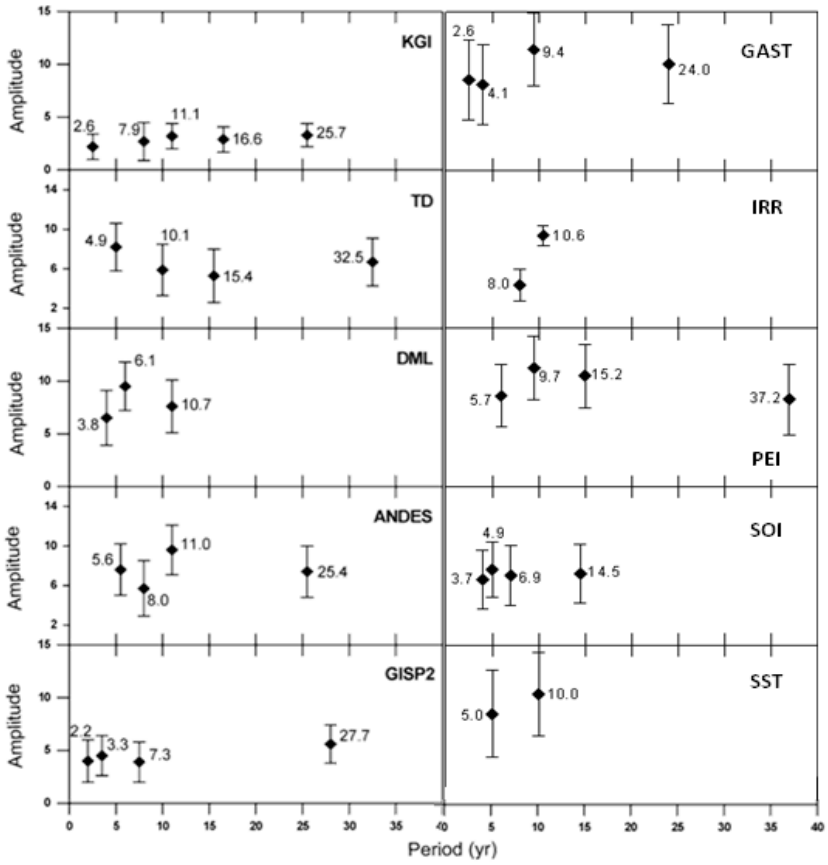

Figure 2.4 – Main periodicities detected at the time series by the ARIST spectral method.

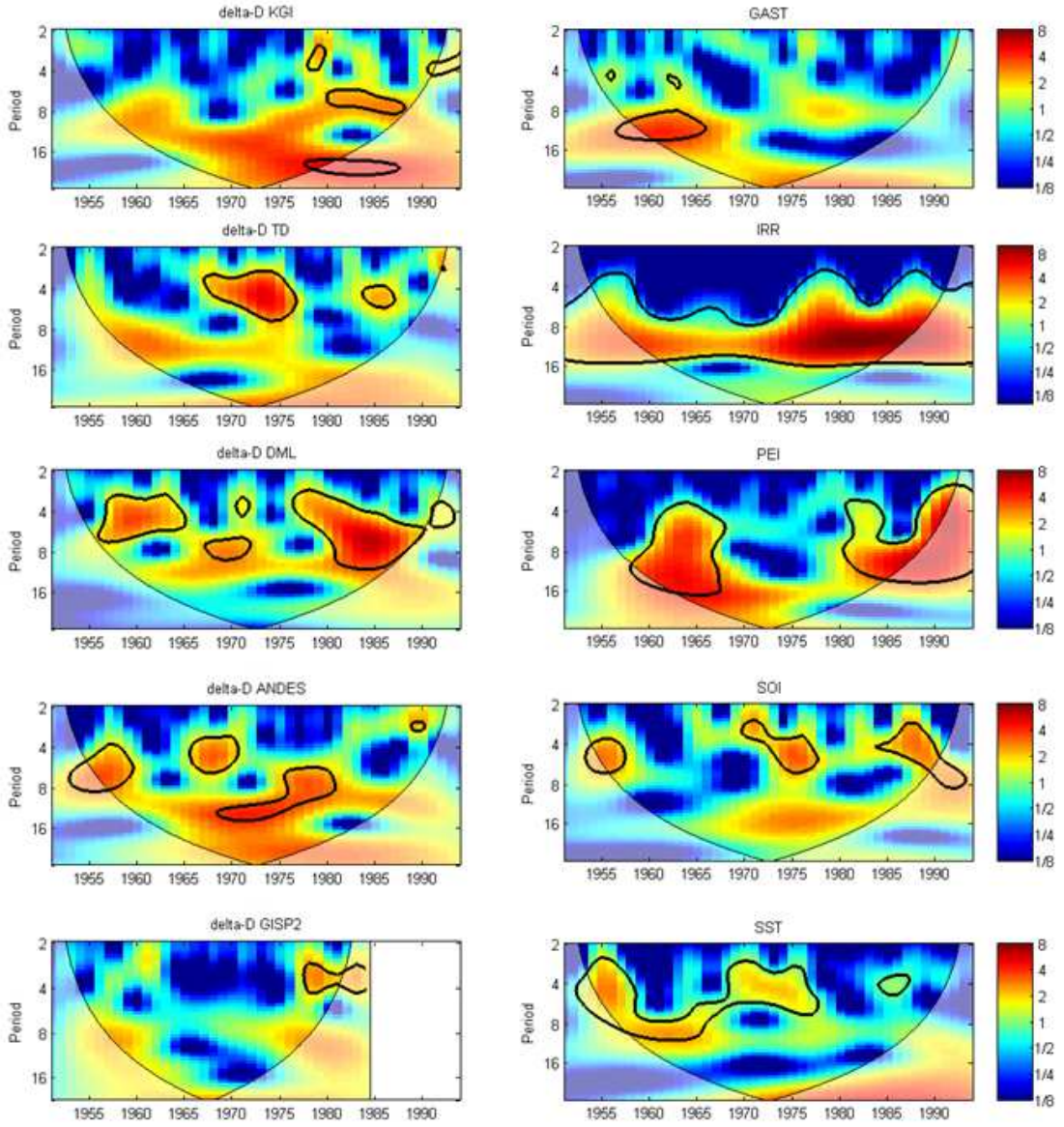

Figure 2.5 – Spectral features detected at the time series by the wavelet method.

For most of the climatic time series, the semi decadal and decadal periodicities predominated (in PEI, a multi-decadal component was also detected). Because of the limited time covering of the data used in this study (44 years), it was not possible to identify long term periodicities within significant level. This limitation can be noted at the analysis of the IRR time series, in which we just found the solar activity periodicities of 8 and 11 years, while it is well known the existence

of longer modulations (like the Hale cycle - 22yr; Gleissberg cycle: 80–90 years; and Suess cycle: 180–200 years).

This decadal periodical band was, obviously, also found in the time series of the nonprimordial deuterium. Figure 2.6 shows the obtained time series of nonprimordial deuterium produced by solar flares and its spectral features found by the wavelet analysis.

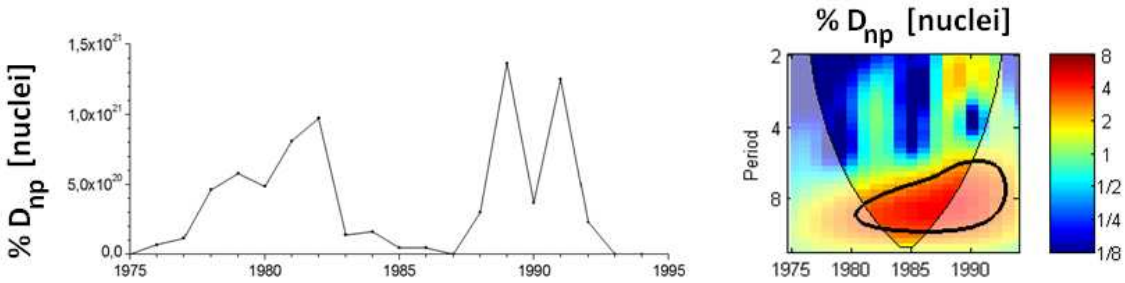

Figure 2.6 – Estimative of the nonprimordial deuterium number arriving the Earth and its spectral features.

The differences and similarities in the set of periodicities among the investigated sites can be interpreted as an indication of globally or regionally specific influences acting on the isotopic fractionation exhibited in the results. A first step as an attempt to better understand the influence of climatic-solar parameters on δD modulation is to search for similar periodicities in related environmental parameters.

To compare the spectral features found at isotopic modulation and its possible drivers, we have applied the Morlet wavelet coherence between each δD time series and our solar / climate / $\%D_{np}$ database (Figures 2.7 to 2.11).

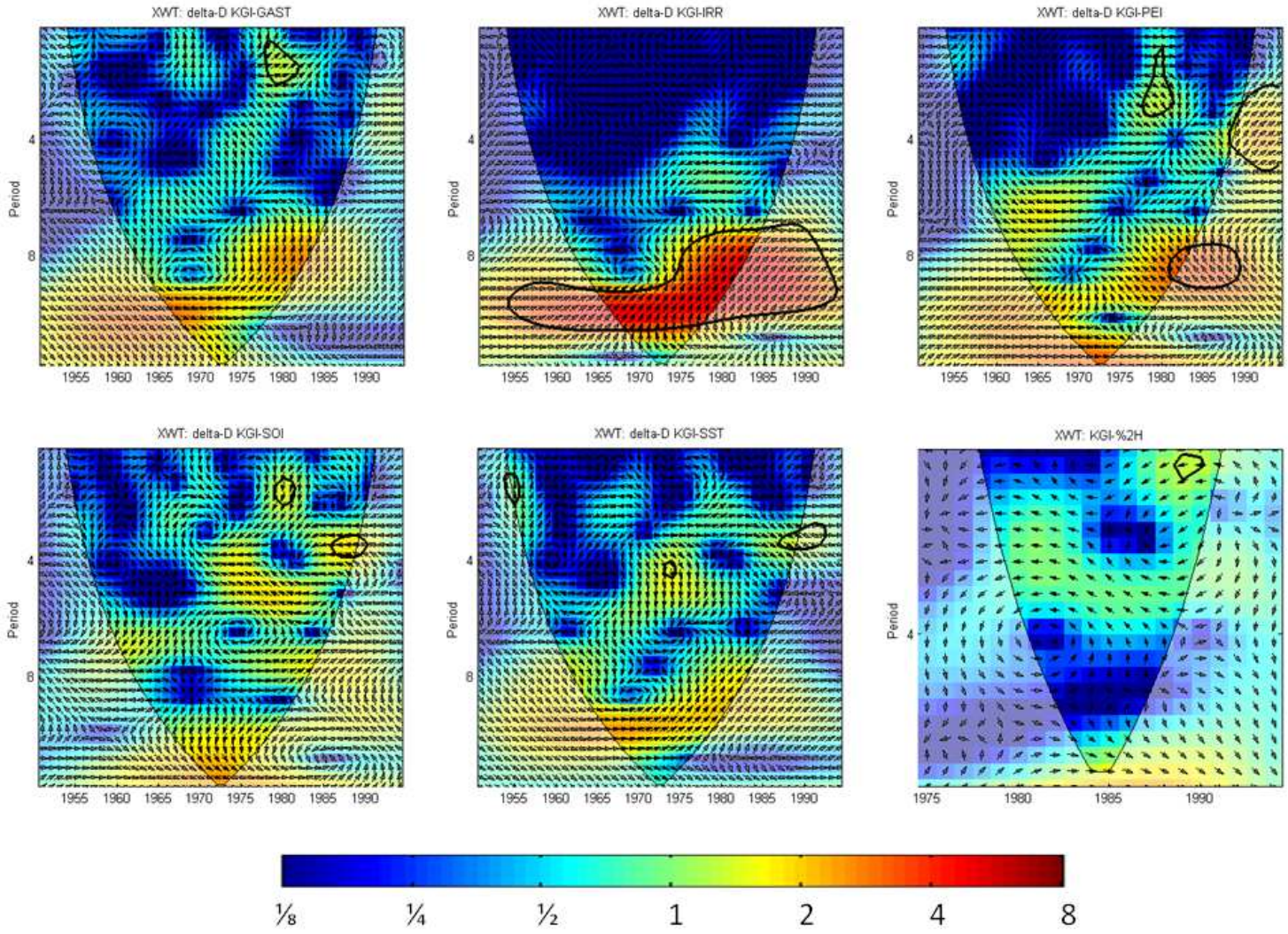

Figure 2.7 – Wavelet coherence between the δD time series from KGI and the IRR / climate / $\%D_{np}$ time series.

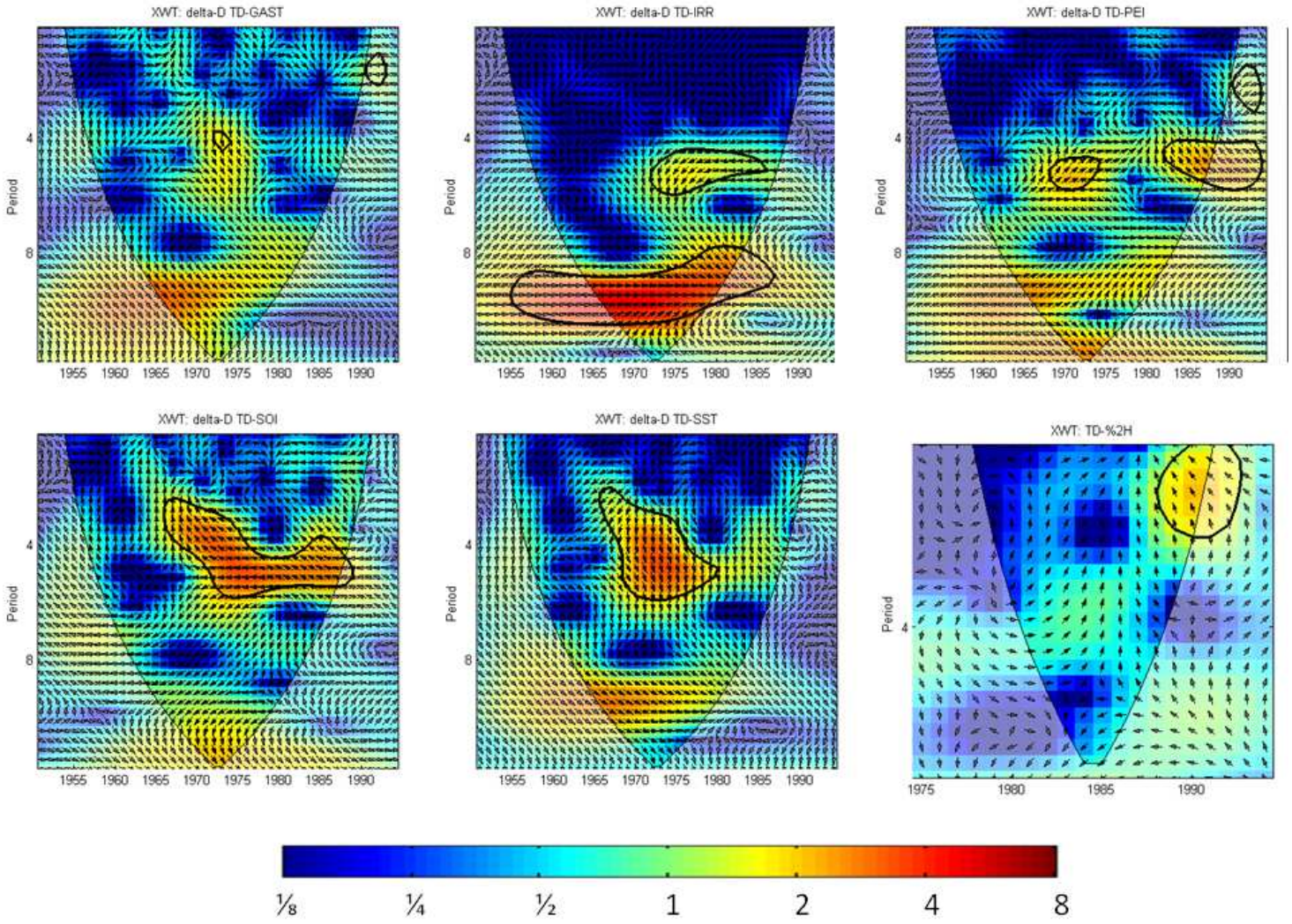

Figure 2.8 – Similar to Figure 2.7 but for δD from TD site.

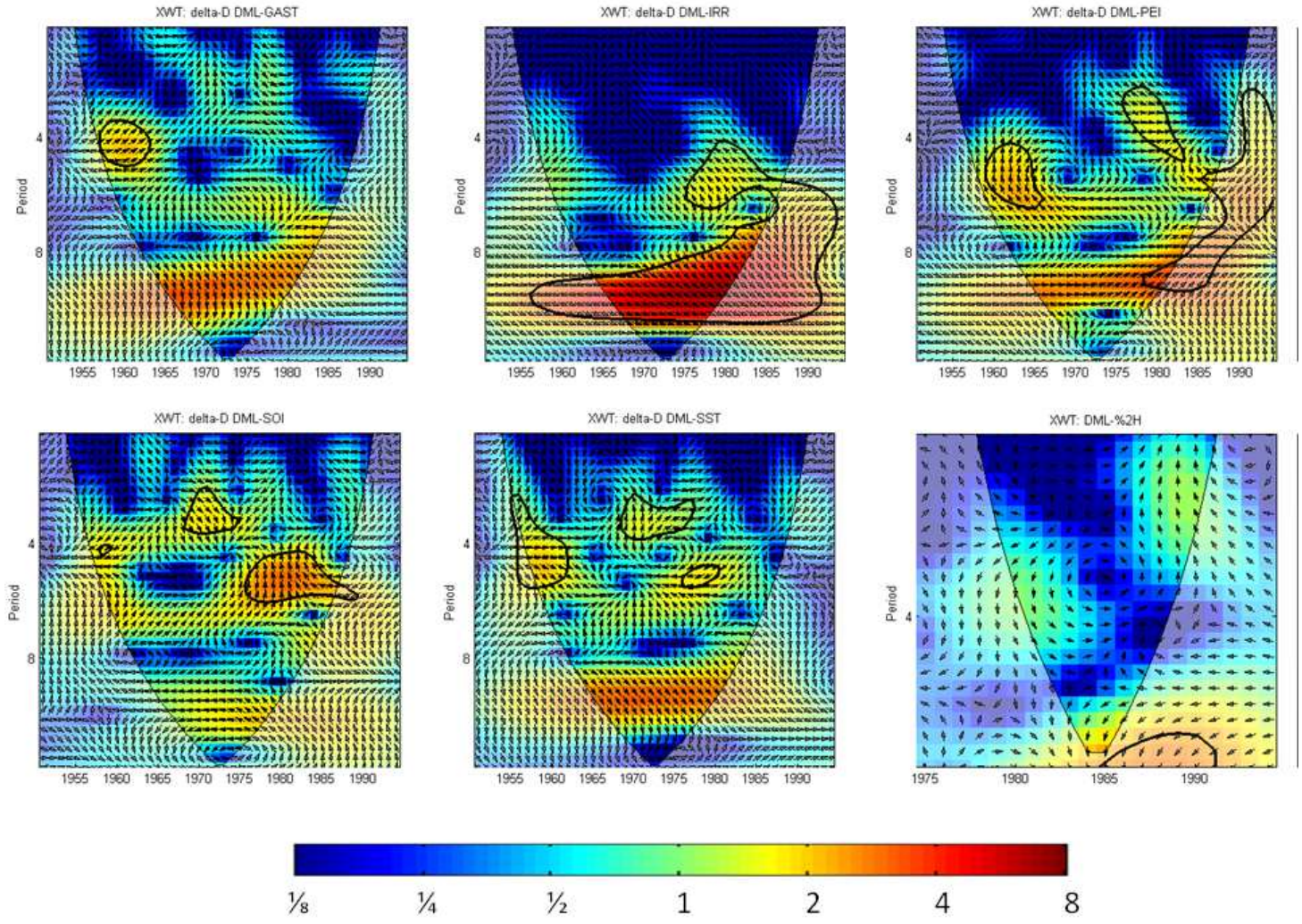

Figure 2.9 – Similar to Figure 2.7 but for δD from DML site.

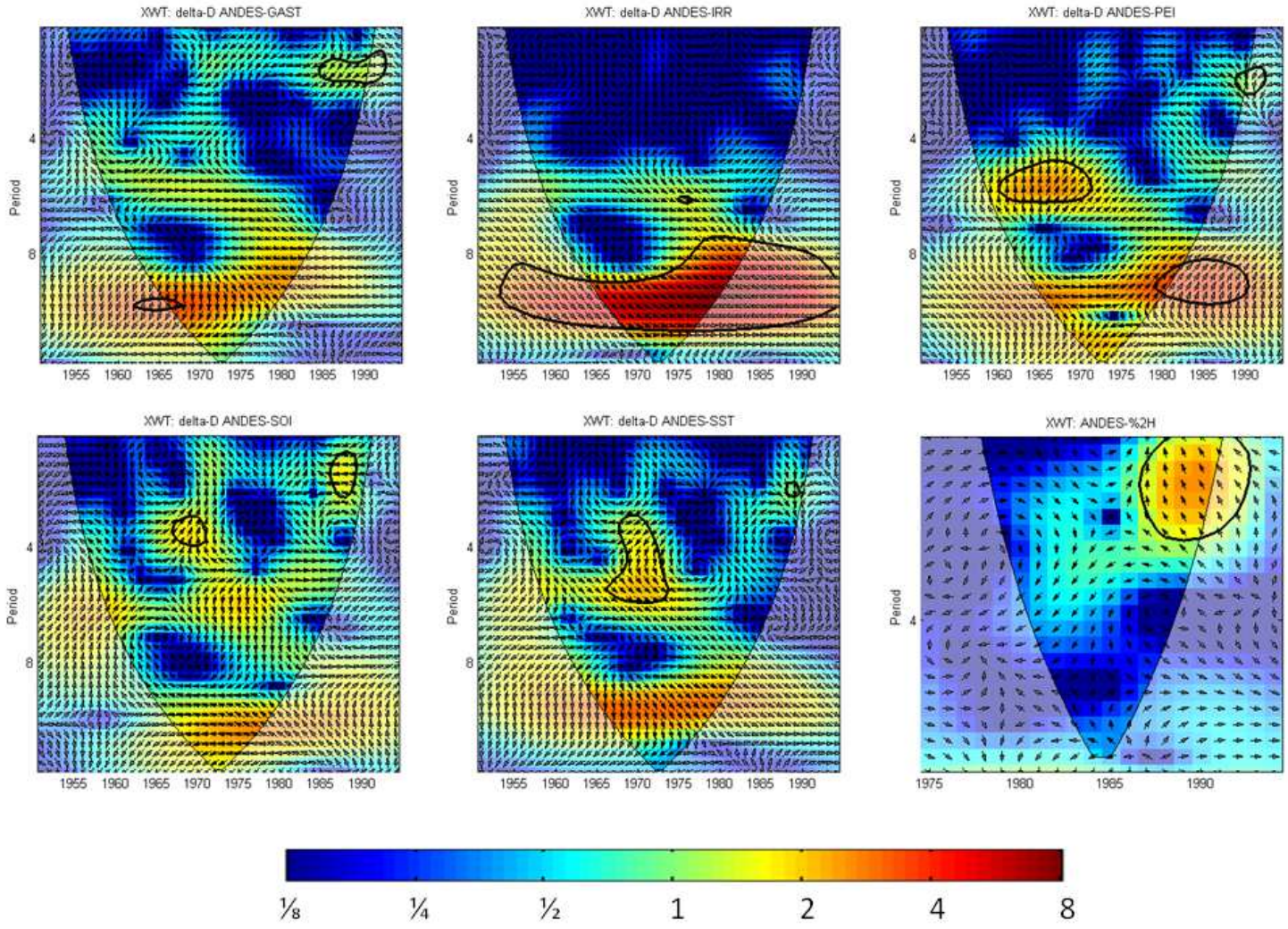

Figure 2.10 – Similar to Figure 2.7 but for δD from ANDES site.

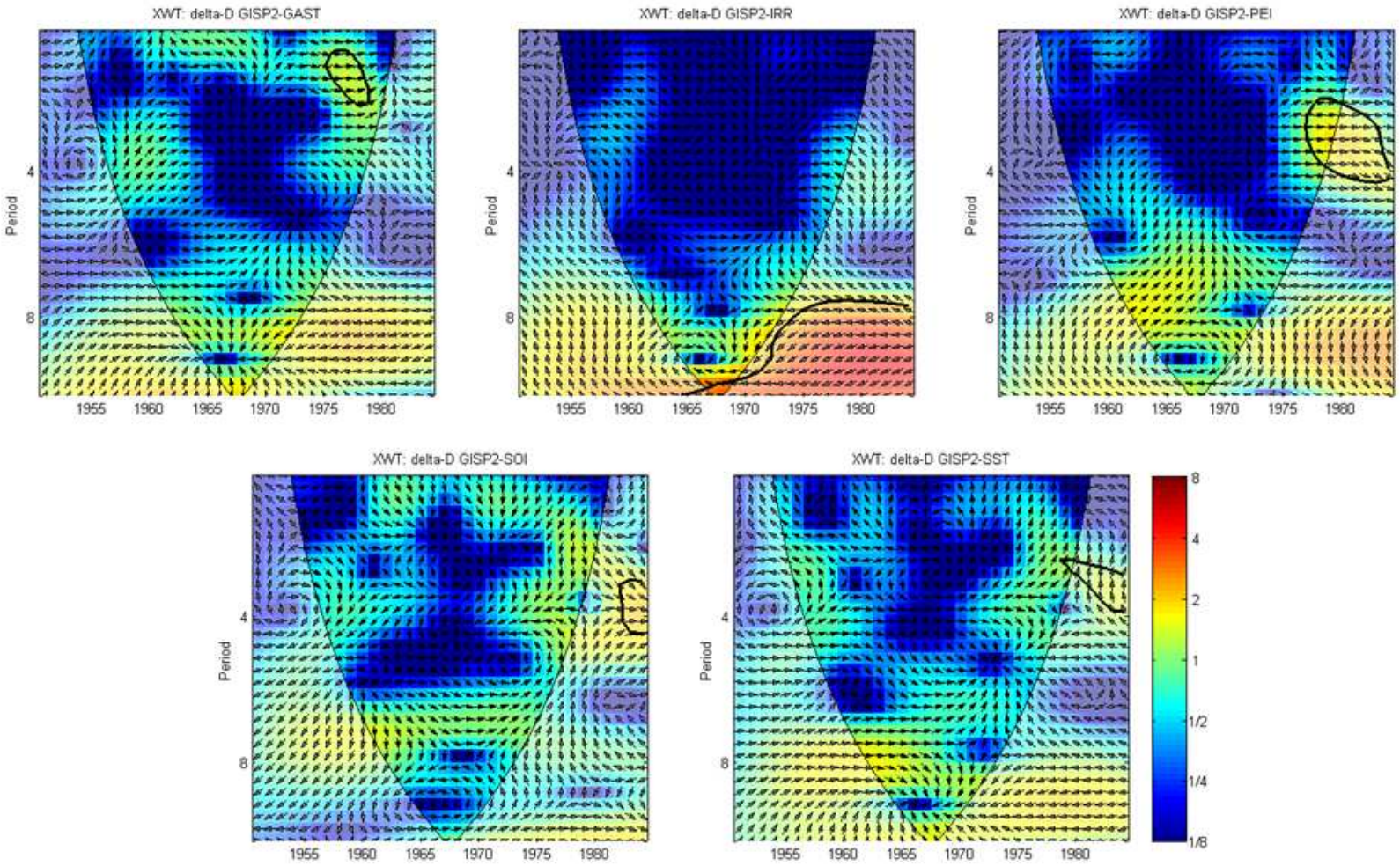

Figure 2.11 – Similar to Figure 2.7 but for δD from GISP2 site (due to the limited time covering, there is no significant coherence map between δD and $\%D_{np}$ in this case.

The colors represent the magnitude of the coherence (from blue: 0 to red: 1). Regions with highly significant coherence (>95%) are bounded by the solid black lines. The local phase between the δD and drivers series is depicted by arrows (→: the driver series at a given frequency and time is in phase with the isotopic one; ↓: driver is leading by a quarter of the period; ← : they are an anti-phase; ↑: driver is lagging by a quarter of the period).

It is interesting to note that the decadal periodicities of the δD time series have a strong coherence with Schwabe IRR cycle, while the possible modulation caused by the input of nonprimordial deuterium nucleons does not seem strong enough. Due to the limited time coverage, this suggestion is not conclusive. For the recent δD time series studied here, the decadal coherence with Schwabe solar cycle impressed in the IRR data is evidently stronger than the coherence with D_{np}, making the hypothesis 2 more reliable. Moreover, the time lags between the IRR and δD series, indicated by the arrows, are smaller than 2 years, which is an acceptable uncertainty for ice-cores studies.

The semi-decadal periodic patterns found at isotopic time series presents coherence with the climatic parameters, although for all of the isotopic time series studied in this work, this coherence with climatic time series were much weaker than that found with solar data. This can be interpreted as the globally distributed dominant solar irradiance influence over the surface of oceans, acting on δD fractioning along the water cycle.

To take into account the relative importance of the solar-climate parameters over the δD modulation, a cross-correlation between the isotopic oscillatory signals and corresponding ones, detected on the environmental time series, were performed. Table 1 summarizes the r-Pearson correlation coefficients obtained in the study.

Table 2.1 - Correlation coefficients R-Pearson for common frequency signals extracted from δD and environmental parameters. Statistically significant values are in bold (P>0.05).

	Periods [yr]	δD of ANDES	δD of DML	δD of GISP2	δD of KGI	δD of TD
GAST	3	--	--	0.10	**0.63**	--
	4	0.04	**0.50**	--	--	0.06
	10	0.10	**0.35**	--	**0.39**	**0.73**
IRR	24	0.04	--	0.30	**0.72**	--
	8 + 11	**0.79**	**0.87**	**0.46**	**0.76**	**0.83**
PEI	6	**0.51**	--	--	--	0.14
	10	**0.46**	**0.66**	--	0.10	**0.72**
	15	--	--	--	**0.73**	**0.95**
	37	--	--	--	--	0.06
SOI	4	--	0.24	0.06	0.001	--
	5	0.10	--	--	--	**0.96**
	7	--	**0.32**	**0.76**	--	--
	15	--	--	--	**0.72**	**0.78**
SST	5	0.02	0.02	--	--	0.30
	10	0.14	**0.45**	--	**0.71**	**0.74**

We have found several significant values of r-Pearson coefficients, which are somewhat evidence that the decomposed analysis can reflect the multiple modulations of the selected parameters over the δD decomposed periodic signals. We have found a large difference while using the correlation between the oscillatory signals in spite of the original time series (which has initially provided coefficients of low values). For example, in the IRR case, coefficients obtained in the original time series were 0.1 for δD of Andes, 0.3 for δD of DML, -0.1 for δD of KGI and 0.1 for δD of TD. On the other hand, coefficients using the decomposed signal of 8+11 years were 0.79, 0.87, 0.46, 0.76 and 0.83, respectively. This occurs because of two factors: (1) the complex nature of the stable isotope time series, especially at sites where there is a constant influence of several synoptic systems as well as high marine and sea ice variability influences such as at KGI or TD; (2) the ability of ARIST method to retrieve the oscillatory signals from those time series.

Considering the time series reconstruction from linear regressions of the oscillatory signals, we restricted the k regressions used in the multiple regression equation (eq. 3) to those that: (1) provided statistically significant r-Pearson coefficients by applying a two-sided t-Student test (P > 0.05), for n=44; (2) linear regressions were tested for different time lags, since the δD response, with respect to a related solar or climatic parameter, would be time lagged considering that the Earth's climate system has considerable thermal Inertia (HANSEN et al., 2005).

Therefore, only the coefficients associated to time lags equal or lower than 2 years were considered. Significant r-Pearson coefficients are indicated in bold font in Table 2.1, which allowed us to interpret the isotopic modulation at each study site from the following parameterization:

$$\delta D'_{DML} = (0.46 + 11.9 \cdot \mathrm{IRR}_{11+8} + 16.4 \cdot \mathrm{PEI}_9 + 33.3 \cdot \mathrm{GAST}_9 + 60.7 \cdot \mathrm{SST}_{10} + 0.88 \cdot \mathrm{SOI}_6 + 60.3 \cdot \mathrm{GAST}_4) - 349{,}8 \quad (2.8)$$

$$\delta D'_{GISP2} = (0.03 + 0.88 \cdot \mathrm{SOI}_6 - 3.55 \cdot \mathrm{IRR}_{11+8}) - 268.98 \quad (2.9)$$

$$\delta D'_{ANDES} = (-0.08 + 18.27 \cdot \mathrm{PEI}_9 + 17.57.55 \cdot \mathrm{IRR}_{11+8} + 17.43 \cdot \mathrm{PEI}_6) - 122.38 \quad (2.10)$$

$$D'_{RG} = (0.30 - 38.04 \cdot \mathrm{GAST}_{24} + 7.75 \cdot \mathrm{PEI}_{15} + 0.57 \cdot \mathrm{SOI}_{14} + 16.33 \cdot \mathrm{GAST}_9 + 6.36 \cdot \mathrm{IRR}_{11+8} + 59.23 \cdot \mathrm{SST}_{10} + 24.61 \cdot \mathrm{GAST}_2) - 75.90 \quad (2.11)$$

$$D'_{TD} = (0.43 + 1.12 \cdot \mathrm{SOI}_{15} + 8.13 \cdot \mathrm{PEI}_{15} + 13.90 \cdot \mathrm{PEI}_9 + 55.06 \cdot \mathrm{GAST}_9 + 8.77 \cdot \mathrm{IRR}_{11+8} + 78.00 \cdot \mathrm{SST}_{10} - 2.03 \cdot \mathrm{SOI}_5) - 289.41 \quad (2.12)$$

A notorious aspect raised from the comparison of the results obtained for the three continental sites: the different number of parameters employed to build up

the reconstruction model. In Antarctica (with 2 δD drilling sites at the western sector), apparently all environmental selected parameters exhibited an “oscillatory imprint” over δD time series, while Andes and Greenland were represented only by 2 parameters. This means that along the decades of 1950 to 1990, at the Antarctic coastal region, the influence of the sea surface and air temperatures, solar modulation and ENSO phenomena were well recognized.

According to Turner et al. (2005) the Antarctic Peninsula could be strongest influenced by ENSO, with a Rossby wave train often extending towards the Bellingshausen Sea from the tropical Pacific mainly during strong El Niño events. In recent decades, these events have been more frequent and of greater intensity, rising the possibility that tropical forcing may have played a role in some of the climatic changes observed in the Antarctic Peninsula. Climatic data from the western Antarctica pointed out to considerable environmental changes of accumulation rate (OHMURA et al., 1996), air temperature (CHAPMAN; WALSH, 2007) and sea ice variability, since satellite images were available. In contrast, from spatially distributed Antarctic meteorological stations, Doran et al. (2002) demonstrated that a net cooling at DML (Eastern Antarctica) region could be projected between 1966 and 2000, particularly during summer and autumn.

The correlation coefficient between the 7yr-band detected in SOI and the same periodic band at δD of DML presented the lowest value among all sites (r=0.32). Moreover, the Nevado Illimani ice core record is located in the eastern Cordillera near La Paz and Lake Titicaca and is primarily exposed to the humid and warm moisture coming from the Amazon Basin and the Equatorial Atlantic Sea. This location seemed to minimize the impact of the Pacific warming sea surface waters during El Niño events (here represented by the SOI parameter), as well as the influence of dryer atmospheric regimes imposed by the strong Peruvian upwelling process, which seemed to be less significant to induce an oscillatory imprint on δD time series.

None value of r-Pearson was statistically significant between all oscillatory signals of GAST and of δD from Nevado Illimani. It is plausible to link this result to previous studies (DANSGAARD, 1964; ROZANSKI et al., 1992; RAMIREZ et al., 2003) in which it is assumed that if from one hand in site at high latitudes, the isotopic composition of meteoric water is usually interpreted as an air temperature proxy, in low latitudes such relation breaks down and instead, precipitation amount dominates the signal. However, for high elevation of tropical glaciers, it is not yet clear which effect dominates, as well as the role of the regional atmospheric circulation (HOFFMANN et al., 2003).

It is known that due to the water recycling over the Amazon Basin, there is an enhancement of the Andean deuterium-excess compared to the d-excess from another sites (RAMIREZ et al. 2003), but there is not a satisfactory model that could associate directly a water isotopic time variability with a specific meteorological or oceanic parameter (THOMPSON et al. 2003). The 8+11 yr band of IRR was the only signal to occur at each reconstruction function, independently of the study site. This can be interpreted as the globally distributed solar irradiance influence over the surface of oceans, acting on δD fractioning along the water cycle.

Applying the above mathematic method we were able to reconstruct the δD time series (reconstructed δD'), according to the equations below and as depicted in figure 2.12 (in red, over the original time series).

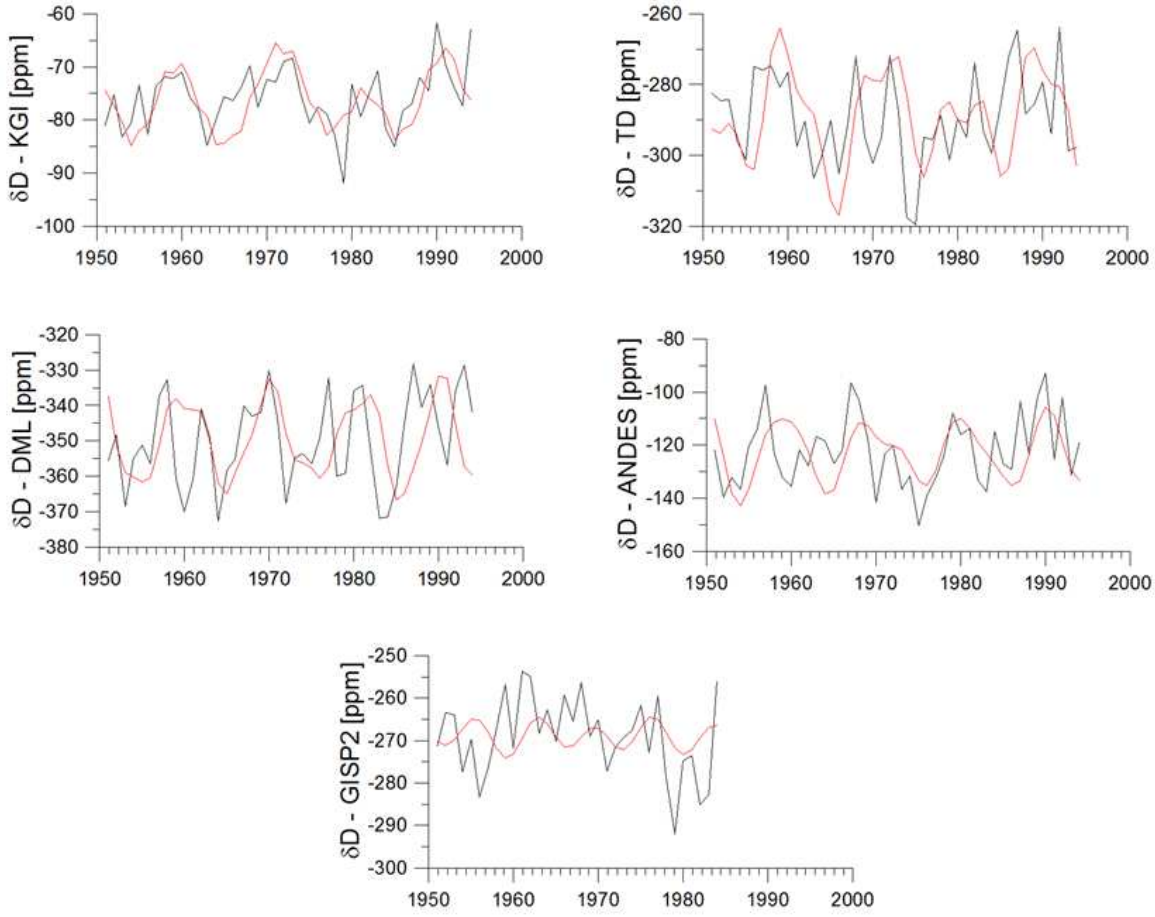

Figure 2.12 – Comparison of reconstructed δD, based on ARIST technique and the original δD time series derived from King George Island, Talos Dome, DML, Nevado Illimani and GISP2 ice cores.

The correlation coefficients (between original δD time series from GISP2, ANDES, KGI, DML and TD and their oscillatory reconstruction, considering the acceptable lag of 2 years) were, respectively: 0.2, 0.6, 0.7, 0.6 and 0.6. We obtained statistically significant correlations, which in general could explain between 36 to 49% of total δD variance from the Andean and Antarctic regions. An exception was the Greenlander δD modulation, in which we could not build a statistical significant reconstruction function, explaining only 4% of the observed modulation.

These results probably indicat that the isotopic content of ice layers at GISP 2 results from different parametrizations that are more relevant to the Northern hemisphere domain and associated to Greenland climatology. This is particularly true in the case of interhemispheric differences of solar energy budget, since the Northern Hemisphere has a larger terrestrial extent.

A possible interpretation of these results is that a significant part of the variance of the δD fractioning would respond to global thermodynamic process involving IRR and GAST, in contrast to processes that take part at sea surface, including episodic ENSO events or local-to-regional variability. The above results do not reflect the entire climatic forcing acting on each step of the water fractionation, responsible by measured δD variations, since only few parameters were selected in this study. But judging from r-Pearson values obtained from the reconstruction method, which simply considers only the oscillatory component of the time series, the set of solar-climatic parameters can be considered as primordial parameterization.

In Figure 2.13 we illustrated a schematic interpretation of our analysis, showing the parameters IRR and GAST as “primordial parameters” on δD fractioning, while the marine derived parameters (PEI, SOI and SST) configured as of second order parameters.

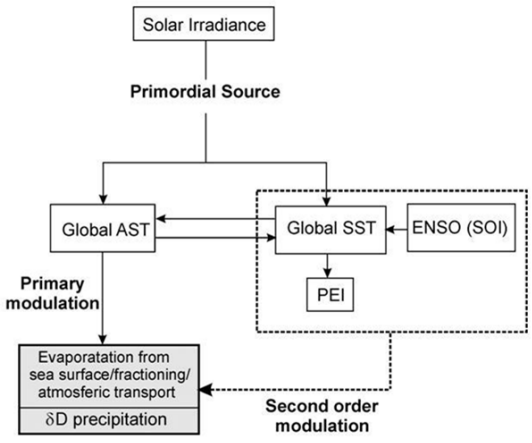

Figure 2.13 – Schematic interpretation of our results.

3 BERYLLIUM ISOTOPE: ^{7}Be

The Beryllium element (Be_4) has seven isotopes, among which only the ^{9}Be is stable. The others are unstable, or radioisotopes, decaying in a specific time interval, turning it selves in other elements. The decay phenomenon (also called disintegration) is a spontaneous process that occurs obeying the following exponential function:

$$N(t) = N_0 \cdot \exp\left(-{}^{t}/_{\tau}\right) \tag{3.1}$$

where: N(t) is the number of radioactive nuclei in a specific instant of time t, N_0 is the number of nuclei in the initial time (t=0) and τ is the radioactive time constant, characteristic of the specific radioisotope.

The radioactive period (T) of a specific radioisotope, or its half-life, is defined by the time range necessary to decay 50% of the initial total amount of radioactive nuclei. The most part of beryllium radioisotopes (^{6}Be, ^{8}Be, ^{11}Be e ^{12}Be) decays with a half-life shorter than one second, and only two of them (^{7}Be e ^{10}Be) takes more time than that to decay (MCHARGUE; DAMON, 1991).

The ^{7}Be has half-life of 53.22 $\pm$ 0.06 days and decays through the electron capture process, turning itself in a Lithium (Li) element after use one electron of its electrosphere to transform one nuclear neutron in to a proton, releasing a neutrino (ν) particle ($^{7}Be_4 + e^{-} \rightarrow {}^{7}Li_3 + \nu$). This decay process can produces directly the stable ^{7}Li, or a ^{7}Li atom with an excess of energy in its nucleus (called excited atom and represented by $^{7}Li^{*}$). The probability of occurrence of the last case is around 10%, and in this case the resulting $^{7}Li^{*}$ will release this energy excess through a γ-ray photon (E_γ = 477.6 keV), becoming a stable nucleus (TILLEY et al, 2002).

The ^{10}Be has a much longer half-life, around $1.5 \cdot 10^6$ years, and its decay is called β^- decay, where its nucleus is turned into a Boron-10 nuclei releasing an electron (with energy up to 550 keV) and an anti-neutrino particles ($^{10}Be_4 \rightarrow {}^{10}B_5 + e^- + \bar{\nu}$).

Both of these radioisotopes, ^7Be and ^{10}Be, are called cosmogenic radionuclides, because they are produced by the spallation of atmospheric constituents (mainly oxygen and nitrogen) by cosmic-rays particles. To make this spallation reaction possible in the atmosphere, and then produces the cosmogenic isotopes, it is necessary to collide a CR particle with energy up to 10 MeV with the atmospheric constituent. Considering the vertical profile of the target-constituents concentration and the energy losses of the cosmic ray in the atmosphere, the optima condition for this production occurs around 20 km above the sea-level (YOSHIMORI et al. 2005). Thus, the concentration of these cosmogenic radionuclides is highest in the low stratosphere and decreases with the altitude. After its production in the atmosphere, the isotopes ^7Be and ^{10}Be gets attached predominantly to small aerosols (diameter ~3 μm) and follow their transport and deposition process (LAL; PETERS, 1967).

The fact that the cosmogenic production is due to the CR incident flux in the atmosphere explains the anti-correlation found between the production rate of these cosmogenic isotopes and the solar cycle (see discussion regarding the CR flux and spectral modulation by the IMF conditions along the solar activity cycle in section 1.2.1), and also explains the geographical dependence observed. Before interacting with the terrestrial atmosphere, the charged particles of the CR flux respond to the local geomagnetic cutoff rigidity (Pc), which is a local threshold for CR energy spectrum that can penetrate into the atmosphere of a certain geographical site. Figure 3.1 shows this Pc dependence of the CR flux reaching the ground-level, measured by CR station geographically distributed (for the same solar activity level).

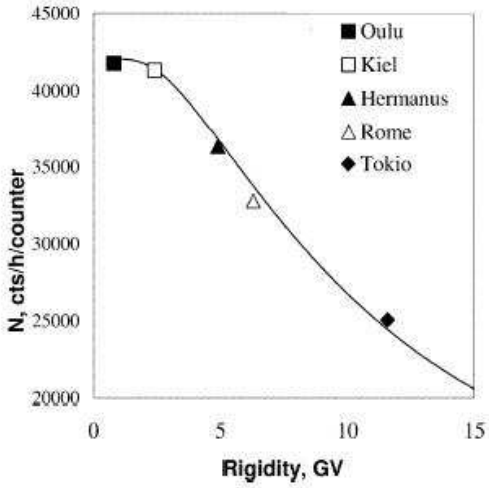

Figure 3.1 – Dependence between the CR secondary flux incident in the terrestrial surface and the local cutoff rigidity Pc.

Source: lecture private notes, Usoskin.

The combination of these two magnetic influences (IMF and Pc) on the cosmogenic production can be seen in Figure 3.2, where annual average of the ^{7}Be concentration measurements made in near-ground air in different sites is shown along the solar activity cycle.

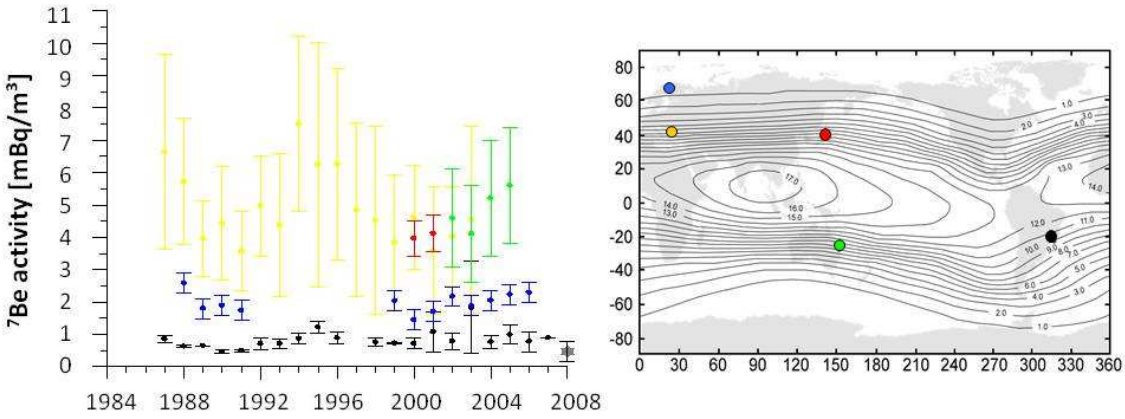

Figure 3.2 – The geographical and solar activity dependence of the ^{7}Be measurements in near-ground air (yellow: Greece (PAPASTEFANOU & IOANNIDOU, 2004), red: Japan (SAKURAI et al, 2005), green: Australia (Doering & Akber, 2008), blue: Finland (data kindly provided by STUK / Finland), and black: Brazil (Angra's data, black dots, and UERJ's data, gray star).

Thus, temporal variations of the cosmogenic beryllium concentration in the near-surface atmosphere can provide information on the air mass dynamics, precipitation patterns, stratosphere-troposphere coupling and cosmic ray variations (MCHARGUE; DAMON, 1991).

Although the production of these cosmogenic isotopes occurs more effectively in the atmosphere, the secondary CR flux may interact with the Earth's surface, producing cosmogenic beryllium *in situ*, imprinting the solar and climate conditions in the superficial natural archives (like rocks).

Many authors have studied details of ^{7}Be atmospheric transport near the ground level at different sites (Japan: YOSHIMORI (2005); Spain: AZAHRA et al. (2003); Australia: DOERING; AKBER (2008), and others), and have found multiple sources of its temporal variations. The relative importance of those different sources of ^{7}Be modulation (like air mass movement - vertical and horizontal, wet scavenging, strato-tropospheric air exchange and cosmic ray modulation) is different at different scales.

Usoskin et al. (2009) showed that the isotope variations measured in the lower atmosphere in time scales longer than synoptic can be well explained by the combined effect of production and large-scale atmospheric dynamics. However, their model appeared unable to reproduce the observed variations on the day-to-day scale, likely because of the smearing of local-regional atmospheric processes in the atmospheric general circulation models (SCHMIDT et al., 2006).

For time scales shorter than synoptic (4 - 7 days), the small-scale atmospheric dynamics produces a not negligible impact on the cosmogenic isotopic concentrations near the ground. This fact seems to be masking the production modulation signal in the near-ground concentration data (ALDAHAN et al.,

2008), making the role of atmospheric local process important to modulate the ^{7}Be radioisotope (YAMAGATA et al., 2010).

Before ^{7}Be time variability can be fully utilized as a quantitative atmospheric tracer, the seasonal and inter-annual variations in surface air ^{7}Be concentrations must be properly understood.

Using ^{7}Be time series measured in air samples at Rio de Janeiro state, Brazil, ***we made an effort to identify the relative importance between the main drivers of the atmospheric ^{7}Be local modulation, including solar activity cycle (through the modulation of the cosmic rays flux) and climate phenomena.***

The data and methods applied in the atmospheric ^{7}Be investigation are described in the next session (section 3.1), followed by the description of the results obtained and pertinent discussion concerning this analysis (section 3.2).

Besides of the analysis of the atmospheric ^{7}Be variability, a study of the climatic changes using ^{10}Be concentration found in morainas' rocks was initiated during the period of this thesis. Rock samples from South America and Antarctic were collected, allowing the determination of their exposure time using ^{10}Be measurements, and the consequent interpretation of the glacier retrieve velocities and global warming impact (occurred since the Last Glacial Maximum, in 25000 years) over different latitudes of South Hemisphere.

However, due to some unexpected difficulties occurred during the measurement stage of this work, no results were obtained until the conclusion of this thesis. Because of that, all the experimental procedures related to the sampling and ^{10}Be measurements tries are detailed in the attachment A, as well as the justification and the perspectives of the cited work.

3.1. Data & Methods

The present study was based on the analysis of two ^{7}Be time collected in air samples from Rio de Janeiro state, Brazil between 1987 and 2009. Figure 3.3 shows the study area and some details concerning this ^{7}Be database.

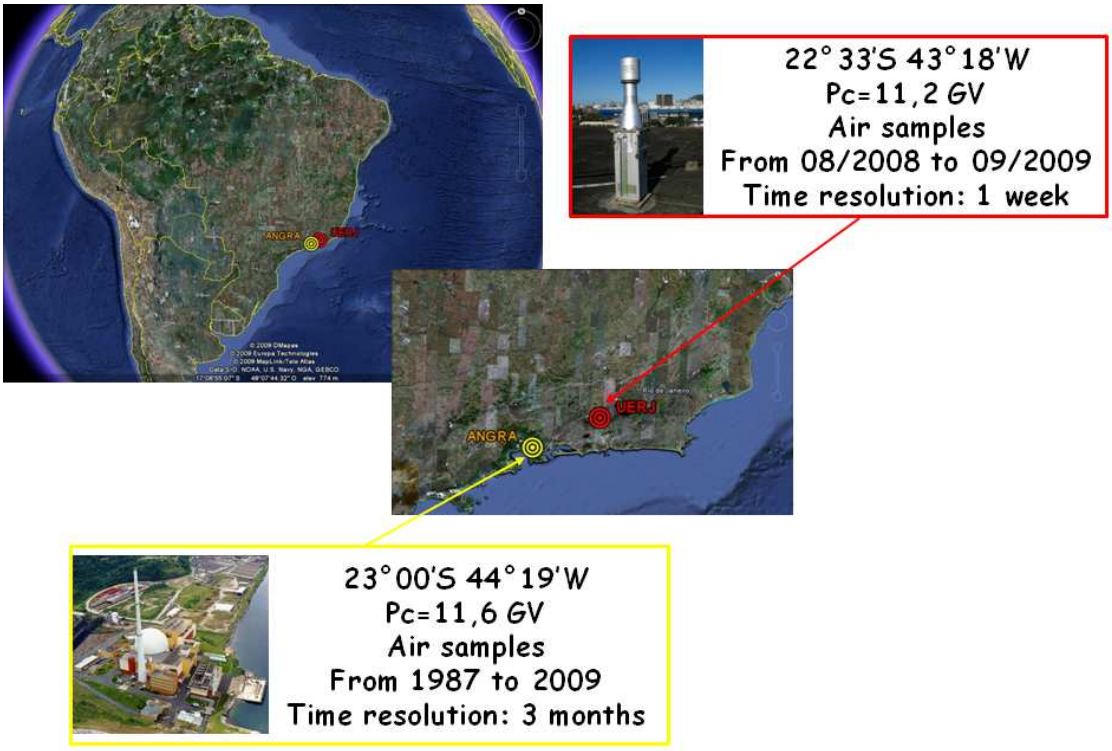

Figure 3.3 – Study areas using atmospheric ^{7}Be time series. The latitude, cutoff rigidity (Pc) and time resolution / covering are highlighted in this figure.

The Rio de Janeiro state is located around 20°S to 25°S, and so it is potentially an important location to the stratospheric ^{7}Be monitoring, because is directly related to the descendent air flow which characterizes the convergence area of the atmospheric circulation cells: Hadley and Ferrel cells. These cells are generated by the coupling between the terrestrial rotation movement and the global thermal equilibrium. Besides, Rio de Janeiro region presents a high cutoff magnetic rigidity (Pc ~ 11 GV), hindering the entrance of CR in the low atmosphere, reducing the local ^{7}Be production. Moreover, the beryllium isotopic concentration in the near-ground air is dependent on several climatic systems

involved in the local climatology, which can carry ^{7}Be atoms from different latitudes to the specific site.

The local atmospheric circulation pattern is affected by many Southern hemisphere climatic systems, which the most important is the ENSO. However, Southern hemisphere sites seem to be partially dependent on SAM signal (SILVESTRE; VERA, 2003). SAM index, also referred as Antarctic Oscillation (AAO) is defined as the difference in the normalized monthly zonal-mean sea level pressure between 40°S and 70°S (NAN & LI, 200 3).

To measure ^{7}Be in air samples, it is necessary to pump the ambient air through a glass fiber filter during a period, to collect the existent ^{7}Be-aerosols. After the collection, filters are analyzed by a hyper-purity germanium (HPGe) gamma-detector mounted inside a lead castle (for the reduction of background radiation). The intensity of the 477.59 keV − line, corresponding to the decay of ^{7}Be, is determined from the measured spectrum. Values in units of Bq/m^{3} (number of disintegrations per second per m^{3}) were obtained from counts after consideration of the detector efficiency at ^{7}Be photopeak (477.6 keV). The overall uncertainty of the measurements is typically 7–8% (USOSKIN et al., 2009).

For the last 20 years, air samples by filtering have been collected weekly around the Angra Nuclear Power Stations to monitoring possible escape of radioactive elements of the Power Station, and ^{7}Be has been measured with 3-month time resolution. The atmospheric ^{7}Be activity is routinely measured in the framework of radiation safety monitoring in many regions and sites around the globe. This 20 years of data (Figure 3.4) was kindly available by Angra Power Station and is the first part of the ^{7}Be database used in this work.

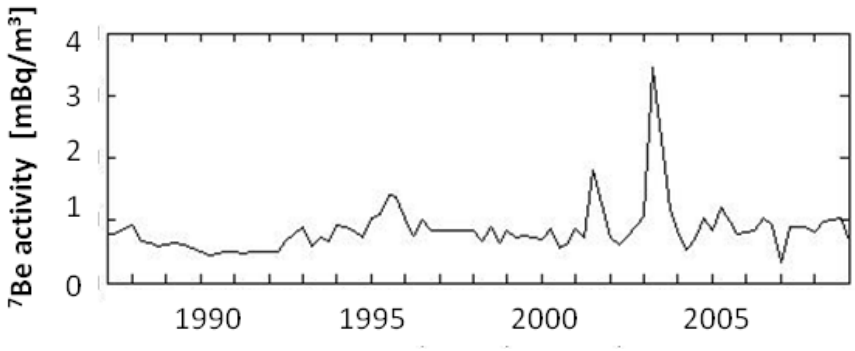

Figure 3.4 –The 3-month time resolution ^{7}Be data from Angra (Rio de Janeiro).

The ^{7}Be Angra's data was analyzed using spectral analysis tools wavelet and ARIST (described in section 2.1) and compared with a cosmogenic theoretical local production model in the upper troposphere and local climatic indices in order to study the external factors influencing ^{7}Be concentration in ambient air at Rio de Janeiro's ground level. The results of this analysis are presented and discussed in the next sub-section.

The local climatic indices used in this investigation (Figure 3.5) were obtained from the internet: SOI (referent to the ENSO phenomena) data was described in section 2.1 and SAM index was found at http://www.lasg.ac.cn/staff/ljp/data-NAM-SAM-NAO/SAM-AAO.htm.

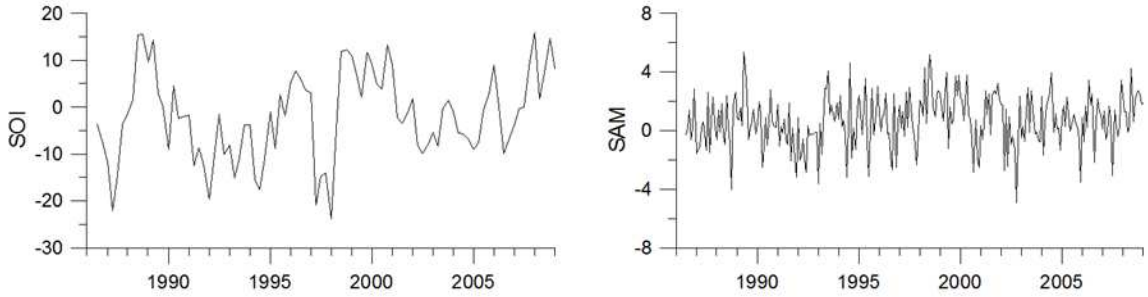

Figure 3.5 – Local climatic index for Rio de Janeiro state, Brazil (SOI, SAM).

The theoretical ^{7}Be production rate was computed using the numerical model CRAC:7Be (Cosmic Ray induced Atmospheric Cascade in application to ^{7}Be) (Usoskin and Kovaltsov, 2008b), which computes a 3-D (altitude, latitude and

longitude) production rate of ^{7}Be [in atom g^{-1} s^{-1}] in realistic conditions and in which results agrees with the available experimental data (USOSKIN & KOVALTSOV, 2008b; USOSKIN et al., 2009; KOVALTSOV; USOSKIN, 2010). The employment of this model and the interpretation of the correspondent analysis were only possible due to a personal collaboration with Dr. Ilya Usoskin, from University of Oulu (Finland), during a five months joint work (from Feb to Jun 2010). The main input parameters for the model are the local geomagnetic cuttoff rigidity (Pc [GV]), the atmospheric depth (h [g/cm^2]) and the solar activity function (ϕ [MV). The Pc value corresponding to the Rio de Janeiro state is shown in Figure 3.3 and was calculated according to the eccentric dipole approximation following the algorithm described in the Appendix of Usoskin et al. (2010), and using the IGRF-10 coefficients (found at http://www.ngdc.noaa.gov/IAGA/vmod/igrf10coeffs.txt), and the solar function ϕ was found in Usoskin et al. (2005) work. Figure 3.6 shows the production rate at Rio de Janeiro site predicted by CRAC7Be model for different altitudes in the atmosphere (represented by the atmospheric depth parameter) and for different periods of the solar activity cycle.

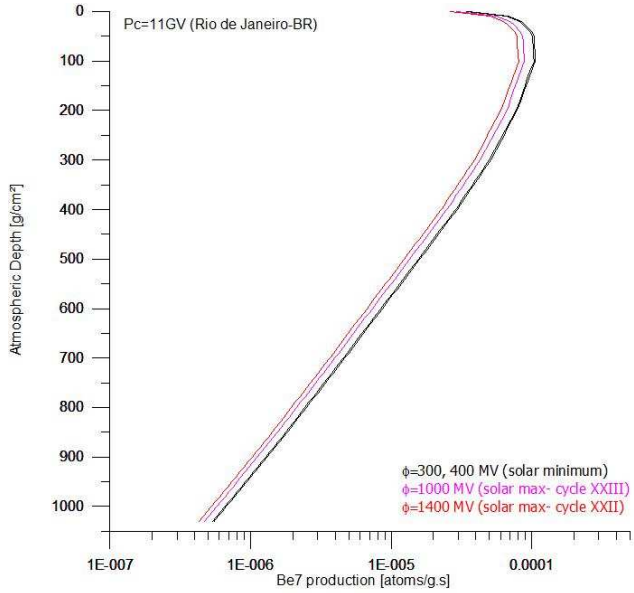

Figure 3.6 – ^{7}Be theoretical production rate for Rio de Janeiro site in different conditions of solar modulation (from CRA7Be model).

Since the time resolution of Angra's data is 3-month, the investigation of short-term variations was not possible. To solve this limitation, a higher time resolution (1-week) ^{7}Be time series from Rio de Janeiro was developed for this work. The ^{7}Be monitoring was initiated in August 2008 with the installation of a high-volume air sampler (PM10 Wedding & Associates) on the roof of the Haroldo Lisboa da Cunha Building (approximately 30 m above the ground), inside the University of Rio de Janeiro State's (UERJ's) campus, and keeps working since then.

Atmospheric aerosols smaller than 10 μm (including the ^{7}Be-aerosols type) are collected for 25 hours / week on a glass fiber filter. The total collection hours (25 h) are distributed in 5 days during the hours with lower local concentration of traffic's aerosols (between 11 am and 4 pm, local time) to avoid the filter saturation due to pollutant particulate. Figure 3.7 shows the implemented system.

Figure 3.7 – ^{7}Be acquisition system installed in UERJ's campus.

After the collection, filters are sliced into 10 identical circles (showed in Figure 3.8) and piled up to fit exactly the detector diameter of 7 cm. We used a Canberra hyper-purity gamma-ray coaxial germanium detector (extended energy range - HPGe).

Figure 3.8 – collected glass filter been sliced to be measured.

The detector was shielded by a lead castle with 10 cm to 20 cm thickness and an inner copper cover, which reduces significantly the background radiation level. Its relative efficiency is 20%, and its energy resolution varies from 1.8 keV at 1.33 MeV to 0.85 keV at 122 keV. The MCA-Maestro II (multi-channel analyzer / EG&G ORTEC) and MCC / IRD-CNEN-Brazil software tools were used to provide the gamma-ray spectral data in counts ($\underline{C}$, in counts per second, or cps). To calculate the ^{7}Be activity, in mBq/m^{3}, we have applied the equation 3.2:

$$^{7}\mathrm{Be} \qquad \frac{\overline{\qquad}}{\qquad} \qquad \frac{\overline{\qquad}}{\qquad\qquad} \qquad 3.2$$

Where $\underline{\varepsilon}$ is the detection efficiency of the system for the energy of the ^{7}Be γ-ray line (and is equivalent, in this case, to 0,032 cps/Bq), $\underline{f}$ is the area factor (and means the fraction of the filter through which the air was sampled, and in our case is 0,878), ($\underline{t}$-$\underline{t_0}$) is the time range between the end of the sampling period and the moment of the measurement, and $\underline{V}$ is the equipment flow (calculated using the atmospheric pressure and temperature, measured *in situ*, and the manometric pressure. The measurement time period of each sampled filter was 24 hours.

The sampling conditions adopted in this work were enough to detect ^{7}Be activity during all the operation period. The spectral resolution of our detector also allows the clear distinction between the γ-ray line of 477.9 keV (associated to the decay of the ^{7}Be) and the γ-ray background line around 510 keV (related to the pair production occurring naturally into the detector).

These facts can be seen in Figure 3.9, which shows an example of the detected gamma spectra (in black) along with the background measurements (in red)

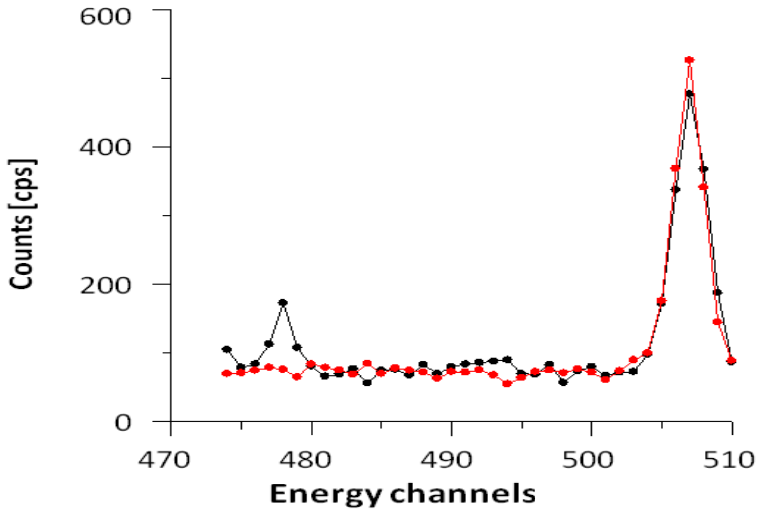

Figure 3.9 – Obtained γ-ray spectrum in the energy range containing the ^{7}Be line (477.9 keV), along with the background level (in red) for the same range.

Since August 2008, a nearly continuous weekly air sampling has been performed, and the ^{7}Be time series obtained until September 2009 was compared to local climatic parameters, in order to understand its seasonal behavior. These climatic data was collected in situ or available in CPTEC webpage (http://www.cptec.inpe.br). Figure 3.10 shows this database along with its superimposed trends (represented by a forth order polynomial fit).

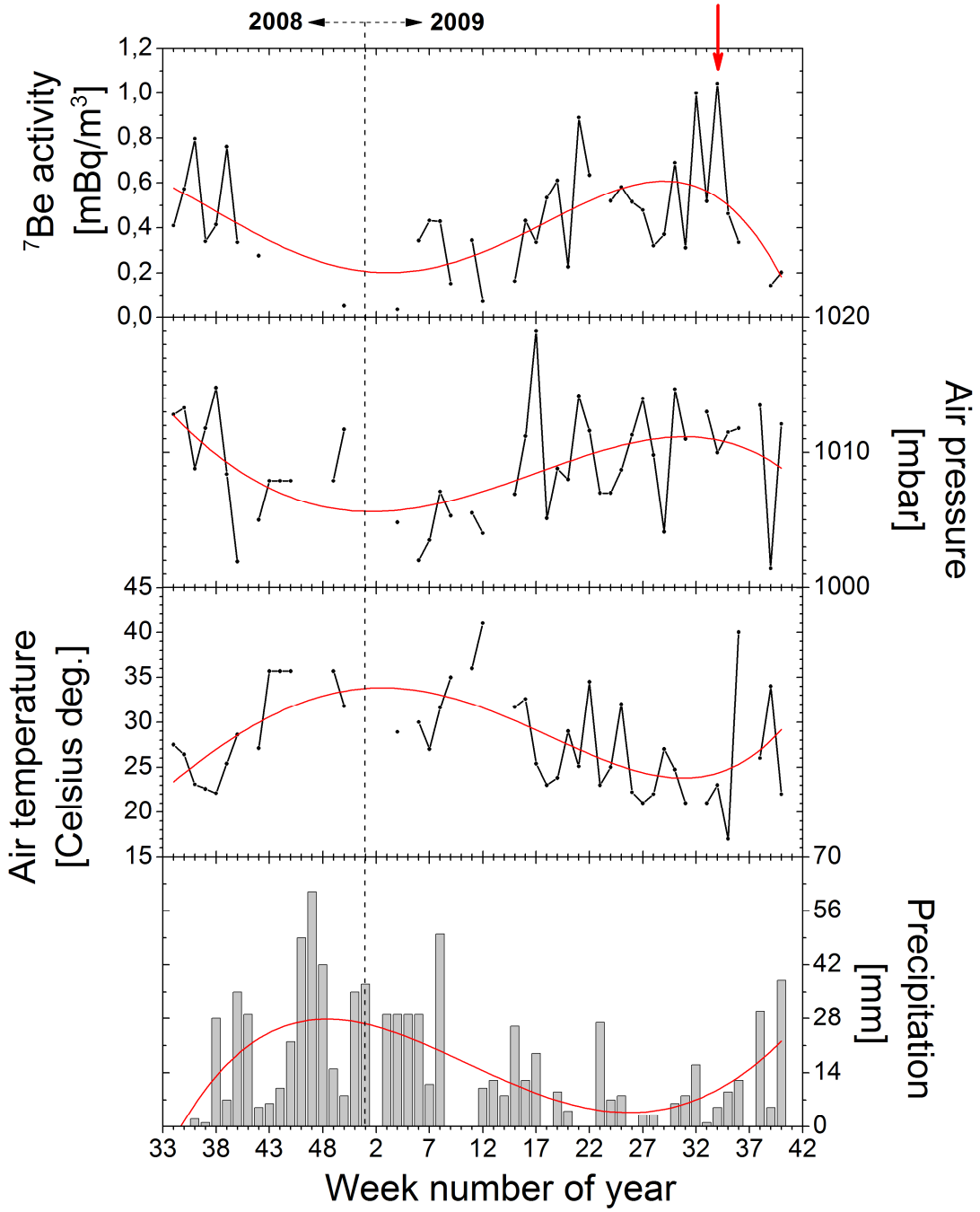

Figure 3.10 –^{7}Be data obtained from UERJ instrument between Aug 2008 and Sep 2009, and the correspondent climatic indices. This entire database is present along with their long trend (in red) represented by a 4th-order polynomial fit.

The results and discussions concerning the analysis of the cosmogenic database described above are presented in the next sub-section.

3.2. On the ^{7}Be response on climate and solar variations

Through the analysis of both ^{7}Be data series, it was possible to study the short-term and the long trend variability. The first step was to identify the trends in each ^{7}Be series, using the wavelet and ARIST spectral methods for the long dataseries (ANGRA's data) and a polynomial fit for the short one (UERJ's data). Figure 3.11 shows the spectral features that have been found in our long cosmogenic time series by wavelet and the inter-annual trend found in the short time series is shown in Figure 3.10 (red line).

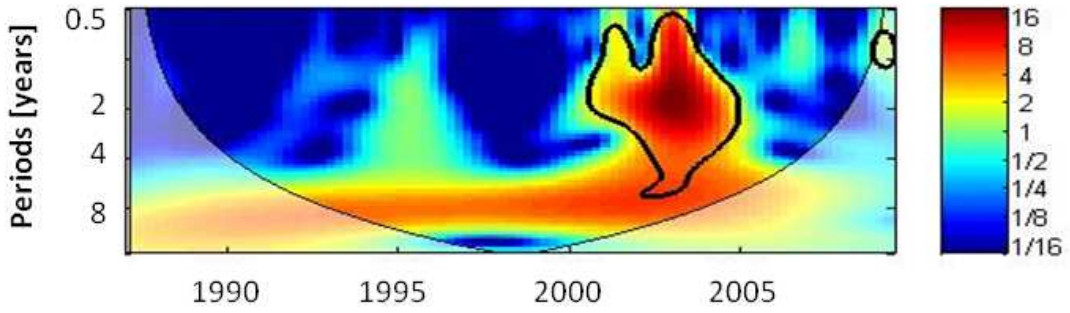

Figure 3.11 –Spectral features found in Angra's ^{7}Be timeseries using the wavelet method.

One can see a suggestion of a decadal trend present in the ANGRA's 3-month data and a seasonal trend in the UERJ's weekly data. The ARIST method couldn't identify any significant (above 2-sigmas) periodicities in the ANGRA's data, but the wavelet result (presented in Figure 3.11) shows a decadal period into the confidence. Moreover, there is also a spectral significant short-term feature occurring only between 2000 and 2005, and it is related to the existence of two extreme measurements taken in Apr-May-Jun of 2001 and 2003 (see Figure 3.4).

In order to understand the spectral features found in the long time series, we analyzed the coherence of the ^{7}Be data series from ANGRA with the local

production Q (from CRAC7Be model) and the dominant climate models at this site: SOI and SAM (Figure 3.12).

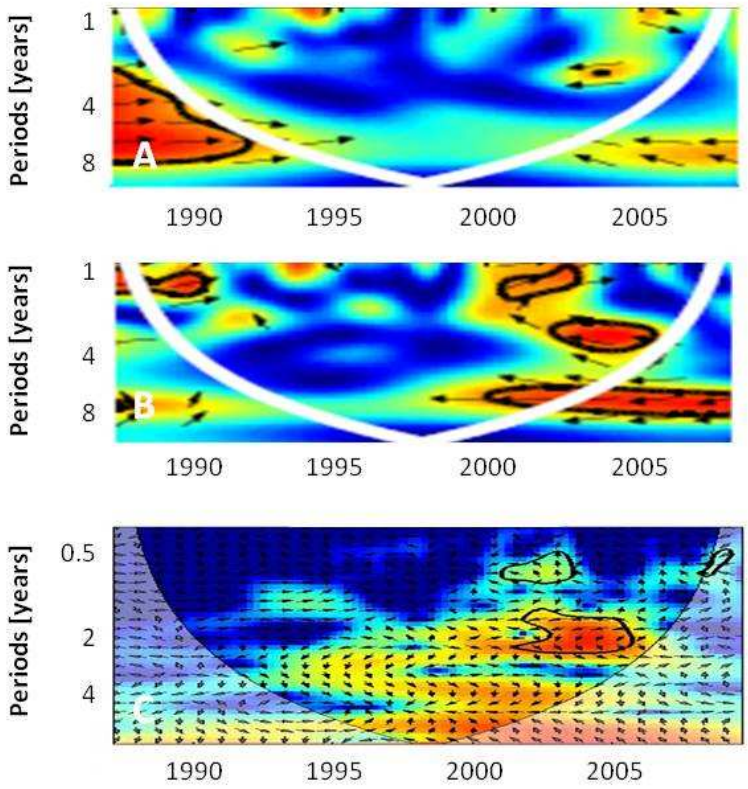

Figure 3.12 –Wavelet coherence found between ^{7}Be ANGRA database and the external forcings (Q , SAM and SOI, boxes A, B and C, respectively).

Concerning to the decadal feature, we can note in Figure 3.12 that there is no coherence between the ^{7}Be modulation and the solar cycle imprints in the cosmogenic production rate (box A) neither with the SOI variability (box C). In this decadal spectral range, there is only a not very strong possibility of coherence with the climate SAM signals after 2000 (box B). A reliable hypothesis for this fact is that the SAM pattern is dominant in a non-seasonal tropospheric circulation variations (below 20°S), affecting the climate patterns in latitudinal direction while ENSO effects mainly in longitudinal direction, making its impression in ^{7}Be concentration data. Moreover, it is known that SAM patterns can produces a significant effect on temperature and precipitation over

different Southern Hemisphere areas (not directly on Rio de Janeiro), producing changes on the regional wind pattern (GILLETT et al, 2006). This fact could also explain the weak relation found between ^{7}Be ANGRA's data and SAM climate index.

The total absence of the cosmogenic production imprints over the ^{7}Be data can be associated to the local high Pc, and can suggests that an important part of the total ^{7}Be atoms available in Rio de Janeiro site is not produced locally, but brought by air-masses from other sites and turning the atmospheric dynamics a dominant driver of the cosmogenic modulation measured in near-ground air.

Through an international collaboration (involving Brazil and Finland), we have compare the results presented above with results obtained using the same analysis with ^{7}Be data from Fennoscandia region (Sweden and Finland). We have found an indication that the cosmogenic production modulation (due to solar cycle, mainly) could be observed only at near-surface air data from sites where the geomagnetic cutoff rigidity is low and the local climatic systems are relatively stable (LEPPÄNEN et al., 2010). These conditions are not met at Brazilian southeast coast making the atmospheric ^{7}Be measured in Rio de Janeiro a potential proxy for atmospheric dynamics.

In this context, to identify the main atmospheric drivers of the ^{7}Be modulation we have analyzed the high resolution time series obtained from UERJ site. First, we separated the UERJ's ^{7}Be data in two seasons (wet season, from September to March, and dry season, from April to August), according to the suggested modulation showed in Figure 3.10.

Figure 3.13 shows the histograms of the measured ^{7}Be activity values obtained for each season along with the best-fit normal distribution. One can see that the values are nearly normally distributed around the correspondent mean value (Q_{DRY} = 0.5 and Q_{WET} = 0.3 mBq/m^{3}) with a spreading within 2 standard

deviations (indicated by the dashed vertical line). There is a single outlier during the dry season (Q_{OUT} = 1.0 mBq/m^3), which is highlighted by the red arrow in Figures 3.10 and 3.13, and it was studied in great details.

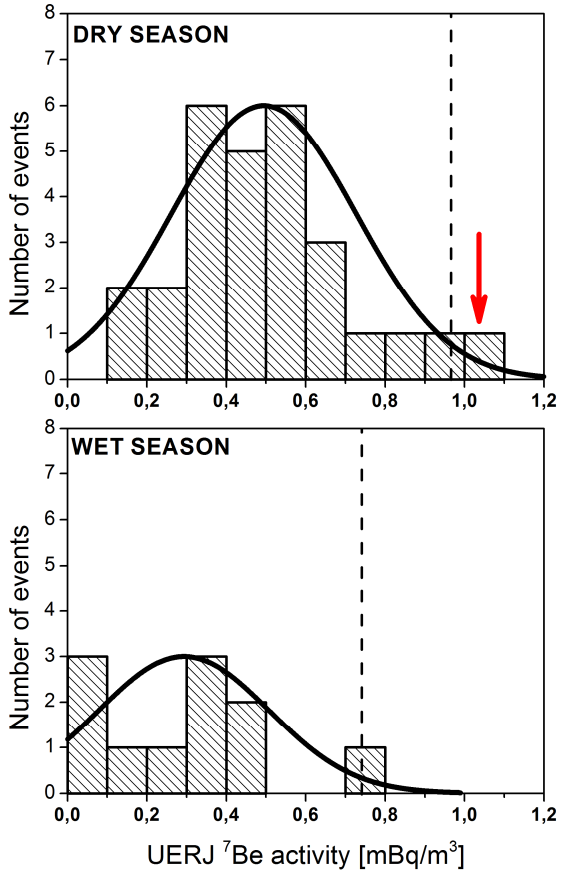

Figure 3.13 – Histogram of UERJ's data series (separated according to the seasons).

From the mean activity values, we estimate the local seasonal ^{7}Be concentration (N_{DRY} and N_{WET}, in atom/g), simply applying the radioisotope decay (τ_s = 6.6x10^6 s), including the decay along the 5 days sampling period, and adopting the typical atmospheric density at the ground level (ρ=1200 g/m^3) through the relation:

$$N = {(Q \cdot \tau_s)}/{\rho} \qquad (3.3)$$

Thus, we have found: N_{DRY} = 2.77 and N_{WET} = 1.64 atom/g. In order to identify the atmospheric drivers of these seasonal differences, we made a simple quantitative estimate of the ^{7}Be concentration expected to be found, in each season, in the atmospheric convective layer (CL, from ground level up to 4 km of altitude) based on the equilibrium condition: production versus losses.

We considered two sources of ^{7}Be production in CL (the *in situ* cosmogenic production, represented by $\underline{g_{II}}$, and sedimentation of ^{7}Be atoms from the upper layer, represented by $\underline{g_{D}}$), and two removal mechanisms (radioactive decay and depositional flux). The wet deposition process in CL for removal due to collisions between the aerosol and the raindrops is generally represented using the washout coeficient (Λ in h^{-1}), described by (APSIMON et al., 1985) as:

(3.4)

Figure 3.14 shows the distribution maps of total accumulated rain in each season in South America from CPTEC / INPE database.

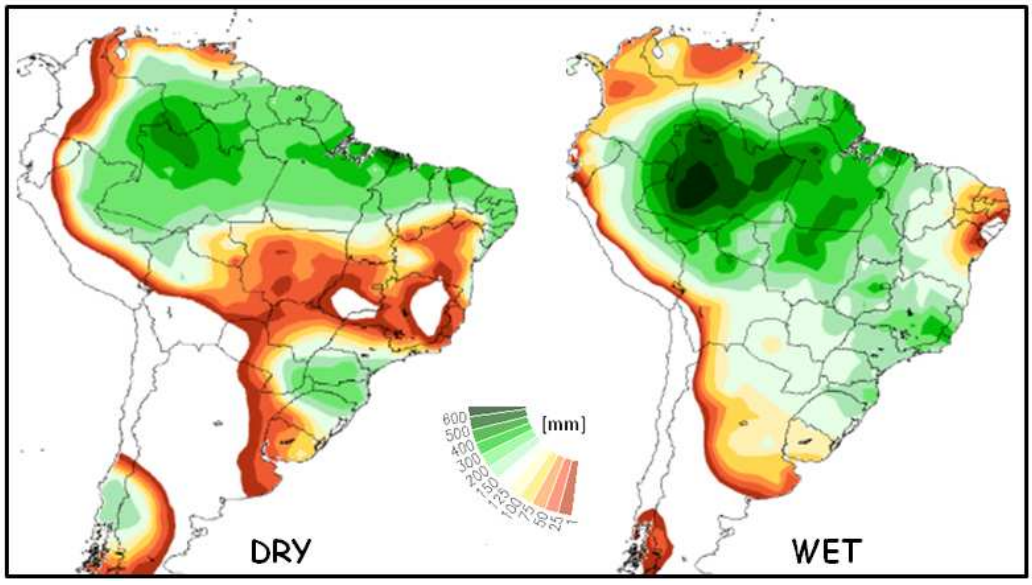

Figure 3.14 – Precipitation maps of South America in each season: wet and dry

SOURCE: modified from http://clima1.cptec.inpe.br/siac/index_ams.html

Based on these maps and applying the relation 3.4, we have computed the seasonal washout coefficients: Λ_{WET}=0.029 h^{-1} and Λ^{DRY} =0.023 h^{-1}.

Figure 3.15 shows a scheme of the conceptual equilibrium model adopted in our calculations. It consists of the upper tropospheric layer (called Layer I, from 4 km to the tropopause) and the CL (Layer II).

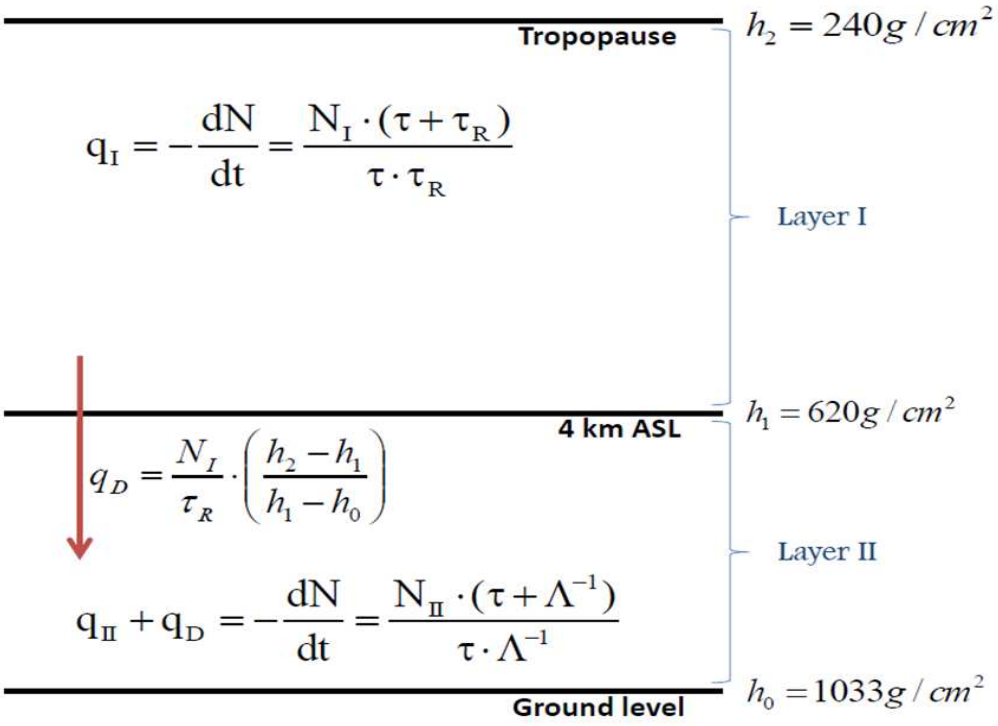

Figure 3.15– Conceptual model of the ^{7}Be dispersion.

In Layer I, we assume the equilibrium between the cosmogenic production and losses due to radioactivity decay and the depositional downward flux. The in situ cosmogenic production for each layer is represented by q_I and q_{II}, respectively, and in both cases the radioactivity decay was considered (represented by the ^{7}Be life time,τ). The mean residence time in the troposphere, τ_R (28.8 days, according to Papastefanou (2009)), was considered to compute the depositional flux of ^{7}Be atoms from the Layer I to the Layer II.

The q_I and q_{II} values ($6.4 \cdot 10^{-5}$ and $5.2 \cdot 10^{-6}$ [atom·g^{-1}·s^{-1}], respectively) were computed also using the numerical production model CRAC:7Be and represent the mean production rate of ^{7}Be in each layer between 0 and 60 degrees of latitude. This latitudinal range was chosen because Rio de Janeiro is located at the convergence area of two atmospheric circulation cells (Hadley and Ferrel), receiving influence from a wide range of latitudes.

The depositional rate from Layer I to Layer II, q_D was computed according to the simple model depicted in Figure 3.14, neglecting more detailed consideration of the atmospheric horizontal diffusion, and the obtained value was $1.6 \cdot 10^{-5}$ atom·g^{-1}·s^{-1}. Comparing this $\underline{q_D}$ value with the ^{7}Be production rates in Layer II, $\underline{q_{II}}$, one can see that $\underline{q_D}$ is 3 times larger than $\underline{q_{II}}$, suggesting that the depositional process is the dominant source of ^{7}Be atoms in CL.

Considering the conceptual equilibrium condition described above, it was also possible to estimate the seasonal values of ^{7}Be concentration in the atmospheric convective layer, as well as the ^{7}Be activity values theoretically expected (N_{II}(DRY) = 3.2 and N_{II}(WET) = 2.6 atoms/g; Q_{DRY} = 0.6 and Q_{WET} = 0.5 mBq/m³). Table 3.1 summarizes the results obtained and makes their comparison with the measured values, showing that our purely theoretical approach (without any normalization for the observed data) provided results really close to the measured activities within 1 standard deviation, well reproducing the seasonal ^{7}Be variability.

Table 3.1 – Observed values (left column) compared to our theoretically expectation (right column).

N_{DRY} [atom/g]	2.77	3.2
N_{WET} [atom/g]	1.64	2.6
Q_{DRY} [mBq/m³]	$0.5 \cdot 10^{-3} \pm 0.2$	0.6
Q_{WET} [mBq/m³]	$0.3 \cdot 10^{-3} \pm 0.2$	0.5

Besides this result, extra information was presented by our study: a ^{7}Be residence time in the troposphere. This parameter was obtained comparing the computed ^{7}Be production rates in the CL (q_{II} and q_D) for a specific solar cycle condition with the measured seasonal ^{7}Be concentrations ($N_{SEASONAL}$, that could be N_{DRY} or N_{WET}), one can also estimate the residence time ($\underline{t_r}$) of the ^{7}Be caring aerosols in CL layer. For that, the equilibrium condition between ^{7}Be production and losses should be considered, through the relation:

$$q_{II} + q_D = (N_{SEASON} \cdot (\tau_s + t_R))/(\tau_s \cdot t_R) \quad (3.5)$$

The residence time found for each season (wet: 0.9 day; dry: 1.5 day) can be compared to the ^{7}Be removal time due to washout process (calculated from the Λ_{WET} and Λ_{DRY} values), which is smaller than 2 days in both cases. These values are much smaller than the ^{7}Be radioactive decay time, showing that the wet deposition is the dominant ^{7}Be losses process in the local CL, even during the dry season (cf. FIELD et al., 2006).

Applying the same methodology, we have tried to explain the variability observed in the ANGRA's data (which were associated mainly to the climatic variability in the coherence analysis previously described). Using the precipitation data correspondent to the first 3-month periods of 1991, 1999, 2000 and 2009 years (correspondent to the maximum and minimum of the solar cycles XXII and XXIII, sequentially) and to the second 3-month period of 2003 (correspondent to the anomalous peak), and also using the theoretical ^{7}Be production expected by the CRAC7Be model in each period of the solar cycle, we found the results (in green) plotted along with the ANGRA's ^{7}Be data in Figure 3.16.

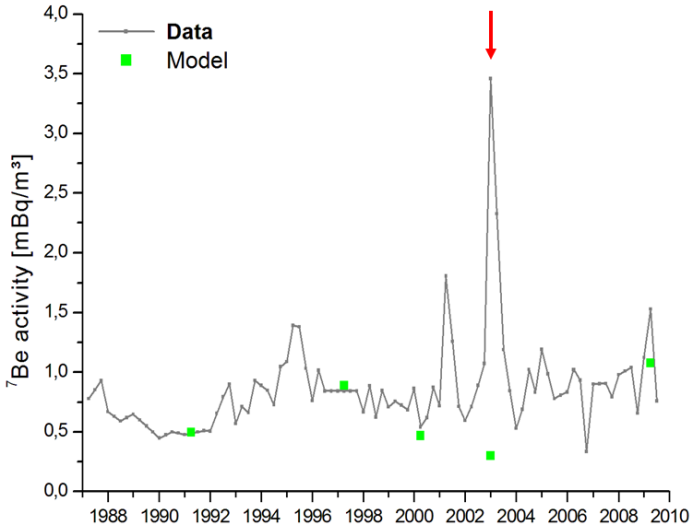

Figure 3.16 – Results obtained with our theoretical approach for different periods of the solar cycles and for an anomalous period, compared to the ANGRA's data.

Thus, one can see in Figure 3.16 and table 3.1 that both ^{7}Be variabilities (decadal and inter-annual) observed in our database collected in near-ground air in Rio de Janeiro were well reproduced by the numerical approach presented here and the good results obtained indicates that the assumptions made for the calculations are reliable, suggesting that the washout mechanism is a dominant forcing to the ^{7}Be seasonal modulation at the studied site. On the other hand, the anomalous measurements, indicated by red arrows in Figures 3.10 and 3.16, could not be reproduced by our theoretical approach.

In order to understand the outlier datapoint from the UERJ's data series, we have applied a more detailed study to infer the contribution of air-masses dynamics to this peculiar ^{7}Be activity value. This effort was only possible for this data series (and not for ANGRA's data) due to the high temporal resolution, that allowed the investigation of air-masses contribution to the observed measurement (as described below).

First, we have investigated the origin of the air-masses reaching Rio de Janeiro during the sampling period corresponding to the outlier datapoint. For that, we

have used the NOAA / HYSPLIT transport and dispersion model (Hybrid Single-Particle Lagrangian Integrated - available at http://ready.arl.noaa.gov), which computes air-mass back trajectories (with the altitude, latitude and longitude information) starting in any tropospheric height, with hourly resolution. The use of HYSPLIT for ^{7}Be-aerosols tracing was validated by Yamagata et al. (2010).

We have used the default meteorological dataset of HYSPLIT which is the NCAR / NCEP reanalysis database to perform a 120-hour back tracing for each of the five collection days (starting at 00 UTC of the specific collection day and at UERJ's location) during the correspondent week. This time limit (120 h) for the back trajectories was chosen after a test of the robustness of the HYSPLIT model results for the Rio de Janeiro location.

In order to do that, we have compared the back tracings obtained in same conditions (starting time and coordinates) but for different starting altitudes (500 m, 1000 m and 2000 m), and we found that at this time scale, the results obtained diverge from each other (Figure 3.17). Although this backtracing period is much shorter than the ^{7}Be life-time, it is in fact longer than the local residence time estimated above. Thus, we expect that the 5-day back-tracing period is sufficient for our purpose.

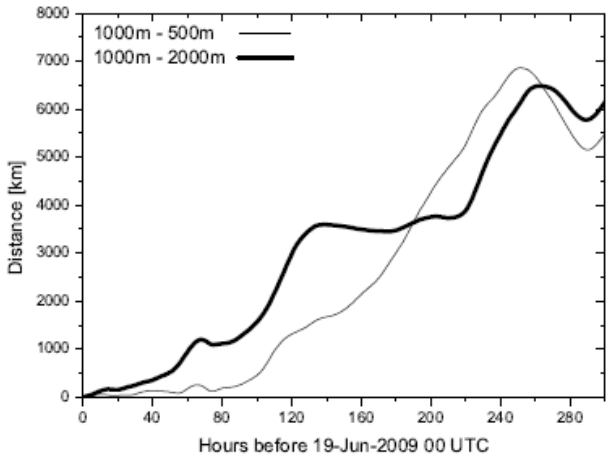

Figure 3.17 - Distance between the locations of air-masses which reach Rio de Janeiro on 19-Jun-2009 at 1000 m and its upper parcel (at 2000 m) and lower parcel (500 m).

We consider the starting point of the back-trajectory of the air mass located at the top of the sampling site atmospheric boundary layer (1000 m). The results obtained with HYSPLIT model (latitude/longitude and altitude of the air-masses) are shown in Figure 3.18, along with the precipitation map for the corresponding collection week.

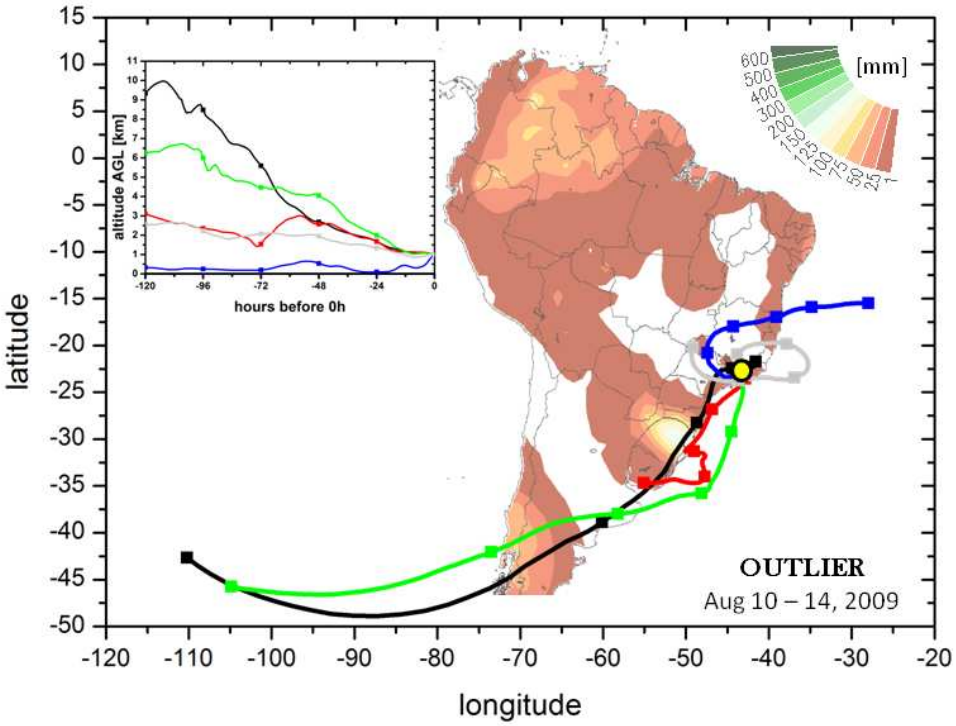

Figure 3.18 - Back-traced paths of the air-masses that were related to the UERJ's outlier data are shown along with the distribution map of accumulated precipitation over the South America during the correspondent period. Different colors denote air sampling days: Gray, blue, green, red and black for the first through fifth day, respectively. The tropospheric altitudes of the back-tracing are shown in the incut. The yellow circle indicates the Rio de Janeiro position. The color scale (upper right corner) is related to the precipitation level (in mm of rain).

One can see that during those collection days, the air-masses which reached Rio de Janeiro came from different areas, both continental and oceanic ones. It is important to note that there are two cases (indicated in Figure 3.18 by black and green colors) in which the traced air-masses came from latitudes higher than 40°S and from altitudes higher than 5 km.

For every hourly sampled location of the air back-tracing obtained with HYSPLIT model, we have computed the ^{7}Be production rate using the numerical production model CRAC:7Be, adopting ϕ=300 MV as a typical value for solar minimum period (according to Usoskin et al. (2005)), since for the UERJ's data acquisition period (2008-2009) the solar activity cycle was still on its minimum.

From the computed ^{7}Be production rate q_i in each $\underline{i}$ hours of the air mass trajectory (from 1 to 120), we have calculated the correspondent concentration (N_i in atom/g) as $N_i=q_i \cdot \Delta t$, where Δt is the total time that the air-mass spends at the same position: considered here as 3600 s. After that, we calculated the total ^{7}Be amount, N'_j (in atoms/g), expected to be found in the filter due to the arrival of the traced air-mass on the specific collection day $\underline{j}$ ($\underline{j}$ stands for the collection day, from 1 to 5). For that, we applied the radioisotope decay (τ_H = 1842.67 hours) and the additional losses rate, $\underline{T_L}$ (in hours). The value of $\underline{T_L}$ was considered as Λ^{-1} from the DRY season, during the periods the air-masses spent in Layer II (where the washout process is dominant), and as τ_R when the air-masses were in Layer I (where the deposition process is dominant). The calculations can be summarized in the following sum:

$$N'_j = \sum_{i=0}^{120} N_i \cdot exp\left(-\frac{(120-i)\cdot(\tau_H+T_L)}{\tau_H \cdot T_L}\right) \quad (3.6)$$

Note that the sum starts from i=0, because we are considering the ^{7}Be concentration found in the equilibrium scenario before the beginning of the traced air-mass movement. The N_0 value was adopted according to the altitude position of each air-mass when the traced movement was initiated. For those which were in the CL altitudes range (between the ground level and 4 km), N_0 = N_{DRY}, and for those which came from Layer I, N_0 = N_I. It is important to note that, when the air-masses crossed the hypothetical border between Layer I and Layer II, the dilution term was applied, as described above.

Thus, considering the mean ground-level local density (ρ) and applying the radioactivity decay occurred during the sampling period, it was possible to compute the expected ^{7}Be activity (Q^{*}_{OUT}), as a sum of the total amount reaching the filter during the five collection days:

$$Q^{*}_{OUT} = \frac{1}{5 \cdot \tau_D} \cdot \sum_{j=1}^{5} \rho \cdot N_j^{'} \cdot exp\left(-\frac{(5-j)}{\tau_D}\right) \quad (3.7)$$

Note that the decay factor is expressed here in days, τ_D = 76.8 days.

The computed value (Q_{OUT} = 2.0 mBq/m^3) is 2 times larger than the measured one (Q_{OUT} = 1.0 mBq/m3). This difference can be associated with the rough assumptions presented in our numerical approach (like the adoption of the dilution coefficient instead of a more realistic diffusion parameter). Besides that, our results indicate that the role of the air-mass dynamics in the anomalous ^{7}Be activity measured in near-surface air samples is important. In this outlier case, two air-masses that reached the filter during the collection week came from the south of the continent, and rised up to 9000 m above the ground induced by the orography of the Andean Cordillera. This fact explains the high ^{7}Be activity found on that week, since the cosmogenic production is very efficient at high altitudes and high latitudes, and the removal rate at higher altitudes is less efficient compared to the washout process occurring in the CL (in which the most part of the air-mass dynamics occur).

4 CONCLUSION & PERSPECTIVES

In this work, we have made an effort to understand the solar and climate information contained in isotopic data series obtained from different natural archives. We have chosen a stable isotope of hydrogen (deuterium), which temporal variability reflects changes on the global hydrological cycle, and a radioactive cosmogenic isotope of beryllium (beryllium-7), which responds to atmospheric dynamic variations. Both of them are also dependent (directly or indirectly) on the solar activity cycle, and all of these climatic and solar information are combined to modulate their concentrations found in the terrestrial surface. This mix of information consists in a main source of doubts and uncertainties for paleo-environmental studies which uses those isotopes as proxies of the solar and climate conditions in the past, hampering the future projection of these conditions.

Using data series of the isotopic concentration (obtained from the internet or acquired by our own instrumentation), solar data and climatic indices combined with spectral programs, conceptual and numerical models (obtained through international collaboration or developed in the context of this work), we have made an investigation of the relative importance between the different drivers of the isotopic modulation observed in our data. After all the work described in this thesis, and considering the modern results available in the literature, this subject is still an open question, due to the complexity of the physical phenomena involved.

The merit of this work consists in the exploration of some important points concerning this question, which can help to narrow the range of future paths to be followed, improving the knowledge of these natural proxies variabilities. Moreover, this thesis was the agent of the institutional connections established along these four years of work. Such collaborations will not be interrupted with the publication of this thesis, providing continuous interchange of knowledge,

researchers, data and models, representing the most important legacy of this thesis.

The conclusions extracted by our results, along with the correspondent perspectives opening by this thesis, can be summarizes in two main topics:

1- The temporal variability of δD obtained from ice-cores is geographically dependent, due to the contribution of the different set of local climatic systems. However, there is a globally imprint of a solar activity decadal cycle, which was better associated with the total solar irradiance modulation than with the input of nonprimordial deuterium synthesized in solar flares along the solar cycle. This result suggests a directly influence of the solar irradiance in the global water cycle, changing some climatic parameters involved in the evaporation, transport and precipitation of the water. This influence will impact in a different way in different sites, make the regional detailed study necessary. Other possible mechanisms of the solar cycle influence on terrestrial climate (like cosmic rays inducing clouds) were not evaluated in this work, and consist in an important next step to be done.

2- The atmospheric ^{7}Be modulation measured in near-ground air is also strongly geographically dependent, because it is sensible to the local climatic systems and to the local cutoff rigidity, reflecting the regional precipitation condition and also the air-masses patterns. Our results shows that in sub-tropical latitudes, the depositional flux and the air-mass transport are the dominant sources of ^{7}Be in the low atmosphere, overwhelming changes on the *in situ* cosmogenic production. Moreover, we have found that the isotopic removal process due to the rain occurrence is the most important forcing of the near-ground atmospheric ^{7}Be seasonal variability, even in the dry season period. These results is a clear warning to the rough use of the ^{10}Be time series as a direct solar

activity proxy, since this cosmogenic isotope has the same atmospheric dynamics as the studied ^{7}Be.

Our results points to a necessity of more careful interpretations of the studied proxies during paleo-environmental works, mainly because they are regionally dependent. For all of the future works suggested here, the use of 3D Global Circulation Models (GCM) is strongly recommended. Nowadays, the tendency of Solar-climate linkage studies is combine data, proxies and climatic models aiming to reproduce and understand the observed variabilities. The use of GCM models will allows the simulation of the solar activity effects (through different agents like irradiance, cosmic rays and solar wind) on the terrestrial stratosphere, troposphere and oceans dynamics, and the quantitative study of the aerosols dynamics, which drives the geochemical cycles of the cosmogenic isotopes in each environment.

Besides the GCM's necessity for further works, it is also clear the importance of the inter-comparison of results obtained with different isotopes and the insertion of other climatic and atmospheric tracers in the future analysis. This procedure will provide complementary information, which is crucial to solve questions like the non-explained anomalous ^{7}Be peak measured in Rio de Janeiro in 2003.

Unfortunately, we conclude this thesis with an incomplete work concerning to the ^{10}Be use to study glacier retreats, which would provide a precious paleo-information about the latitudinal impact of the global warming (see Attachment A). The conclusion of this experimental work also composes an important further work and depends, primarily, on the rock samples preparation, quartz extraction and ^{10}Be measurements (using AMS equipment).

REFERENCES

ALDAHAN, A.; HEDFORS, J.; POSSNERT, G.; KULAN, A.; BERGGREN, A.-M; SÖDERSTRÖM, C. Atmospheric impact on beryllium isotopes as solar activity proxy. **Geophys. Res. Lett.** v. 35. L21812, 2008.

ANGLIN, J.D.; DIETRICH, W.F.; SIMPSON, J.A. Deuterium and Tritium from Solar Flares at ~ 10 MeV Per Nucleon. **Astrophysical Journal**, v. 186, p. L41, 1973.

APSIMON, H.; GODDARD, A.; WRIGLEY, J.; CROMPTON, S. Long-range atmospheric dispersion of radioisotopes-II. application of the MESOS model. **Atmospheric Environment.** v. 19 , n. 1, p. 113-125. 1985.

ARAGUÁS-ARAGUÁS, L.; FROEHLICH, K.; ROZANSKI, K. Deuterium and oxygen-18 isotope composition of precipitation and atmospheric moisture. **Hydrological Process***,* v. 14, n. 8, p. 1341-1355, 2000.

AZAHRA, M.; CAMACHO-GARCÍA, A.; GONZÁLEZ-GÓMEZ, C.; LÓPEZ-PEÑALVER, J. J.;EL BARDOUNI, T. Seasonal ^{7}Be concentrations in near-surface air of Granada (Spain) in the period 1993-2001. **Appl. Rad. Isotopes,** v. 59, n. 2-3, p. 159-164, 2003.

BAKER, D.N. Effects of the Sun on the Earth's environment, **Journal of Atmospheric and Solar-Terrestrial Physics**, v. 62, p. 1669-1681, 2000.

BARLOW, L. K., GISP2 Stable Isotopes (Deuterium, High Resolution), **PANGAEA**, doi:10.1594/PANGAEA.56089, 1999.

BAZILEVSKAYA, G.; KRAINEV, M.; MAKHMUTOV, V. Effects of cosmic rays on the Earth's environment. **Journal of Atmospheric and Solar-Terrestrial Physics**, v. 62, p. 1577–1586, 2000.

BRIGGS, R.P. ; CARLISLE, R.J. **Solar physics and terrestrial effects** – Chapter 2, 1996. Available in: www.sec.noaa.gov/Curric_7-12/index.html).

CHAPMAN W.L.; WALSH, J. E. A Synthesis of Antarctic Temperatures. **Journal of Climate**, v. 20, p. 4096-4117, 2007.

CHUPP, E. L.; FORREST, D. J.; HIGBIE, P. R.; SURI, A. N.; TSAI, C.; DUNPHY, P. P. Solar Gamma Ray Lines observed during the Solar Activity of August 2 to August 11, 1972. **Nature**, v. 241, p. 333-335, 1973

COLGATE, S.A. The formation of Deuterium and the Light elements by Spallation in Supernova Shocks. **Astrophysical Journal**, v. 187, p. 321-332, 1974

DANSGAARD, W. Stable isotopes in precipitation, **Tellus***,* v. 16, p. 436 – 468, 1964.

DEWIT, J.C.; VANDERSTRAATEN, C.M. ; MOOK, W.G. Determination of the absolute hydrogen isotopic ratio of V-SMOW and SLAP, **Geostandards Newslett.**, v. 4, p. 33-36, 1980

DICKINSON, R.E. Solar variability and the Lower Atmosphere, **Bull. Amer. Met. Soc**, v. 56, p. 1240-1248, 1975

DORAN, P. T.; PRISCU, J. C.; LYONS, W. B.; WALSH, J. E.; FOUNTAIN, A. G.; MCKNIGHT, D. M.; MOORHEAD, D. L.; VIRGINIA, R. A.; WALL, D. H.; CLOW, G. D.; FRITSEN, C.H.; MCKAY, C. P.; PARSONS, A. N. Antarctic climate cooling and terrestrial ecosystem response, **Nature**, v. 415, l. 6871, p. 517-520, 2002.

DOERING, C.; AKBER, R. Beryllium-7 in near-surface air and deposition at Brisbane, Australia. **J. Env. Radioact.**, v. 99, n. 3, p. 461-467, 2008.

EDDY, J.A.; GILLILAND, R.L.; HOYT, D.V. Changes in the solar constant and climatic effects, **Nature**, v. 300, p. 689, 1982.

EPSTEIN, R.I.; LATTIMER, J.M.; SCHRAMM, D.N. The origin of deuterium, **Nature**, v. 263, p. 198-202, 1976.

FERRON, F. A.; SIMÕES, J. C.; AQUINO, F. E.; SETZER A.W. Air temperature time series for King George Island, Antarctica, **Pesquisa Antártica Brasileira**, v. 4, p. 155-169, 2004.

FIELD, C.; SCHMIDT, G.; KOCH, D.; SALYK, C. Modeling production and climate-related impacts on ^{10}Be concentration in ice cores. **J. Geophys. Res.,** v. 111, D15107, 2006.

FRIEDMAN, I.; REDFIELD, A. C.; SCHOEN, B.; HARIS, J. The variation of the deuterium content of natural waters in the hydrologic cycle, **Reviews of Geophysics**, v. 2, p. 177-224, 1964.

FRÖHLICH, K.; GIBSON, J. J.; AGGARWAL, P. Deuterium excess in precipitation and its climatological significance. **Study of environmental change using isotope techniques**, C&S Papers Series 13/P, p.p 54-65, International Atomic Energy Agency, Vienna, 2002

GAT, J.R. Oxygen and hydrogen isotopes in the hydrologic cycle, **Annu. Rev. Earth Planet. Sci.,** v. 24, p. 225–262, 1996.

GILLETT, N.P.; KELL, T.D.; JONES, P.D. Regional climate impacts of the southern annular mode, **Geophysical Research Letters**, v. 33, 2006.

GRINSTED, A.; JEVREJEVA , S.; MOORE, J. Application of the cross wavelet transform and wavelet coherence to geophysical time series, **Nonlinear Proc. Geophys.**, v. 11, p. 561–566, 2004.

HAIGH, J.D. The Impact of Solar Variability on Climate, **Science**, v. 272, p. 981-984, 1996

HAIGH, J.D., A GCM study of climate change in response to the 11-year solar cycle, **Quart. J. R. Meteorol. Soc.**, v. 125, p. 871–892, 1999

HAIGH, J.D. The Sun and the Earth's Climate, **Living Rev. Solar Phys.**, v. 4, n. 2, 2007.

HALE, G.E.; ELLERMAN, F.; NICHOLSON, S.B.; JOY, A.H. The Magnetic Polarity of Sun-Spots**, Astrophys. J.**, v. 49, p. 153–178, 1919.

HANSEN, J.; SATO, M.; NAZARENKO, L.; RUEDY, R.; LACIS, A.; KOCH, D.; TEGEN, I.; HALL, T.; SHINDELL, D.; SANTER, B.; STONE, P.; NOVAKOV, T.; THOMASON, L.; WANG, R.; WANG, Y.; JACOB, D.; HOLLANDSWORTH, S.; BISHOP, L.; LOGAN, J.; THOMSON, A.; STOLARSKI, R.; LEAN, J.; WILLSON, R.; LEVITUS, S.; ANTONOV, J.; RAYNER, N.; PARKER, D.; CHRISTY, J. Climate forcings in Goddard Institute for Space Studies SI2000 simulations, **Journal of Geophysical Research**, v. *107*, n. D18, p. 4347, 2002

HANSEN, J.; NAZARENKO, L.; RUEDY, R.; SATO, M.; WILLIS, J.; DEL GENIO, A.; KOCH, D.; LACIS, A.; LO, K.; MENON, S.; NOVAKOV, T.; PERLWITZ, J.; RUSSELL, G.; SCHMIDT, G. A., TAUSNEV, N. Earth's energy imbalance: confirmation and implications, **Science**, v. 380, p. 1431-1435, 2005.

HOFFMANN, G.; RAMIREZ, E.; TAUPIN, J. D.; FRANCOU, B.; RIBSTEIN, P.; DELMAS, R.; DURR, H.; GALLAIRE, R.; SIMÕES, J.; SCHOTTERER, U.; STIEVENARD, M., WERNER, M. Coherent isotope history of Andean ice cores over the last century, **Geophysical Research Letters**, v. 30, n. 4, p. 1179, 2003.

HOYLE, F.; FOWLES, W.A. On the Origin of Deuterium. **Nature,** v. 241, p. 384-386, 1973.

JOUZEL, J.; ALLEY, R.B.; CUFFEY, K.M.; DANSGAARD, W.; GROOTES, P.; HOFFMANN, G.; JOHNSEN, S.J.; KOSTER, R.D.; PEEL, D.; SHUMAN, C.A.; STIEVENARD, M., STUIVER, M., WHITE, J. Validity of the temperature reconstruction from water isotopes in ice cores, **J. Geophys. Res***.,* v. 102, n. C12, p. 26471–2648, 1997.

JOUZEL, J., MASSON-DELMOTTE, V., TIEVENARD, M., LANDAIS, A., VIMEUX, F., JONHSEN, S. J., SVEINBJORNSDOTTIR, A. E., WHITE, J. W. Rapid deuterium-excess changes in Greenland ice cores: a link between the ocean and the atmosphere, **Comptes Rendus Geoscience**, 337, n. 10-11, p. 957-969, 2005.

KIVELSON M.G.; Russell, C.T. **Introduction to space physics.** Cambridge: University Press, 1995. Ch. 3.

KODERA, K. et al. Downward propagation of upper stratospheric mean zonal wind perturbation to the troposphere. **Geophys. Res. Lett.,** v. 17, 1263-1266, 1990

KOVALTSOV, G.A., USOSKIN, I.G. A new 3D numerical model of cosmogenic nuclide ^{10}Be production in the atmosphere, **Earth Planet. Sci. Lett.**, v. 291, p. 182-188, 2010.

LAL, D., PETERS, B., Cosmic ray produced radioactivity on the Earth, **Handbuch der Physik.**, v. 46, p. 551-612, 1967.

LEAN, J., BEER, J., BRADLEY, R. Reconstruction of solar irradiance since 1610: Implications for climate change, **Geophysical Research Letters**, v. 22, p. 3195-3198, 1995.

LEAN, J, RIND, D. Evaluating Sun-climate relationships since the Little Ice Age, **J. Atmosph. Solar-Terr. Phys**, v. 61, n. 1-2, p. 25-36, 1999

LEPPÄNEN, A.-P.; PACINI, A.; ALDAHAN, A.; KOVALTSOV, G.; MURSULA, K.; POSSNERT, G.; USOSKIN, I. Cosmogenic ^{7}Be in air: A complex mixture of production and transport. **J. Atmosph. Solar-Terr. Phys**. v. 72, p. 1036-1043, 2010.

LEVITUS, S.; ANTONOV, J. I.; BOYER, T. P.; STEPHENS, C. Warming of the world ocean, **Science**, v. 287, p. 2225-2229, 2000.

LIU, J., YUAN, X., RIND, D., MARTINSON, D. G. Mechanism study of ENSO and southern high latitude climate teleconnections, **Geophysical Research Letters**, v. 29, n. 14, 2002.

LUZ, B.; BARKAN, E.; YAM, R., SHEMESH, A. Fractionation of oxygen and hydrogen isotopes in evaporation water, **Geochimica et Cosmochimica Acta**, v. 73, p. 6697–6703, 2009.

MCHARGHE, L.R.; DAMON, P.E. The global beryllium 10 cycle, **Rev. of Geophys.**, v. 29, p. 141-158, 1991.

MEEHL, G.A.; ARBLASTER, J.M.; MATTHES, K.; SASSI, F.; VAN LOON, H. Amplifying the Pacific climate system response to a small 11-year solar cycle forcing, **Science**, v. 325, p. 1114, 2009.

MERLIVAT, L.; JOUZEL, J. Global Climatic Interpretation of the deuterium-oxygen-18 relationship for precipitation, **Journal of Geophysical Research**, v. 84, n. C8, p. 5029-5033, 1979.

MIYAHARA, H., et al. Cyclicity of solar activity during the Maunder Minimum deduced from radiocarbon content, **Sol. Phys.**, v. 224, p. 317–322, 2004.

MIYAHARA, H., et al. Possible link between multi-decadal climate cycles and periodic reversals of solar magnectic field polarity. **Earth and Planetary Science Letters,** v. 272, p. 290–295, 2008.

MULLAN, D.J., LINSKY, J.L. Nonprimordial deuterium in the interstellar medium, **Astrophysical Journal**, v. 511, p. 502-512, 1999.

MUSCHELER, R., JOOS, F., BEER, J., MÜLLER, S.A., VONMOOS, M., SNOWBALL, I. Solar activity during the last 1000 yr inferred from radionuclide records, **Quat. Sci. Rev.**, v. 26, p. 82–97, 2007.

NASA – GISS, disponível em www.giss.nasa.gov/data/update/gistemp/. Acesso em: 25/06/2007.

NAN, S., LI, J. The relationship between the summer precipitation in the Yangtze River valley and the boreal spring Southern Hemisphere annular mode. **Geophys. Res. Lett.**, v. 30, p. 2266, 2003.

OERTER, H., GRAF, W., MEYER, H., WILHELMS, F. The EPICA ice core from Dronning Maud Land: first results from stable-isotope measurements. **Annals of Glaciology**,v. 39, p. 307-312, 2004.

OHMURA, A., M. WILD, BENGTSSON L. A Possible Change in Mass Balance of Greenland and Antarctic Ice Sheets in the Coming Century. **Journal of Climate**, v. 9, p. 2124–2135, 1996.

PAPASTEFANOU, C.; IOANNIDOU, A. Beryllium-7 and solar activity. **Applied Radiation and Isotopes**, v. 61, p. 1493-1495, 2004.

PAPASTEFANOU, C.; Beryllium-7 aerosols in ambient air. **Aerosol and Air Quality Research**, v. 09, p. 187-197, 2009.

PETIT, J.R., J. JOUZEL, D. RAYNAUD, N. I. BARKOV, J.-M. BARNOLA, I. BASILE,M. BENDER, J. CHAPPELLAZ,M. DAVISK, G. DELAYGUE, M. DELMOTTE, V. M. KOTLYAKOV, M. LEGRAND, V. Y. LIPENKOV, C. LORIUS, L. PÉPIN, C. RITZ, E. SALTZMANK, STIEVENARD, M. **Nature**, v. 399, p. 429-436, 1999.

RAMIREZ, E., G. HOFFMANN, J.D. TAUPIN, B. FRANCOU, P. RIBSTEIN, N. CAILLON, F.A. FERRON, A. LANDAIS, J.R. PETIT, B. POUYAUD, U. SCHOTTERER, J.C. SIMÕES, STIEVENARD M. A new Andean deep ice core from Nevado Illimani (6350 m),Bolivia, **Earth and Planetary Science Letters**, v. 212, p. 337-350, 2003.

REID, G. C. Solar variability and earth's climate: introduction and overview. **Space Science Review**, v. 94, 1-11, 2000.

RIGOZO, N.R., NORDEMANN, D. J. R. Iterative regression analysis of periodicities in geophysical record time series, **Revista Brasileira de Geofísica***,* v. 16, n. 2-3, p. 149-158, 1998.

RIGOZO, N.R., ECHER, E., NORDEMANN, D. J. R., VIEIRA, L. E. A., FARIA, H. H. Comparative Study Between Four Classical Spectral Analysis Methods, **Applied Mathematics and Computation**, v. 168, p. 411-430, 2005.

ROZANSKI, K., ARAGUÁS-ARAGUÁS, L., GONFIANTINI, R. Relation between long-term trends of O-18 isotope composition of precipitation and climate, **Science**, v. 258, n. 5084, p. 981-985, 1992

SAKURAI, H., SHOUJI, Y., OSAKI, M., AOKI, T., GANDOU, T., KATO, W., TAKAHASHI, Y., GUNJI, S., TOKANAI, F. Relationship between daily variation of cosmogenic nuclide Be-7 concentration in atmosphere and solar activities, **Adv. Space Res.**, v. 36, p. 2492-2496, 2005.

SCHIERMEIER Q. IPCC flooded by criticism. **Nature**, v. 463, p. 596-597, 2010

SCHMIDT, G., ALEINOV, I., BELL, N., BAUER, M., BAUER, S., CAIRNS, B., FALUVEGI, G., HU, Y., KIANG, N. Y., KOCH, D., LERNER, J., NAZARENKO, L., PERLWITZ, J., THRESHER, D., RUEDY, R., CHENG, Y., LO, K., OINAS, V., SATO, M.,TAUSNEV, N., YAO, M.-S., HANSEN, J. E., CANUTO, V., DEL GENIO, A., HALL, T. M., LACIS, A. A., MILLER, R. L., RIND, D., RUSSELL, G. L., SHINDELL, D. T., FRIEND, A. D., KELLEY, M., PERLWITZ, J., STONE, P. H., ROMANOU, A., SUN, S. Present-day atmospheric simulations using giss modele: Comparison to in situ, satellite, and reanalysis data. **J. Clim**., v. 19, n. 2, p. 153-192. 2006.

SILVESTRE, G., VERA, C. Antarctic oscillation signal on precipitation anomalies over southeastern South America, **Geophysical Research Letter**, v. 30, n. 21, 2003.

SIMÕES, J.C., F. A. FERRON, R. T. BERNARDO, A. J. ARISTARAIN, M. STIÉVENARD, M. POURCHET, AND R. DELMAS, Ice core study from the King George Island, South Shetland, Antarctica, **Pesquisa Antártica Brasileira**, v. 4, p. 9-23., 2004.

SHINDELL, D., RIND, D., BALACHANDRAN, N., LEAN, J.L., LONERGAN, P. Solar Cycle Variability, Ozone, and Climate, **Science**, v. 284, p. 305–308, 1999.

SKVARCA, P., W. RACK, H. ROTT AND T. IBARZÁBAL Y DONÁNGELO. Evidence of recent climatic warming on the eastern Antarctic Peninsula, **Annals of Glaciology**, v. 27, p. 628-632, 1998.

SMITH, J.A., SELTZER, G.O., FARBER, D.L., RODBELL, D.T., FINKEL, R.C. Early Local Last Glacial Maximum in the Tropical Andes, **Science**, v. 308, p. 678-680, 2005.

SOLANKI, S.K., USOSKIN, I.G., KROMER, B., SCHUESSLER, M., BEER, J. An unusually active Sun during recent decades compared to the previous 11,000 years, **Nature**, v. 431, p. 1084-1087, 2004.

STENNI, B., PROPOSITO, M., GRAGNANI, R., FLORA, O., JOUZEL, J., FREZZOTTI, M. Eight centuries of volcanic signal and climate change at Talos Dome (East Antarctica), **Journal of Geophysical Research**, v. 107, n. D9, 2002.

STOTT, P.A., JONES, G.S., MITCHELL, J.F.B. Do Models Underestimate the Solar Contribution to Recent Climate Change?, **J. Climate**, 16, 4079–4093, 2003.

THOMPSON, L. G., MOSLEY-THOMPSON, E., DAVIS, M. E., LIN, P.-N., HENDERSON, K., MASHIOTTA, T. A. Tropical Glacier and ice core evidence of climate change on annual to millennial time scales, **Climatic Change**, v. 59, p. 137-155, 2003.

TORRENCE, C., COMPO, G. P. A practical guide to wavelet analysis, **Bulletin of the American Meteorological Society**, v. 79, n. 1, p. 61-78, 1998.

TURNER, J., COLWELL, S. R., MARSHALL, G. J., LACHLAN-COPE, T. A., CARLETON, A. M., JONES, P. D., LAGUN, V., REID, P. A., IAGOVKINA, S. Antartic climate change during the last 50 years, **International Journal of Climatology**, v. 25, p. 279-294, 2005.

USOSKIN, I.G., KANANEN, H., KOVALTSOV, G.A., MURSULA, K., TANSKANEN, P. Correlative Study of Solar Activity and Cosmic Ray Intensity, **J.Geophys.Res.**, v.103, n. A5, p. 9567-9574, 1998.

USOSKIN, I.G., ALANKO, K., MURSULA, K., KOVALTSOV, G.A. Heliospheric modulation strength during the neutron monitor era, **Solar Phys.**, v. 207, p. 389-399, 2002.

USOSKIN, I.G., Long-Term Variations of Cosmic Rays and Terrestrial Environment. In: T.Kajita, Y. Asaoka, A.Kawachi, Y.Matsubara, M.Sasaki (eds.). **Frontiers of cosmic ray science.** Tokyo: Universal Academy Press, p.205-228, 2004.

USOSKIN, I. G., ALANKO-HUOTARI, K., KOVALTSOV, G. A., MURSULA, K., Heliospheric modulation of cosmic rays: Monthly reconstruction for 1951-2004. **J. Geophys. Res.**, v. 110, 2005.

USOSKIN, I.G., G.A. KOVALTSOV, Cosmic rays and climate of Earth: Possible connection, **Compt. Rend. Geosci**., v. 340, p. 441-450, 2008a

USOSKIN, I., KOVALTSOV, G., Production of cosmogenic ^{7}Be isotope in the atmosphere: Full 3d modelling. **J. Geophys. Res**. v. 113, 2008b.

USOSKIN, I. G., FIELD, C. V., SCHMIDT, G. A., LEPPÄNEN, A.-P., ALDAHAN, A.,KOVALTSOV, G. A., POSSNERT, G., UNGAR, R. K. Short-term production and synoptic influences on atmospheric ^{7}Be concentrations. **J. Geophys. Res**., v. 114, 2009.

USOSKIN, I., MIRONOVA, I., KORTE, M., KOVALTSOV, G., Regional millennial trend in the cosmic ray induced ionization of the troposphere. **J. Atmos.Solar-Terrest. Phys.**, v. 72, p. 19-25. 2010.

VALDEZ-GALICIA, J. F. Advances in low energy galactic cosmic rays in the heliosphere. **Adv. Space Res.**, v. 35, n. 5, p. 755-767, 2005

Van den Broeke, M., N. Van Lipzig, Marshall, G. On Antarctic climate and change, **Weather**, v. *59, n.*1, p. 3-7, 2004.

VAUGHAN, D.G. Recent rapid regional climate warming on the Antarctic Peninsula, **Climate Change**, v. *60*, p. 243-274, 2003.

VIEIRA L.E.A., SOLANKI S.K. Evolution of the Solar Magnetic Flux on Time Scale of Years to Millienia, **Astron. Astrophys.**, v. 509, p. A100, 2010.

VIMEUX F., MASSON V., JOUZEL J., STIEVENARD M., PETIT J.-R. Glacial–interglacial changes in ocean surface conditions in the Southern Hemisphere, **Nature**, v. 398, p. 410–413, 1999.

WOLBERG, J.R. Applying method of prediction analysis to problem of peak separation, **Nucelar Instruments & Methods***, v. 56*, n. 2, 209-&., 1967.

YUAN, X. Extra-polar climate impacts on Antarctic sea ice: Phenomenon and mechanisms, **Antarctic Science***, v.* 16, n. 4, p. 415-425, 2004.

YAMAGATA, T., SUGIHARA, S., MORINAGA, I., MATSUZAKI, H., NAGAI, H. Short term variations of ^{7}Be, ^{10}Be concentrations in atmospheric boundary layer. **Nuclear Inst. and Met. Phys. Res. B**, v. 268, n. 7-8, p. 1135-1138, 2010.

YOSHIMORI, M., Beryllium 7 radionucleide as a tracer of vertical air mass transport in the troposphere, **Adv. Space Res**, v. 36, p. 828- 832, 2005.

WHITE, W.R. et al. The climate signal in the stable isotopes of snow from Summit Green Land: results of comparison with modern climate observations. JGR, v. 102, 3255-3266, 1997.

ATTACHMENT A – EXPERIMENTAL EFFORT ON ^{10}BE STUDY

In this attachment, it is present the motivation and methodology of an experimental effort on ^{10}Be measurements that was done during the period of this thesis aiming a latitudinal glaciers retreats study.

The ^{10}Be measurements requires the employment of a mass spectrometry combined with an accelerator (AMS – Accelerator Mass Spectrometry), which basically is a traditional mass spectrometer, with magnetic and electric fields promoting a defined separation of elements with distinct atomic masses. The special point of this AMS method is that the sample is accelerated up to 20 MeV before interact with the fields, excluding eventual background noises due to the presence of isobars in the sample (^{10}B, in this case).

The lack of a Brazilian AMS instrument and the failure to use an existent one during the period of this thesis make the conclusion of this work impossible. However, the sampling stage and a first step of the sample preparation were made on time, and are described in this attachment, as well as the theoretical fundament of this work.

The main motivation was the potential retreat information contained in the moraines at different latitudes of South America and Antarctica which could be accessed through the ^{10}Be concentration measurements in their superficial rocks. From this information, the climate variations of the sub-tropical and sub-polar regions since the LGM (Last Glacial Maximum, 25000 years ago) could be understood.

Moraines are regions which were covered by glaciers in the past and were submitted to erosion and transport of rocks during moments of expansion and retreat of the glacier along the glacial and inter-glacial periods. As soon as the glacier retreats, the moraine region is exposed and the ^{10}Be is produced *in situ*.

Figure A.1 illustrates the process of ^{10}Be production in moraines during the time evolution of the glacier retreat.

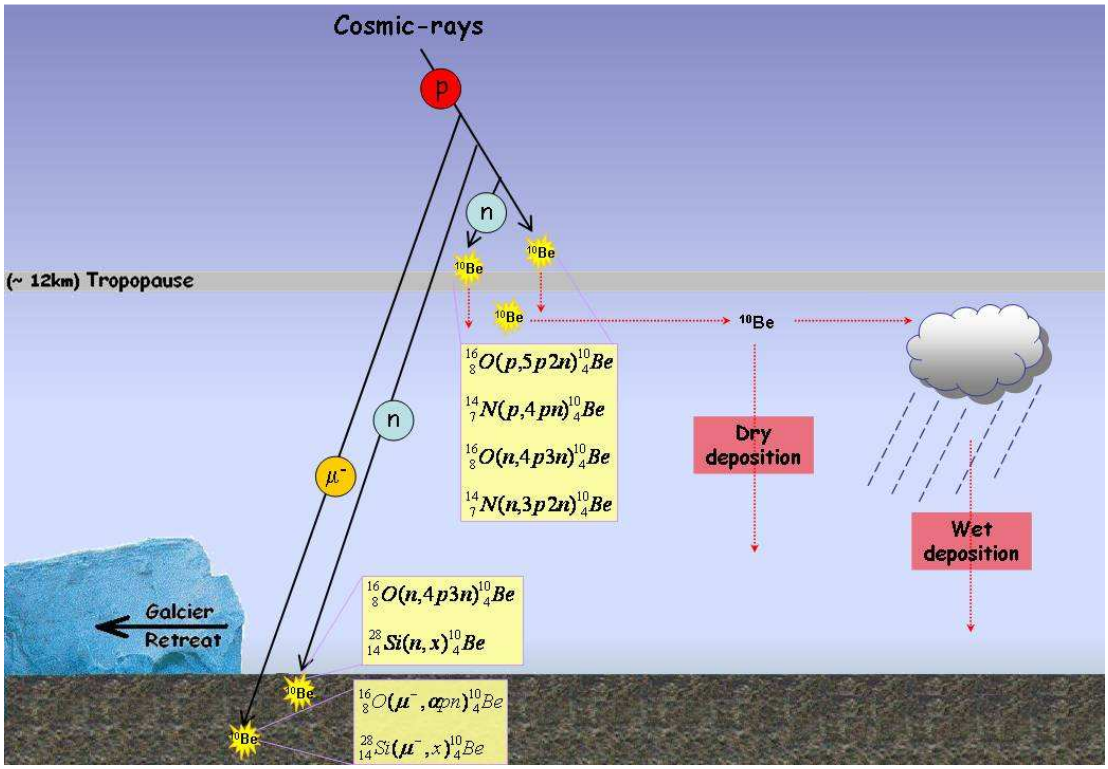

Figure A.1 – Schema of ^{10}Be production in moraines areas. The nuclear reactions occurring in the atmosphere and *in situ* are indicated, as well as the deposition main processes.

The current process of glaciers retreat has been interpreted as an evidence of the global temperatures increase observed since 1860. However, the linkage between the atmospheric temperature and the glacier retreat process is still controversial, and the response of glaciers at different latitudes to this global warming is not fully understood yet.

Through the analysis of ^{10}Be concentration in moraines from Andes, Smith et al. (2005) shows that there was no synchronisms in the glacier retreats process from tropical regions and from higher latitudes, showing the necessity of a detailed latitudinal investigation of this process to understand the impact of the global warming in each region.

In this context, we sampled moraines rocks from sub-tropical and polar regions (areas C and D in Figure A.2) aiming to measure ^{10}Be in it and compare the obtained results with the Smith et al (2005) work (correspondent to tropical area A in the same figure), and with further results from the next sampling region (indicated by B region).

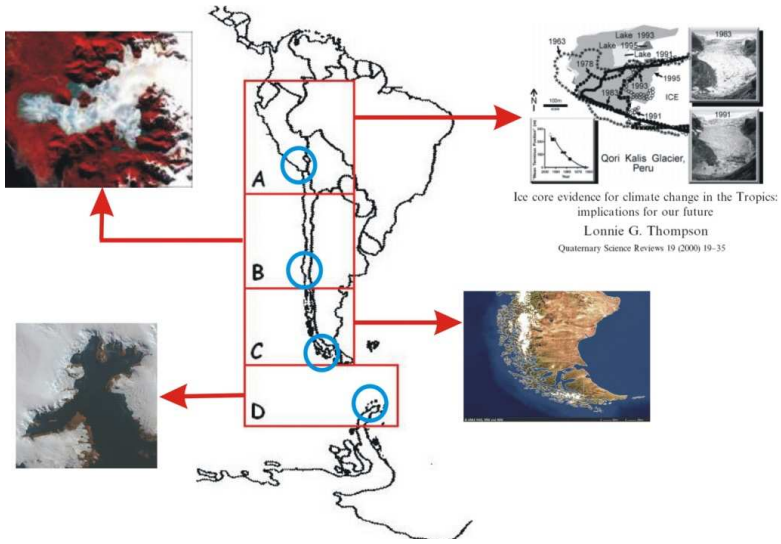

Figure A.2 – Study areas of this work.

The Antarctic region was included here due to its essential contribution to the planetary climatic system and to its evident sensibility to the recent global changes. Air temperature data from surface meteorological stations and satellites show that an important increase is occurring at the Antarctica Peninsula region, which is considered one of the most sensible regions to climatic changes in the world (NASA-GISS, 2004; HANSEN et al., 2001; SKVARCA, et al., 1998). This feature makes this Antarctic region one of the main natural laboratories to study the environmental response to climate change.

For the sampling process in the Antarctic Peninsula area (area D), we had the logistic support from Brazilian Antarctic Program (PROANTAR), due to the

collaboration of the MIDIAPI project (Microbial Diversity of Terrestrial and Maritime Ecosystems in Antarctic Peninsula, USP / Brazil). In the period from 18th Feb 2008 and 14th Mar 2008, four different moraines were sampled in the Almirantado bay, King George Island, as one can see in figure A.3.

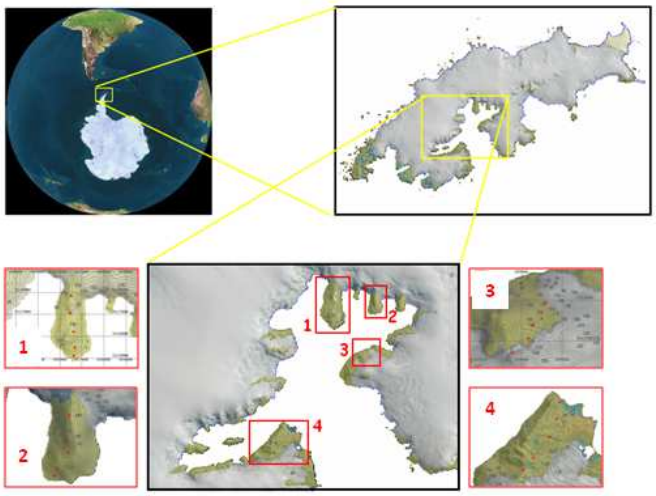

Figure A.3 – Four moraines sampled in Almirantado bay, King George Island, Antarctic Peninsula (area D in Figure A.2).

Aiming to estimate the velocity of the glacier retreat, we have sampled rocks (3 samples of 2 kg each) from five fixed exposed blocks found in the sea-glacier path (indicated by the red dots in Figure A.3 incuts), in each moraine (1 to 4, in Figure A.3), in different altitude levels (from sea level up to 250 m above it). Figure A.4 shows the sampling process and the work field team responsible for the sampling in Antarctica.

Figure A.4 – Sampling process in Antarctica and the work field team: Lia Rocha (MIDIAPI), Alessandra Pacini, Emanuelle Kuhn (MIDIAPI) and Roberto Vilella (CAP).

From 15th Mar 2008 to 18th Mar 2008, it was realized the sampling process in the moraine correspondent to the retreat of the Gray Glacier, in Chilean Patagonia (region C), Chile (Figure A.5).

Figure A.5 – Sampling points in the Chilean moraine of the Gray Glacier (area C in Figure A.2).

In this case, we have taken one rock sample (~5 kg) from each exposed block found in the moraine (red dots in figure A.5). Figure A.6 show the patagonian sampling process and the correspondent work field team (composed by Drs. Heitor Evangelista, Erling Johnson e Vincent Jomelli).

Figure A.6 – Sampling team working at Chilean Patagonia moraines.

To date the exposure time of the moraines' rocks, it is necessary to determine the concentration of the cosmogenic ^{10}Be produced *in situ*, removing from the sample the contribution of the ^{10}Be atoms brought from the atmosphere during the deposition processes (see Figure A.1). Therefore, it is necessary to measure the cosmogenic concentration into the quartz molecules, because they are composed by silicon and oxygen atoms (SiO_2), which are the main target for the cosmic rays to produce ^{10}Be *in situ*.

Thus, it was made an effort to extract the quartz from the sampled rocks, mechanically and magnetically, without any chemical attack (since we don't have the know-how for that procedure in our laboratories). Therefore we broke one piece of sample in small grains (< 1 mm), and after washed and dried it, we separated only the non-magnetic parcel (composed by quartz + feldspar), using an electro-magnet. This stage was done in the Geological Laboratory of Samples Processing (LGPA / UERJ) and is represented in Figure A.7.

Figure A.7 – Rock processing stage

In closing, using the non-magnetic parcel of our sample, we tested an alternative methodology to measure the ^{10}Be concentration: the Plasma Desorption Method Spectromety (PDMS), in PUC / Rio de Janeiro, Brazil, but no result was obtained.

The dating of the sampled rocks and the analysis of the obtained results composes the next step of this work.